TWO ANGULAR FORCE MODELS FOR THE LATTICE DYNAMICS OF CUBIC METALS

by

Pui Sum Yuen

Submitted in partial fulfillment
of the requirements for the degree of
Master of Science

Department of Physics,
Faculty of Pure and Applied Science,
The University of Ottawa,
Ottawa, Canada.

September 1966.

ACKNOWLEDGMENTS

I wish to express my deep gratitude to Dr. Yatendra P. Varshni for suggesting this problem and for his constant advice and encouragement during this investigation.

Thanks are due to Dr. Ramesh C. Shukla and Mr. Robert J. Blanchard for many helpful discussions.

TABLE OF CONTENTS

ABSTRACT

We have used two angular force models to investigate the lattice dynamical properties of some cubic metals. Each of these two models consists of central force interaction between a particle and each of its first and second neighbours. In addition the first model also has an angular force interaction between a particle and each of its first and second neighbours (treated in de Launay's article [12]), while the second model has an angular force interaction between a particle and two of its first and second neighbours (treated in the paper by Cazis et al. [24]). Each model involves two central and two angular force constants.

For the second model, we give an alternative derivation of the results obtained by Clark et al. [23] for the b.c.c. lattice.

We apply both models to copper, aluminum and nickel (f.c.c.). It is found that the second model gives reasonably good results, better than those provided by the first model.

For b.c.c. lattice, we find that the two models are equivalent to each other and equivalent to the second neighbour tensor-force model, as far as the frequency spectrum is concerned. We apply this model to sodium, tantalum, molybdenum, tungsten and iron. For those metals whose dispersion curves are not complicated (e.g. Na, Fe), the second neighbour tensor-force model can be used with fair success.

CHAPTER I

INTRODUCTION

In order to explain the variation of specific heats at constant volume with changes of temperature for different materials, Einstein [1], in 1907, proposed a model of solid which consists of atoms, vibrating independently with the same frequency about their own positions of equilibrium. Though this model provides only a qualitative agreement with the experimental variation of the specific heats with temperature, it still serves as a great milestone in the studies of solids.

In 1912, Debye [2] developed a model of solid which employs as a postulate that all the atoms in a solid are not vibrating independently, but instead, are coupled together and vibrate collectively. Only the normal modes of vibration are taken as the motion of the system in reality. This laid down the foundation of the modern lattice dynamic theory of solids. A Debye cut-off frequency was introduced artificially so that the total number of normal modes is equal to that of the degrees of freedom of the system.

In Debye's theory, a crystal is treated as a continuum which is not true in reality. On the experimental side it is found that, the Debye temperature is not a constant at low temperatures. Born and von Kármán [3], in 1912, proposed their famous model of solid which treats the crystal as a discrete lattice as it actually is. An artificial periodic boundary condition was introduced by Born ([4], p. 567), so that only those

solutions of the equations of motion, which satisfy this boundary condition are the normal modes of vibration.

The interactions between the particles are expressed in terms of the elastic constants when passing to the long-wave limit. This is a good method of obtaining the characteristics of some microscopic quantities in terms of their asymptotic behaviour.

Blackman [5], Montroll [6], Bowers and Rosenstock [7] applied this model to a two-dimensional lattice with central force interaction between a particle and each of its first and second neighbours.

Fine [8] applied this model to the body-centered cubic lattice and Leighton [9] to the face-centered cubic lattice. These models assume central force interaction between a particle and each of its first and second neighbours. Though their results agree qualitatively with experiment, their basic assumption of purely central force interaction leads to the Cauchy relation which is not obeyed in metals.

The subject of lattice dynamics has been reviewed in recent years by Blackman [10] Born and Huang [11], de Launay [12], Cochran [13] and Maradudin, Montroll and Weiss [14].

The most general force constant model is that proposed by Begbie and Born [15] in 1947, now known as the tensor-force model. Begbie [16] applied this model to the face-centered cubic and the close-packed hexagonal lattices. Curien [17] has used this model for the b.c.c. lattice;

simplified versions have been used by Singh and Bowers [18] and by Hendricks, Riser and Clark [19]. Squires [20,21] has given general equations for interactions out to n neighbours on this model. The number of force constants required for each shell of atoms for the tensor-force model for b.c.c. and f.c.c. lattices are shown in Table I.

Table 1. The number of force constants required for each shell of neighbours for the tensor-force model.

	Shells of neighbours								
	1	2	3	4	5	6	7	8	9
f.c.c.	3	2	4	3	4	2	6	2	4
b.c.c.	2	2	3	4	2	2	4	4	4

In recent years several models have been proposed which make special assumption as to the type of forces involved. The number of force constants for each shell of neighbours in these models is often less than the corresponding number on the tensor force model. Three of these models are identified below.

1. Besides the central force, de Launay [12] has discussed a second type of force which depends on the angle which the line joining the moving atoms

makes with the equilibrium position of the line; this type is called an "angular force".* The mechanical analogy is a rod connecting the particles, the rod being fastened at its ends to the equilibrium positions by springs perpendicular to the rod. This model uses two force constants for each shell of neighbours. It is referred to as the "Angular Force Model I" (AFM-I) in this thesis.

2. Recently Clark, Gazis and Wallis [23] have investigated the frequency spectra of b.c.c. lattices using a model in which interatomic forces include angular forces of the type introduced by Gazis, Herman and Wallis [24]. This model contains angular forces as well as central forces between nearest and next-nearest neighbours and has four force constants; it will be referred to as the "Angular Force Model II" (AFM-II).

3. Lehman, Wolfram and De Wames [25] have proposed an axially symmetric model for lattice dynamics of metals. The basis of the model is the assumption that the internal energy of the system can be obtained by simply adding up all the bond-stretching and axially symmetric bond-bending terms. Varshni and Shukla [26] have given a treatment of the axially symmetric model when interactions out to any neighbour are considered. This model has two force constants associated with each shell of neighbours.

In the present thesis we have carried out the following investigations:

1) A treatment of the f.c.c. and b.c.c. lattices according to AFM-I.

---

* Angular forces were first introduced in lattice dynamics by Born [22] in his treatment [illegible]

2) An alternative derivation of the results of Clark et al. [23] for the b.c.c. lattice on AFM-II, and further the model has been applied to the f.c.c. lattice.

Since there are four force constants in each of the models and only three elastic constants, we use the experimental values of the frequency of a longitudinal phonon at the zone boundary in the [100] direction. In terms of these four quantities, we obtain the values of the four inter-particle force constants.

After a brief introduction in Chapter I, the Born-von Kármán theory is discussed in Chapter II. In Chapter LII, the angular force model I is discussed and the secular equations for both b.c.c. and f.c.c. lattices are obtained, while in Chapter IV, we deal with the angular force model II.

The two models have been applied to obtain the dispersion curves, vibration spectra and Debye temperatures of copper, aluminum, nickel (f.c.c,) and sodium, tantalum, molybdenum, tungsten and iron (b.c.c.). The results are compared with the experimental values. These are presented in Chapter V and Chapter VI.

CHAPTER II

BORN-VON KÁRMÁN THEORY

In contrast to the continuum assumption of the Debye theory, in the Born-von Kármán theory [3], crystals are treated as a system of interacting particles. The essential features of the theory for a simple Bravais lattice are discussed below.

Consider a system of (N + 1) (finite) identical particles with no constraint imposed on them. These particles are vibrating about their own equilibrium positions which are located at the lattice points of a lattice representing the crystal formed by the (N + 1) particles. Each particle has a mass M. The system has 3(N + 1) degrees of freedom which are represented by 3(N + 1) independent coordinates, g_1, g_2 ..., $g_{3(N+1)}$. In lattice dynamic theory, we are interested in small oscillations of the particles about their equilibrium positions, denoted by g_{01}, ..., $g_{03(N+1)}$.

The deviations of the 3(N+1) coordinates from equilibrium are denoted by ε_i:

$$g_i = g_{oi} + \varepsilon_i \qquad (i = 1, \ldots, 3(N+1)) \tag{2.1}$$

As shown [27] Goldstein, the total potential energy, V, of the

system can be expanded in a Taylor series about the equilibrium.

$$V(g_1, \ldots, g_{3(N+1)}) = V(g_{01}, \ldots, g_{03(N+1)}) + \sum_{i=1}^{3(N+1)} \left(\frac{\partial V}{\partial g_i}\right)_o \varepsilon_i + 1/2 \sum_{i,j=1}^{3(N+1)} \left(\frac{\partial^2 V}{\partial g_i \partial g_j}\right)_o \varepsilon_i \varepsilon_j + S \qquad (2.2)$$

where S is a sum of infinite number of terms involving higher derivatives of V. $V(g_{01}, \ldots, g_{03(N+1)})$, being arbitrary, is chosen equal to 0. Moreover, $\left(\frac{\partial V}{\partial g_i}\right)_o = 0 \qquad (i = 1, \ldots, 3(N+1))$

Assuming that the temperature is low and the displacement of each particle is small in magnitude such that S is negligible in comparing with the sum

$$1/2 \sum_{i,j=1}^{3(N+1)} \left(\frac{\partial^2 V}{\partial g_i \partial g_j}\right)_o \varepsilon_i \varepsilon_j,$$

we have,

$$V = 1/2 \sum_{i,j=1}^{3(N+1)} \left(\frac{\partial^2 V}{\partial g_i \partial g_j}\right)_o \varepsilon_i \varepsilon_j$$

In terms of $\varepsilon_1, \ldots, \varepsilon_{3(N+1)}$ by making use of (2.1)

$$V = \frac{1}{2} \sum_{i,j=1}^{3(N+1)} \left(\frac{\partial^2 V}{\partial \varepsilon_i \partial \varepsilon_j}\right)_o \varepsilon_i \varepsilon_j \cdot \qquad (2.3)$$

Total kinetic energy of the system,

$$T = \frac{1}{2} M \sum_{i=1}^{3(N+1)} \dot{\epsilon}_i^2 \tag{2.4}$$

where $\dot{\epsilon}_i = \frac{d\epsilon_i}{dt}$

Lagrangian of the system,

$$L = T - V$$

$$= \frac{1}{2} M \sum_{i=1}^{3(N+1)} \dot{\epsilon}_i^2 - \frac{1}{2} \sum_{i,j=1}^{3(N+1)} \left(\frac{\partial^2 V}{\partial \epsilon_i \partial \epsilon_j}\right)_o \epsilon_i \epsilon_j \tag{2.5}$$

The Lagrange's equations are

$$M\ddot{\epsilon}_i + \sum_{j=1}^{3(N+1)} \left(\frac{\partial^2 V}{\partial \epsilon_i \partial \epsilon_j}\right)_o \epsilon_j = 0 \qquad (i=1, \ldots, 3(N+1)) \tag{2.6}$$

We use the cartesian coordinates

$x_o, y_o, z_o, \ldots, x_n, y_n, z_n$ as the 3(N+1) independent coordinates. With x_o, y_o, z_o, ..., x_n, y_n, z_n, representing the deviations of the particles from equilibrium, the Lagrange's equations (2.6) becomes

$$M\ddot{u}_m + \sum_{n=o}^{N} \left[\left(\frac{\partial^2 V}{\partial u_m \partial x_n} \right)_o x_n + \left(\frac{\partial^2 V}{\partial u_m \partial y_n} \right)_o y_n \right.$$

$$\left. + \left(\frac{\partial^2 V}{\partial u_m \partial z_n} \right)_o z_n \right] = 0$$

$$(u = x, y, z; \quad m = 0, \ldots, N) \tag{2.7}$$

In the following, we denote $\left(\frac{\partial^2 V}{\partial u_m \partial v_n} \right)_o$ by

$$V\begin{pmatrix} u & v \\ m & n \end{pmatrix} \qquad \begin{pmatrix} u = x, y, z; & v = x, y, z \\ m = 0, \ldots, N; & n = 0, \ldots, N \end{pmatrix},$$

and all the summations will be taken from 0 to N, unless otherwise stated. We have

$$V\begin{pmatrix} u & v \\ m & n \end{pmatrix} \equiv V\begin{pmatrix} v & u \\ n & m \end{pmatrix} \tag{2.8}$$

We use as a trial solution of (2.7), a plane wave function

$$\left.\begin{aligned} \vec{s} &= \vec{A}\, e^{i(\vec{q}.\vec{r}-\omega t)} \\ \text{or} \quad x &= A_1\, e^{i(\vec{q}.\vec{r}-\omega t)} \\ y &= A_2\, e^{i(\vec{q}.\vec{r}-\omega t)} \\ z &= A_3\, e^{i(\vec{q}.\vec{r}-\omega t)} \end{aligned}\right\} \tag{2.9}$$

By substitution of (2.9) into (2.7), we obtain a set of 3(N+1) equations:

$$\left.\begin{aligned} -\omega^2 M A_1 + A_1 \sum_n V\,(^{x\ x}_{m\ n})\, e^{i\vec{q}.(\vec{R}_n - \vec{R}_m)} \\ + A_2 \sum_n V\,(^{x\ y}_{m\ n})\, e^{i\vec{q}.(\vec{R}_n - \vec{R}_m)} \\ + A_3 \sum_n V\,(^{x\ z}_{m\ n})\, e^{i\vec{q}.(\vec{R}_n - \vec{R}_m)} = 0 \end{aligned}\right\} \quad (2.10)$$

and two similar equations for y and z for each value of m. Moreover, m takes all the values from 0 to N ($\vec{R}_n$ is the equilibrium position of the particle n).

In order to have nontrivial solutions of A_1, A_2 and A_3, for each m, the determinant

$$\begin{vmatrix} \sum_n V(^{x\ x}_{m\ n})\, e^{i\vec{q}.(\vec{R}_n - \vec{R}_m)} - \omega^2 M & \sum_n V(^{x\ y}_{m\ n})\, e^{i\vec{q}.(\vec{R}_n - \vec{R}_m)} & \sum_n V(^{x\ z}_{m\ n})\, e^{i\vec{q}.(\vec{R}_n - \vec{R}_m)} \\ \sum_n V(^{y\ x}_{m\ n})\, e^{i\vec{q}.(\vec{R}_n - \vec{R}_m)} & \cdots & \\ \sum_n V(^{z\ x}_{m\ n})\, e^{i\vec{q}.(\vec{R}_n - \vec{R}_m)} & \cdots & \sum_n V(^{z\ z}_{m\ n})\, e^{i\vec{q}.(\vec{R}_n - \vec{R}_m)} - \omega^2 M \end{vmatrix} = 0 \quad (2.11)$$

(m runs from 0 to N)

Because the interatomic force in a crystal are essentially short range in comparison with the dimensions of the crystal, $V\binom{u\ v}{m\ n}$ will be negligible for distant neighbours of a particle. Since, in general, N is very large (e.g. of the order of 10^{23}), for most particles which are located inside the crystal, their environment will be identical. For these particles, $\sum_n V\binom{x\ x}{m\ n}$ for different values of m will be identical. This is also true for other values of $\sum_n V\binom{u\ v}{m\ n}$ $(u = x,y,z;\ v = x,y,z)$. Therefore, these particles will have the same equation (2.11). For those particles located near the surface of the crystal, they will have equation (2.11) different from those of the particles located well inside the specimen.. Since these particles are small in number in comparison with the number of particles located well inside the specimen (it varies as $6N^{2/3}/N$, i.e. $N^{-1/3}$ and is of the order of 0 when N is of the order of 10^{23}), we shall disregard their special equations. Therefore, we can assume that for all the N particles, we have the same equation (2.11) and, hence, the same ω, $\vec{k}$ relationship and the same ratios of A_1, A_2 and A_3 for each value of $\vec{k}$. This justifies the choice of the plane wave function (2.9) as a solution of all the 3(N+1) equations in (2.7).

We take the origin of our coordinate system on a lattice point located well inside the crystal. The particle whose equilibrium position is at this lattice point is called the particle 0. The equation obtained by putting m = 0, $\vec{R}_m = 0$ into (2.11) is the secular equation of the crystal,

$$\begin{vmatrix} \sum_n V\binom{x\ x}{o\ n} e^{i\vec{q}.\vec{R}_n} - \omega^2 M & \sum_n V\binom{x\ y}{o\ n} e^{i\vec{q}.\vec{R}_n} & \sum_n V\binom{x\ z}{o\ n} e^{i\vec{q}.\vec{R}_n} \\ \sum_n V\binom{y\ x}{o\ n} e^{i\vec{q}.\vec{R}_n} & \sum_n V\binom{y\ y}{o\ n} e^{i\vec{q}.\vec{R}_n} - \omega^2 M & \sum_n V\binom{y\ z}{o\ n} e^{i\vec{q}.\vec{R}_n} \\ \sum_n V\binom{z\ x}{o\ n} e^{i\vec{q}.\vec{R}_n} & \sum_n V\binom{z\ y}{o\ n} e^{i\vec{q}.\vec{R}_n} & \sum_n V\binom{z\ z}{o\ n} e^{i\vec{q}.\vec{R}_n} - \omega^2 M \end{vmatrix} = 0$$

(u = x, y, z; v = x, y, z; includes n = 0) (2.12)

$$\text{i.e.} \left| \sum_n V\binom{u\ v}{o\ n} e^{i\vec{q}.\vec{R}_n} - \omega^2 M \delta_{uv} \right| = 0$$

(u = x, y, z; v = x, y, z;

$$\delta_{uv} = \begin{cases} 1 & u = v \\ 0 & u \neq v \end{cases}) \qquad (2.13)$$

If we put $\vec{q} = 2\pi\vec{k}$, $\omega = 2\pi\nu$ into (2.13), it becomes

$$\left| \sum_{n} V\begin{pmatrix} u & v \\ o & n \end{pmatrix} e^{i2\pi\vec{k}.\vec{R}_n} - 4\pi^2\nu^2 M\delta_{uv} \right| = 0$$

$$(u = x, y, z; \quad v = x, y, z) \tag{2.14}$$

All distinct physical motions of the lattice represented by (2.9) are taken into account when the values of $\vec{k}$ are restricted to one reciprocal lattice cell (Born & Huang [11], p. 68 to 70).

The usual periodic boundary condition is imposed on the solutions (2.9) to give the normal modes of vibration of the crystal. $\vec{k}$ is restricted to some discrete values. The total number of vibrational modes, with $\vec{k}$ restricted to a reciprocal lattice cell, is exactly 3(N+1) which is equal to the total number of degrees of freedom in this system of (N+1) particles. Hence, plane waves with distinct wave vectors $\vec{k}$ in the same reciprocal cell and satisfying the periodic boundary condition, do correspond to distinct normal modes of vibration. Also, an artificial maximum frequency such as that introduced by Debye, is not required. (See, e.g. Born & Huang [11], p. 45, 46, 70)

Remark 2.1 - Essentially, we are interested in particles located well inside the crystal. For these particles (e.g. particles n_1, n_2, n_3 and n_4), because of symmetry of the lattice, the determinant in (2.13) is symmetrical and we have

$$V\binom{u\ v}{n_1 n_2} = V\binom{u\ v}{n_3 n_4} \text{ if } \vec{R}_{n_1} - \vec{R}_{n_2} = \pm(\vec{R}_{n_3} - \vec{R}_{n_4}) \tag{2.15}$$

i.e., $V\binom{u\ v}{m\ n}$ depends on the separation of the lattice points only.

In particular,

$$\left.\begin{aligned} V\binom{u\ v}{o\ n_1} &= V\binom{u\ v}{o\ n_2} \\ = V\binom{v\ u}{n_1 o} &= V\binom{v\ u}{n_2 o} \end{aligned}\right\} \text{ if } \vec{R}_{n_1} = -\vec{R}_{n_2} \tag{2.16}$$

In order to emphasize the fact expressed by equation (2.15), some authors prefer to use the notation $V\binom{u\ \ v}{m\ -n}$ or $V\binom{u\ \ v}{\vec{m}\ -\vec{n}}$ (see, e.g., Born & Huang [11], equation (6.12) or Smith [28], equation (21)). Because in what follows, we need only use $V\binom{u\ v}{o\ n}$, we prefer to stick to the notation $V\binom{u\ v}{m\ n}$.

Moreover, it has been shown by Smith [28] (p. 213 to 215) that:

$$\text{(i)} \sum_n V\binom{u\ v}{o\ n} = \sum_n V\binom{v\ u}{n\ o} = 0$$

$$(u = x, y, z;\ v = x, y, z) \tag{2.17}$$

$$\text{i.e. } V\binom{v\ u}{o\ o} = -\sum_{n=1}^{N} V\binom{v\ u}{n\ o}$$

$$(u = x, y, z;\ v = x, y, z) \tag{2.18}$$

(ii) when $q \to 0$, $\omega \to 0$

(iii) ω^2 is an even function of $\vec{q}$.

Remark 2.2 - For a given value of $\vec{q}$, equation (2.12) will have six roots of ω. Out of these six roots, only those real roots do correspond to physical wave motion, and need to be considered.

Actually, in (2,9), only the real components of $\vec{s}$ are considered as representing physical motion, i.e.,

$$\vec{s}\,(\text{real}) = \vec{A} \cos (\vec{q}.\vec{r}-\omega t) \tag{2.19}$$

Since ω^2 is an even function of $\vec{q}$ and if ω_1 and $-\omega_1$ are two real roots for a given wave vector $\vec{q}_o$, they will also be two real roots of $-\vec{q}_o$. But the wave

$$\vec{s}\,(\text{real}) = \vec{A} \cos (\vec{q}_o.\vec{r}-(-\omega t_1)t)$$

$$= \vec{A} \cos ((-\vec{q}_o).\vec{r}-\omega_1 t)$$

is actually the same as the wave with $\vec{q} = -\vec{q}_o$, $\omega = \omega_1$. Similarly, the wave with $\vec{q} = -\vec{q}_o$, $\omega = -\omega_1$ and the wave with $\vec{q} = \vec{q}_o$, $\omega = \omega_1$ are the same wave. Therefore, for equation (2.12), we need only consider the positive roots of ω.

CHAPTER III

ANGULAR FORCE MODEL I - DE LAUNAY

This model consists of a cubic lattice with a central force and an angular force interaction between a particle and each of its first and second neighbours. This angular force interaction is of the type discussed in de Launay's article [12], p. 248. The effects of the more distant neighbours are neglected.

We locate the origin of our cartesian coordinate system on a lattice point situated well inside the crystal. The particle vibrating about this lattice point is called particle 0.

In what follows, since we are dealing with b.c.c. and f.c.c. lattices, we denote the positions of a lattice point by

$$\vec{R}_{on} = \vec{R}_n = \frac{a}{2}\vec{N}_n \tag{3.1}$$

where "a" is the length of one side of the cube.

In this notation, (2.14) becomes

$$\left| \sum_n V\binom{u\ v}{o\ n} e^{i\vec{p}\cdot\vec{N}_n} - 4\pi^2\nu^2 M\delta_{uv} \right| = 0 \tag{3.2}$$

where

$$\vec{p} = \pi\vec{ak};$$

$$u = x, y, z; \quad v = x, y, z$$

We shall discuss the general properties of the central force interaction and the angular force interaction before we deal with specific lattices.

(a) Central force interaction -

Let the force constant representing the central force between the particle m and the particle n be α_{mn}.

The potential energy of the system of (N+1) particles due to central forces,

$$V_\alpha = \frac{1}{2} \sum_{\substack{m=0 \\ m \neq n}}^{N} \sum_{n=0}^{N} \left[\frac{1}{2} \alpha_{mn} (r_{mn} - R_{mn})^2 \right] \tag{3.4}$$

where

$$\begin{aligned} R_{mn} &= \left|\vec{R}_{mn}\right| \\ \vec{R}_{mn} &= (X_n - X_m)\vec{i} + (Y_n - Y_m)\vec{j} + (Z_n - Z_m)\vec{k} \\ &= \frac{a}{2}\vec{N}_{mn} \end{aligned} \tag{3.5}$$

is the equilibrium position of the particle n referring to that of the particle m

$$r_{mn}^2 = (X_n + x_n - X_m - x_n)^2 + (Y_n + y_n - Y_m - y_m)^2 + (Z_n + z_n - Z_m - z_m)^2 \tag{3.6}$$

For $n \neq 0$,

$$\left(\frac{\partial^2 V_\alpha}{\partial y_n \partial x_o}\right)_o = V_\alpha \begin{pmatrix} y & x \\ n & o \end{pmatrix} = -\alpha_{on} \frac{Y_n X_n}{R_{on}^2} = -\frac{\alpha_{on}}{N_n^2} (\vec{j}.\vec{N}_n)(\vec{i}.\vec{N}_n) . \qquad (3.7)$$

where $\vec{N}_n$ is defined in (3.1) and $N_n = |\vec{N}_n|$.

$$V \begin{pmatrix} y & x \\ o & o \end{pmatrix} = \sum_{n=1}^{N} \alpha_{on} \frac{Y_n X_n}{R_{on}^2}$$

$$= -\sum_{n=1}^{N} V \begin{pmatrix} y & x \\ n & o \end{pmatrix} \qquad (3.8)$$

and (2.17) is verified.

Similarly for $n \neq o$,

$$V_\alpha \begin{pmatrix} x & x \\ n & o \end{pmatrix} = -\alpha_{on} \frac{X_n^2}{R_{on}^2}$$

$$= -\alpha_{on} \frac{(\vec{i}.\vec{N}_n)^2}{N_n^2} . \qquad (3.9)$$

$$V_\alpha\begin{pmatrix} x & x \\ o & o \end{pmatrix} = \sum_{n=1}^{N} \alpha_{on} \frac{x_n^2}{R_{on}^2}$$

$$= -\sum_{n=1}^{N} V_\alpha\begin{pmatrix} x & x \\ n & o \end{pmatrix} \qquad (3.10)$$

and (2.17) is verified.

(b) Angular force interaction (the type discussed in de Launay's article [12]) –

We denote the angular force constant representing the angular force interaction between the particle m and the particle n by σ_{mn}. From de Launay's article [12], p. 249, the displacement which is effective for the angular force constant σ_{mn} due to displacements $\vec{s}_n$ and $\vec{s}_n$ of the particle m and particle n respectively, $= \vec{\zeta}_n \times (\vec{s}_n - \vec{s}_m)$ where, $\vec{\zeta}_{mn} = \frac{\vec{N}_{mn}}{|\vec{N}_{mn}|}$ is the unit vector from the particle m to the particle n. (N_{mn} is defined in (3.5)

$$\vec{s}_n = x_n\vec{i} + y_n\vec{j} + z_n\vec{k}$$

The change in potential energy due to $\vec{s}_m$ and $\vec{s}_n$,

$$V_{\sigma_{mn}} = \frac{1}{2} \sigma_{mn} [\vec{\zeta}_{mn} \times (\vec{s}_n - \vec{s}_m)]^2 \qquad (3.11)$$

Let V_σ be the change of the total potential energy (angular force portion) due to displacements of all the (N+1) particles. We have, for $n \neq 0$,

$$V_\sigma\begin{pmatrix} y & x \\ n & o \end{pmatrix} = \sigma_{on} [\vec{\zeta}_n \times \vec{j}].[\vec{\zeta}_n \times (-\vec{i})] \tag{3.12}$$

$$= \frac{\sigma_{on}}{N_n^2} (\vec{j}.\vec{N}_n) (\vec{i}.\vec{N}_n) \tag{3.13}$$

where $\vec{N}_n$ is defined in (3.1) and $N_n = |\vec{N}_n|$.

$$V_\sigma\begin{pmatrix} y & x \\ o & o \end{pmatrix} = \sum_{n=1}^{N} \sigma_{on} [\vec{\zeta}_n x (-\vec{j})].[\vec{\zeta}_n \times (-\vec{i})] \tag{3.14}$$

$$= - \sum_{n=1}^{N} V_\sigma\begin{pmatrix} y & x \\ n & o \end{pmatrix} \tag{3.15}$$

and (2.17) is verified.

Similarly, for $n \neq 0$,

$$V_\sigma\begin{pmatrix} x & x \\ n & o \end{pmatrix} = \sigma_{on} [\frac{(\vec{i}.\vec{N}_n)^2}{N_n^2} - 1] \tag{3.16}$$

$$V_\sigma\begin{pmatrix} x & x \\ o & o \end{pmatrix} = - \sum_{n=1}^{N} V_\sigma\begin{pmatrix} x & x \\ n & o \end{pmatrix} \tag{3.17}$$

and (2.17) is verified.

(1) Body-centered Cubic Lattice -

(See Fig. 4-2)

The central force constant between a particle and each of its first neighbours is denoted by α_1, while that between it and each of its second neighbours is denoted by α_2.

The angular force constant between a particle and each of its first neighbours is denoted by η_1, while that between it and each of its second neighbours is denoted by η_2.

The force equations required are given in de Launay's article [12], (equation (7.7)). We can obtain the secular equation by means of equation (3.2). But, for the purpose of illustration, we start from the first principles, following the approach used by de Launay.

The first neighbours of particle 0 are labelled 1, 2, ..., 8, and its second neighbours 9, 10, ..., 14. (Fig. 4-2).

With the displacement of the particle n denoted by $\bar{s}_n$, the equation of motion for the particle 0 are:

$$M\ddot{x}_o = \left\{ -(8\eta_1+6\eta_2)x_o + \eta_1 \sum_{i=1}^{8} x_i + \eta_2 \sum_{i=9}^{14} x_i \right.$$

$$\left. - \frac{\alpha_1-\eta_1}{3} \left(8x_o - \sum_{i=1}^{8} x_i - \sum_{i=1}^{4} y_i + \sum_{i=5}^{8} y_i \right. \right. .$$

$$
\left.
\begin{aligned}
&- z_1 - z_2 \\
&+ z_3 + z_4 - z_5 - z_6 + z_7 + z_8) \\
&-(\alpha_2 - \eta_2)\,(2x_o - x_9 - x_{10})\Big\}
\end{aligned}
\right| \qquad (3.18)
$$

and two similar equations for y and z. By substituting the plane wave solution (2.9) into (3.18) and with $\vec{q} = 2\pi\vec{k}$, $\varkappa = 2\pi\nu$, we obtain

$$
\left.
\begin{aligned}
&\left\{ \frac{8}{3}(\alpha_1+2\eta_1)(1-C_1C_2C_3) + 4\alpha_2 S_1^2 + 4\eta_2 (S_2^2+S_3^2) \right. \\
&\quad -4\pi^2\nu^2 M \Big\} A_1 + \left\{ \frac{8}{3}(\alpha_1-\eta_1) S_1S_2C_3 \right\} A_2 \\
&\qquad + \left\{ \frac{8}{3}(\alpha_1-\eta_1) S_1C_2S_3 \right\} A_3 = 0
\end{aligned}
\right\} \qquad (3.19)
$$

and two corresponding equations for y and z

where $C_j = \pi a k_j$

$S_j = \sin \pi a k_j$

k_1, k_2 and k_3 are the components of $\vec{k}$ in cartesian coordinates.

These lead to the secular equation

$$
\begin{vmatrix}
G_1 - 4\pi^2\nu^2 M & H_{12} & H_{13} \\
H_{21} & G_2 - 4\pi^2\nu^2 M & H_{23} \\
H_{31} & H_{32} & G_3 - 4\pi^2\nu^2 M
\end{vmatrix} = 0 \qquad (3.20)
$$

where

$$G_1 = \frac{8}{3}(\alpha_1 + 2\eta_1)(1-C_1C_2C_3) + 4\alpha_2 S_1^2 + 4\eta_2(S_2^2+S_3^2)$$

$$H_{12} = \frac{8}{3}(\alpha_1-\eta_1) S_1S_2C_3$$

and the others can be obtained by circular permutations of the indices. In the long-wave limit as $k \to 0$, the secular equation becomes

$$\begin{vmatrix} I_1-4\pi^2\nu^2M & J_{12} & J_{13} \\ J_{21} & I_2-4\pi^2\nu^2M & J_{23} \\ J_{31} & J_{32} & I_3-4\pi^2\nu^2M \end{vmatrix} = 0 \qquad (3.21)$$

where

$$I_i = \frac{2}{a}(\alpha_2-\eta_2)k_i^2 + \frac{2}{a}\left(\frac{\alpha_1+2\eta_1}{3} + \eta_2\right)k^2 - \rho\nu^2$$

$$J_{ij} = \frac{4}{3a}(\alpha_1 - \eta_1)k_ik_j$$

$$\rho = \frac{2M}{a^3} \quad \text{(density of the crystal)}$$

This should be identical with the elacticity secular equation (de Launay [12]: Equation (10.9))

$$\begin{vmatrix} (c_{11}-c_{44})k_1^2 + c_{44}k^2 - \rho v^2 & (c_{12}+c_{44})k_1k_2 & (c_{12}+c_{44})k_1k_3 \\ (c_{12}+c_{44})k_1k_2 & (c_{11}-c_{44})k_2^2 + C_{44}k^2 - \rho v^2 & (c_{12}+c_{44})k_2k_3 \\ (c_{12}+c_{44})k_1k_3 & (c_{12}+c_{44})k_2k_3 & (c_{11}-c_{44})k_3^2 + c_{44}k^2 - \rho v^2 \end{vmatrix} = 0 \tag{3.22}$$

By comparing (3.21) and (3.22), we have the identities,

$$2\left(\frac{\alpha_1 + 2\eta_1}{3} + \eta_2\right) = a c_{44} \tag{3.23}$$

$$2(\alpha_2 - \eta_2) = ac_{11} - ac_{44} \tag{3.24}$$

$$\frac{4}{3}(\alpha_1 - \eta_1) = ac_{12} + ac_{44} \tag{3.25}$$

In the [100] direction, the phonon frequency (longitudinal) at the first Brillouin zone boundary (i.e. $k_1 = 1/a$) is given by

$$\nu_b = \frac{2}{\pi}\left[\frac{1}{3M}(\alpha_1 + 2\eta_1)\right]^{1/2} \tag{3.26}$$

From equations (3.23) to (3.26),

$$\alpha_1 = \frac{1}{2} a(c_{12} + c_{44}) + \frac{1}{4}\pi^2 \nu_b{}^2 M \tag{3.27}$$

$$\alpha_2 = \frac{1}{2} ac_{11} - \frac{1}{4}\pi^2 \nu_b{}^2 M \tag{3.28}$$

$$\eta_1 = -\frac{1}{4} a(c_{12} + c_{44}) + \frac{1}{4}\pi^2 \nu_b{}^2 M \tag{3.29}$$

$$\eta_2 = \frac{1}{2} ac_{44} - \frac{1}{4}\pi^2 \nu_b{}^2 M \tag{3.30}$$

Bu substituting (3.27), (3.28), (3.29) and (3.30) into (3.20), we obtain

a secular equation

$$\begin{vmatrix} G_1-4\pi^2\nu^2M & H_{12} & H_{13} \\ H_{21} & G_2-4\pi^2\nu^2M & H_{23} \\ H_{31} & H_{32} & G_3-4\pi^2\nu^2M \end{vmatrix} = 0 \qquad (3.31)$$

where $G_1 = 2\pi^2\nu_b^2M\,(1-C_1C_2C_3) + (2a\,c_{11}-\pi^2\nu_b^2M)S_1^2 + (2a\,c_{44}-\pi^2\nu_b^2M)\,(S_2^2+S_3^2)$

$$H_{12} = 2a\,(c_{12} + c_{44})\,S_1S_2C_3$$

and the others can be obtained by circular permutations of the indices.

(2) Face-centered Cubic Lattice -

(See Fig. 4-3)

The central force constant between a particle and each of its first neighbours is denoted by α_1, while that between it and each of its second neighbours is denoted by α_2.

The angular force constant between a particle and each of its first neighbours is denoted by σ_1, while that between it and each of its second neighbours is denoted by σ_2.

As a matter of illustration, in obtaining the secular equation

for this kind of lattice, we use equation (3.2). Since we only need to use terms of $\left(\frac{\partial^2 V}{\partial u_o \partial v_n}\right)_o$, we can treat the potential energy due to the central force and angular force interactions separately.

(a) Central force (α_1, α_2) interaction -

From (3.7) and (2.16), we have

$$V_\alpha \begin{pmatrix} y & x \\ n & o \end{pmatrix} = \begin{cases} 0 & (n=1, 2, 3, 4) \quad (3.32) \\ -\frac{\alpha_1}{2} & (n=5, 6) \quad (3.33) \\ \frac{\alpha_1}{2} & (n=7, 8) \quad (3.34) \\ 0 & (n=9, 10, 11, 12) \quad (3.35) \\ 0 & (n=13, 14, \ldots, 18) \quad (3.36) \end{cases}$$

From (3. 8)

$$V_\alpha \begin{pmatrix} y & x \\ o & o \end{pmatrix} = 0 \qquad (3.37)$$

Since from (2.8),

$$V \begin{pmatrix} u & v \\ m & n \end{pmatrix} \equiv V \begin{pmatrix} v & u \\ n & m \end{pmatrix},$$

we have

$$\sum_n V_\alpha \begin{pmatrix} x & y \\ o & n \end{pmatrix} e^{i\vec{p}.\vec{N}_n} = 2\alpha_1 S_1 S_2 \tag{3.38}$$

where S_1, S_2 are defined in (3.19). Similarly from (3.9), (2.16) and (3.10),

$$V_\alpha \begin{pmatrix} x & x \\ n & o \end{pmatrix} = \begin{cases} -\frac{1}{2}\alpha_1 & (n=1, 2, \ldots, 8) \quad (3.39) \\ 0 & (n=9, 10, 11, 12) \quad (3.40) \\ -\alpha_2 & (n=13, 14) \quad (3.41) \\ 0 & (n=15, 16, 17, 18) \quad (3.42) \\ 4\alpha_1 + 2\alpha_2 & (n=0) \quad (3.43) \end{cases}$$

Making use of (2.8) and (3.39) to (3.43), we have

$$\sum_n V_\alpha \begin{pmatrix} x & x \\ o & n \end{pmatrix} e^{i\vec{p}.\vec{N}_n} = 4\alpha_1 - 2\alpha_1 C_1 (C_2+C_3) + 4\alpha_2 S_1^2 \tag{3.44}$$

where C_i, S_i are defined in (3.19).

Equations (3.38) and (3.44) have also been obtained by de Launay ([12], equation (11.6)).

(b) Angular force (σ_1, σ_2) interaction -

Since (3.13) can be obtained from (3.7) by replacing σ_{on} with

$-\sigma_{on}$, the result obtained for the central forces, namely, equation (3.38), can be used to obtain the corresponding result for the angular forces. Therefore,

$$\sum_n V_\sigma\binom{x\ y}{o\ n}\, e^{i\vec{p}.\vec{N}_n} = -2\sigma_1 S_1 S_2 \tag{3.45}$$

From (3.16), (2.16) and (3.17),

$$V_\sigma\binom{x\ x}{n\ o} = \begin{cases} -\frac{1}{2}\sigma_1 & (n=1, 2, \ldots, 8) \quad (3.46) \\ -\sigma_1 & (n=9, 10, 11, 12) \quad (3.47) \\ 0 & (n=13, 14) \quad (3.48) \\ -\sigma_2 & (n=15, 16, 17, 18) \quad (3.49) \\ 8\sigma_1 + 4\sigma_2 & (n=0) \quad (3.50) \end{cases}$$

Making use of (2.8) and (3.46) to (3.50), we have

$$\sum_n V_\sigma\binom{x\ x}{o\ n}\, e^{i\vec{p}.\vec{N}_n}$$

$$= 8\sigma_1 - 2\sigma_1 C_1(C_2+C_3) - 4\sigma_1 C_2C_3 + 4\sigma_2 (S_2^2+S_3^2) \ . \tag{3.51}$$

Combination of α_1, α_2, σ_1, σ_2 -

After substitution of (3.38), (3.44), (3.45) and (3.51) into (3.2), we have a secular equation

$$\begin{vmatrix} K_1 - 4\pi^2\nu^2 M & L_{12} & L_{13} \\ L_{21} & K_2 - 4\pi^2\nu^2 M & L_{23} \\ L_{31} & L_{32} & K_3 - 4\pi^2\nu^2 M \end{vmatrix} = 0 \qquad (3.52)$$

where

$$K_1 = 4\alpha_1 + 8\sigma_1 - 2(\alpha_1+\sigma_1)\, C_1\,(C_2+C_3) - 4\sigma_1\, C_2C_3 + 4\alpha_2\, S_1^2 + 4\sigma_2\,(S_2^2+S_3^2)$$

$$L_{12} = 2(\alpha_1 - \sigma_1)\, S_1\, S_2$$

and the remainder can be obtained by circular permutations of the indices.

In the long-wave limit as $k \to 0$, with $\rho = 4M/a^3$, the secular equation obtained should be identical with the elasticity secular equation (3.22). Therefore, by comparison, we have

$$2\alpha_1 - 2\sigma_1 = a\, c_{12} + a\, c_{44} \qquad (3.53)$$

$$\alpha_1 + 4\alpha_2 - \sigma_1 - 4\sigma_2 = a\, c_{11} - a\, c_{44} \qquad (3.54)$$

$$\alpha_1 + 3\sigma_1 + 4\sigma_2 = a\, c_{44} \qquad (3.55)$$

(longitudinal)

In the [100] direction, the phonon frequency/at the first Brillouin

zone boundary (i.e., $k_1 = 1/a$) is given by

$$\nu_b = \frac{1}{\pi}\left[\frac{2}{M}(\alpha_1 + \sigma_1)\right]^{1/2} \tag{3.56}$$

From (3.53) to (3.56), we have

$$\alpha_1 = \frac{1}{4} a (c_{12}+c_{44}) + \frac{1}{4}\pi^2\nu_b{}^2 M \tag{3.57}$$

$$\alpha_2 = \frac{1}{4} a c_{11} - \frac{1}{4}\pi^2\nu_b{}^2 M \tag{3.58}$$

$$\sigma_1 = -\frac{1}{4} a (c_{12}+c_{44}) + \frac{1}{4}\pi^2\nu_b{}^2 M \tag{3.59}$$

$$\sigma_2 = \frac{1}{8} a (c_{12} + 3 c_{44}) - \frac{1}{4}\pi^2\nu_b{}^2 M \tag{3.60}$$

By substituting (3.57), (3.58), (3.59) and (3.60) into (3.52), we obtain a secular equation

$$\begin{vmatrix} K_1 - 4\pi^2\nu^2 M & L_{12} & L_{13} \\ L_{21} & K_2 - 4\pi^2\nu^2 M & L_{23} \\ L_{31} & L_{32} & K_3 - 4\pi^2\nu^2 M \end{vmatrix} = 0 \tag{3.61}$$

where $K_1 = -a (c_{12} + c_{44}) + 3\pi^2\nu_b{}^2 M$

$$-\pi^2\nu_b{}^2 M C_1 (C_2+C_3)$$

$$+ (a c_{12} + a c_{44} - \pi^2 \nu_b{}^2 M)\, C_2 C_3$$

$$+ (a c_{11} - \pi^2 \nu_b{}^2 M)\, S_1{}^2$$

$$+ \left(\frac{1}{2} a c_{12} + \frac{3}{2} a c_{44} - \pi^2 \nu_b{}^2 M\right) (S_2{}^2 + S_3{}^2)$$

$$L_{12} = a (c_{12} + c_{44})\, S_1 S_2$$

and the others can be obtained by circular permutations of the indices.

CHAPTER IV

ANGULAR FORCE MODEL II

This model consists of central force between a particle and each of its first and second neighbours, as well as angular forces which depend on the changes of angles in the triangles formed by the particle and its first and second neighbours. This type of angular force has been used by Gazis et al. [24] and Clark et al. [23]. The effects of the more distant neighbours are neglected.

In what follows, the general properties of the central forces and the angular forces are discussed before dealing with specific lattices.

(a) Central force interaction -

This is the same as that used in the angular force model I. The properties of these forces are discussed in Chapter III.

(b) Angular force interaction -

There are two types of triangles in which we are interested. One is formed by a particle and two of its first neighbours, called type (1) triangles. The other is formed by a particle, one of its first neighbours and one of its second neighbours, called type (2) triangles. (A more detailed discussion of this point will be given when we deal with

specific lattices).

The changes in the angles of a triangle are obtained by comparing the triangle of the equilibrium positions of these particles with the projection of the triangle of these particles, onto the plane of their equilibrium positions.

Consider the triangle formed by three particles a, b and c (Fig. 4-1). Let A, B and C denote their equilibrium positions; $\vec{s}_a$, $\vec{s}_b$ and $\vec{s}_c$ denote their small displacements.

$\vec{n}_{A,B,C}$ is defined as a unit vector which is in the plane A, B, C and normal to the vector $\vec{R}_{A,B}$. We are dealing with the angle Θ_A at A. The convention for the direction of $\vec{n}_{A,B,C}$ is that, when $\vec{n}_{A,B,C}$ is applied to the particle B, it reduces the angle Θ_A. (From definition

$$\vec{n}_{A,B,C} \equiv \vec{n}_{B,A,C}) \qquad (4.1)$$

$\vec{R}_{A,B}$ is the position vector of B relative to A and $R_{A,B} = |\vec{R}_{A,B}|$. $\vec{w}$ denotes a unit vector normal to the plane A,B,C in a direction such that $\vec{R}_{A,C}$, $\vec{R}_{A,B}$ and $\vec{w}$ form a right-handed system. The projection of the displacement $\vec{s}_b$ on the plane A,B,C,

$$\vec{s}_{bp} = (\vec{w} \times \vec{s}_b) \times \vec{w}$$

Since the displacement $\vec{s}_b$ is small in magnitude, the effective change in the angle Θ_A (as far as the angular force is concerned) due to $\vec{s}_b$

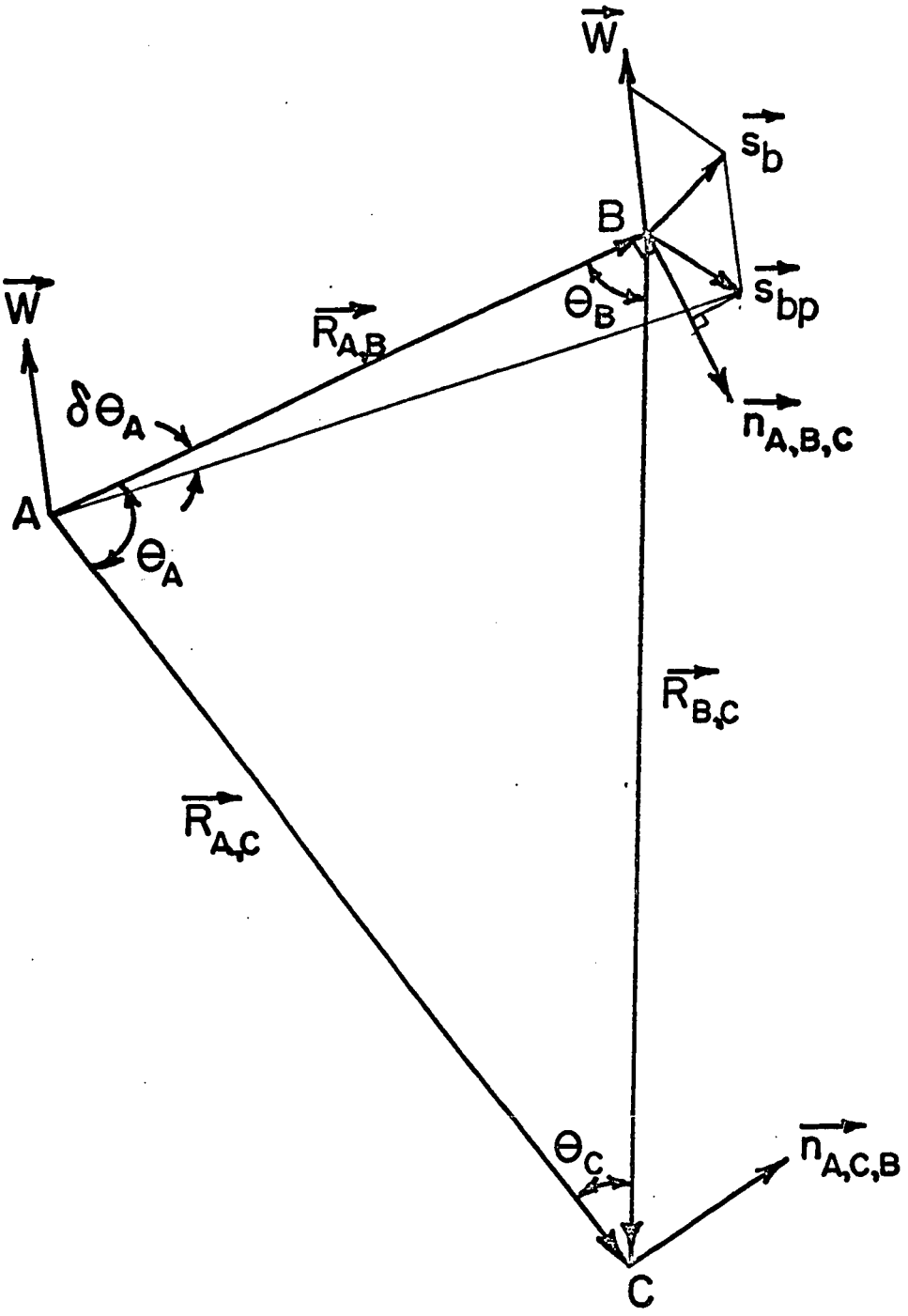

Fig. 4-1. Angular Force.

$$= - \frac{\vec{s}_{bp} \cdot \vec{n}_{A,B,C}}{R_{A,B}}$$

$$= - \frac{\vec{s}_{b} \cdot \vec{n}_{A,B,C}}{R_{A,B}} \qquad (4.2)$$

The change in the angle Θ_A due to the displacements $\vec{s}_a$, $\vec{s}_b$ and $\vec{s}_c$,

$$\delta\Theta_A = \frac{(\vec{s}_a - \vec{s}_b) \cdot \vec{n}_{A,B,C}}{R_{A,B}} + \frac{(\vec{s}_a - \vec{s}_c) \cdot \vec{n}_{A,C,B}}{R_{A,C}} \qquad (4.3)$$

Similarly, $\delta\Theta_B$ and $\delta\Theta_C$ can be obtained. The change in the potential energy due to $\delta\Theta_A$, $\delta\Theta_B$ and $\delta\Theta_C$,

$$= \frac{1}{2} \gamma_A (\delta\Theta_A)^2 + \frac{1}{2} \gamma_B (\delta\theta_B)^2 + \frac{1}{2} \gamma_C (\delta\theta_C)^2 \qquad (4.4)$$

where γ_A, γ_B and γ_C are the angular force constants associated with the angles θ_A, θ_B and θ_C respectively.

(1) Body-centered Cubic Lattice

(See Fig. 4-2)

Clark et al. [23] have obtained the secular equation for the angular force model II for the b.c.c. lattice from first principles. In this paper, we obtain the same secular equation (equation (4.51)) by means of equation (3.2)

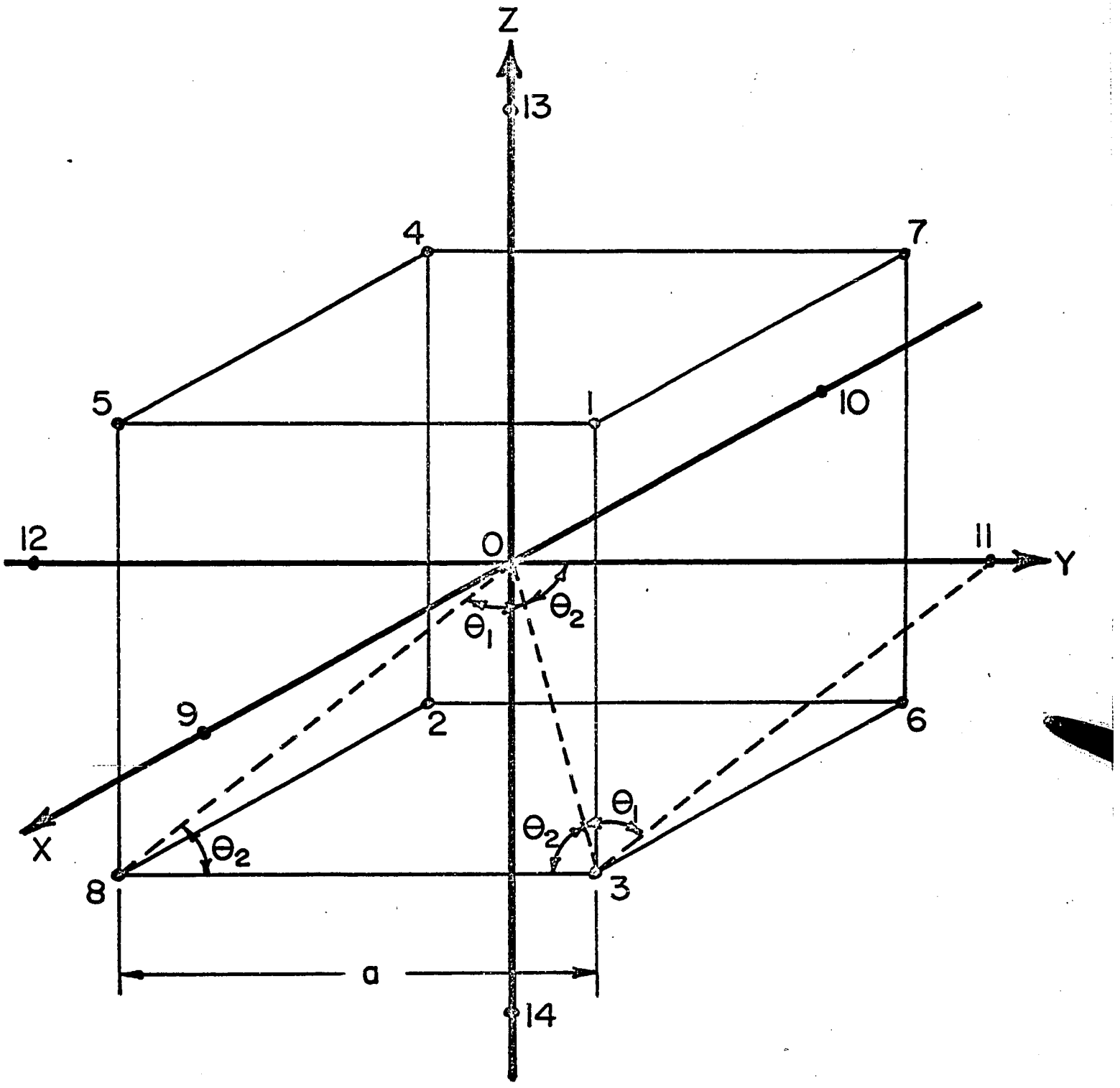

Fig. 4-2. The first and second neighbours of the particle O of the b.c.c. lattice.

Since we only need to use terms of $\left(\frac{\partial^2 V}{\partial u_o \partial v_n}\right)_o$, we can treat the potential energy due to the central force interaction and the angular force interaction separately.

(a) Central force (α_1, α_2) interaction -

The central force constant between a particle and each of its first neighbours is denoted by α_1, while that between it and each of its second neighbours is denoted by α_2. From (3.7), (2.16), (3.8) and (2.8), we have

$$V_\alpha \begin{pmatrix} y & x \\ n & o \end{pmatrix} = \begin{cases} -\frac{\alpha_1}{3} & (n=1, 2, 3, 4) \quad (4.5) \\ \frac{\alpha_1}{3} & (n=5, 6, 7, 8) \quad (4.6) \\ 0 & (n=9, 10, \ldots, 14) \quad (4.7) \\ 0 & (n=0) \quad (4.8) \end{cases}$$

and

$$\sum_n V_\alpha \begin{pmatrix} x & y \\ o & n \end{pmatrix} e^{i\vec{p}.\vec{N}_n}$$

$$= \frac{8\alpha_1}{3} S_1 S_2 C_3 \quad (4.9)$$

where S_i, C_i are defined in (3.19). Similarly, from (3.9), (2.16), (3.10) and (2.8), we have

$$V_\alpha\begin{pmatrix} x & x \\ n & o \end{pmatrix} = \begin{cases} -\frac{\alpha_1}{3} & (n=1, 2, \ldots, 8) \quad (4.10) \\ -\alpha_2 & (n=9, 10) \quad (4.11) \\ 0 & (n=11, 12, 13, 14) \quad (4.12) \\ \frac{8\alpha_1}{3} + 2\alpha_2 & (n=0) \quad (4.13) \end{cases}$$

and

$$\sum_n V_\alpha\begin{pmatrix} x & x \\ o & n \end{pmatrix} e^{i\vec{p}.\vec{N}_n}$$

$$= \frac{8\alpha_1}{3}(1 - C_1C_2C_3) + 4\alpha_2 S_1^2 \quad (4.14)$$

where C_i, S_i are defined in (3.19). Equations (4.9) and (4.14) have also been obtained by de Launay ([12], (equation (11.5))

(b) Angular force (μ_1, μ_2) interaction -
(See Fig. 4-2)

There are two types of triangles which we are going to consider. The first one is that formed by a particle and two of its first neighbours. They are triangles equivalent to $\Delta 0, 3, 8$ in Fig. 4-2; particle 8 is a

second neighbour of particle 3. This type of triangles is called type (1) triangles.

The other one is that formed by a particle, one of its first neighbours and one of its second neighbours. They are triangles equivalent to $\Delta O, 3, 11$; particle 11 is a first neighbour of particle 3. This type of triangles is called type (2) triangles.

There are, in all, twelve type (1) triangles and twenty-four type (2) triangles, referring to the particle O. As shown in Fig. 4-2, all the thirty-six triangles are identical and each is isosceles with two equal angles θ_2. We shall associate with each angle θ_1 in the triangles an angular force constant μ_1, and each angle θ_2, an angular force constant μ_2.

The unit normals $\vec{n}_{A,B,C}$ in (4.1) are given by

$$\vec{n}_{i,o,j} = \left(\sqrt{\frac{8}{3}}\right)\frac{1}{\frac{a}{2}} (\vec{N}_j - e\vec{N}_i) \frac{a}{2} \tag{4.15}$$

$$= \sqrt{\frac{3}{8}} (\vec{N}_j - \frac{1}{3}\vec{N}_i) = \vec{n}_{o,i,j} \tag{4.16}$$

$$\vec{n}_{i,j,o} = -\frac{1}{\sqrt{2}a} (\vec{N}_i + \vec{N}_j) \frac{a}{2}$$

$$= -\frac{1}{\sqrt{8}} (\vec{N}_i + \vec{N}_j) = \vec{n}_{j,i,o} \tag{4.17}$$

$$\vec{n}_{i,m,o} = \frac{1}{\sqrt{\frac{8}{3}}\frac{a}{2}} \left[-\vec{N}_i - e(\vec{N}_m - \vec{N}_i)\right] \frac{a}{2}$$

$$= -\frac{1}{\sqrt{24}} (\vec{N}_m + 2\vec{N}_i) = \vec{n}_{m,i,o} \qquad (4.18)$$

$$\vec{n}_{o,i,m} = \frac{1}{\sqrt{\frac{8}{3}}\frac{a}{2}} \left[(\vec{N}_m - \vec{N}_i) - e(-\vec{N}_i)\right] \frac{a}{2}$$

$$= \sqrt{\frac{3}{8}} (\vec{N}_m - \frac{2}{3}\vec{N}_i) = \vec{n}_{i,o,m} \qquad (4.19)$$

$$\vec{n}_{m,o,i} = -\frac{1}{\sqrt{2}a} \left[(\vec{N}_m - \vec{N}_i) + (-\vec{N}_i)\right] \frac{a}{2}$$

$$= \frac{1}{\sqrt{8}} (2\vec{N}_i - \vec{N}_m) = \vec{n}_{o,m,i} \qquad (4.20)$$

where $e = \dfrac{\vec{N}_{kr} \cdot \vec{N}_{kt}}{N_{kr}\, N_{kt}} = \dfrac{1}{3}$ (k, r, t form a type (1) triangle referring to particle k; k takes an appropriate value out of 0, 1, 2, ..., 8), (4.21)

i,j denote the first neighbours of particle 0, and m the second neighbours.

We shall deal with the potential energy corresponding to μ_1 first, then that corresponding to μ_2.

(i) Potential energy corresponding to μ_1 —

$$V_{\mu_1} = \frac{1}{2}\ \mu_1\Big\{\Big[\frac{(\vec{s}_o-\vec{s}_1).\vec{n}_{0,1,3}}{\sqrt{3}(\frac{a}{2})} + \frac{(\vec{s}_o-\vec{s}_3).\vec{n}_{0,3,1}}{\sqrt{3}(\frac{a}{2})}\Big]^2$$

(This is the contribution of the type (1) triangle 0, 1, 3)

+ ... (contribution of the twelve type (1) triangles referring to the particle 0)

$$+\Big[\frac{(\vec{s}_1-\vec{s}_9).\vec{n}_{1,9,0}}{\sqrt{3}(\frac{a}{2})} + \frac{(\vec{s}_1-\vec{s}_o).\vec{n}_{1,0,9}}{\sqrt{3}(\frac{a}{2})}\Big]^2$$

(This is the contribution of the type (2) triangle 0, 1, 9)

+ ... (contribution of the twenty-four type (2) triangles referring to the particle 0).

+ (contribution of all other triangles which do not involve the particle 0)$\Big\}$ (4.22)

By substituting (4.16), (4.18), (4.19) into (4.22), we have

$$V_{\mu_1} = \frac{\mu_1}{4a^2}\ \Big\{[(\vec{s}_o-\vec{s}_1).(\vec{N}_3-\tfrac{1}{3}\vec{N}_1) + (\vec{s}_o-\vec{s}_3).(\vec{N}_1-\tfrac{1}{3}\vec{N}_3)]^2$$

+ ... (contribution of the twelve type (1) triangles referring to the particle 0).

$$+ \left[\frac{1}{3} (\vec{s}_1 - \vec{s}_9) \cdot (\vec{N}_9 + 2\vec{N}_1) + (\vec{s}_1 - \vec{s}_o) \cdot (\vec{N}_9 - \frac{2}{3} \vec{N}_1) \right]^2$$

+ ... (contribution of the twenty-four type (2) triangles referring to the particle 0)

+ (contribution of all other triangles which do not involve the particle 0) $\Big\}$ (4.23)

$$V_{\mu_1} \begin{pmatrix} y & x \\ 1 & 0 \end{pmatrix} = - \frac{\mu_1}{3a^2} \Big\{ [\vec{j} \cdot (\vec{N}_3 - \frac{1}{3} \vec{N}_1)] \, [\vec{i} \cdot (\vec{N}_3 + \vec{N}_1)]$$

$$+ [\vec{j} \cdot (\vec{N}_5 - \frac{1}{3} \vec{N}_1)] \, [\vec{i} \cdot (\vec{N}_5 + \vec{N}_1)]$$

$$+ [\vec{j} \cdot (\vec{N}_7 - \frac{1}{3} \vec{N}_1)] \, [\vec{i} \cdot (\vec{N}_7 + \vec{N}_1)]$$

$$+ [\vec{j} \cdot (\vec{N}_9 - 2\vec{N}_1)] \, [\vec{i} \cdot (\vec{N}_9 - \frac{2}{3} \vec{N}_1)]$$

$$+ [\vec{j} \cdot (\vec{N}_{11} - 2\vec{N}_1)] \, [\vec{i} \cdot (\vec{N}_{11} - \frac{2}{3} \vec{N}_1)]$$

$$+ [\vec{j} \cdot (\vec{N}_{13} - 2\vec{N}_1)] \, [\vec{i} \cdot \vec{N}_{13} - \frac{2}{3} \vec{N}_1)] \Big\} \qquad (4.24)$$

$$= \frac{8\mu_1}{9a^2} \qquad (4.25)$$

From (2.16),

$$V_{\mu_1} \begin{pmatrix} y & x \\ 2 & 0 \end{pmatrix} = \frac{8\mu_1}{9a^2} \qquad (4.26)$$

Similarly,

$$V_{\mu_1}\begin{pmatrix} y & x \\ n & o \end{pmatrix} = \begin{cases} \dfrac{8\mu_1}{9a^2} & (n=3,\ 4) \qquad (4.27) \\ \\ -\dfrac{8\mu_1}{9a^2} & (n=5,\ 6,\ 7,\ 8) \qquad (4.28) \end{cases}$$

$$V_{\mu_1}\begin{pmatrix} y & x \\ 9 & 0 \end{pmatrix} = -\frac{\mu_1}{6a^2}\Big\{ [\vec{j}.(\vec{N}_9+2\vec{N}_1)]\,[\vec{i}.(\vec{N}_9-\tfrac{2}{3}\vec{N}_1)] + [\vec{j}.(\vec{N}_9+2\vec{N}_3)]\,[\vec{i}.(\vec{N}_9-\tfrac{2}{3}\vec{N}_3)] + [\vec{j}.(\vec{N}_9+2\vec{N}_5)]\,[\vec{i}.(\vec{N}_9-\tfrac{2}{3}\vec{N}_5)] + [\vec{j}.(\vec{N}_9+2\vec{N}_8)]\,[\vec{i}.(\vec{N}_9-\tfrac{2}{3}\vec{N}_8)]\Big\} \qquad (4.29)$$

$$= 0 \qquad (4.30)$$

$$V_{\mu_1}\begin{pmatrix} y & x \\ n & o \end{pmatrix} = 0 \qquad (n=10,\ 11,\ \ldots,\ 14) \qquad (4.31)$$

From (2.18)

$$V_{\mu_1}\begin{pmatrix} y & x \\ 0 & 0 \end{pmatrix} = 0 \qquad (4.32)$$

By making use of equation (2.8), (4.25), (4.26), (4.27), (4.28), (4.30), (4.31) and (4.32), we have,

$$\sum_n V_{\mu_1}\begin{pmatrix} x & y \\ o & n \end{pmatrix} e^{i\vec{p}.\vec{N}_n} = -\frac{64\mu_1}{9a^2} \; S_1 S_2 C_3 \tag{4.33}$$

where S_i, and C_i are defined in (3.19). Similarly, and making use of equations (2.18) and (2.8), we have

$$V_{\mu_1}\begin{pmatrix} x & x \\ n & o \end{pmatrix} = \begin{cases} -\frac{16\mu_1}{9a^2} & (n=1, 2, \ldots, 8) \quad (4.34) \\ -\frac{32\mu_1}{9a^2} & (n=9, 10) \quad (4.35) \\ \frac{8\mu_1}{9a^2} & (n=11, 12, 13, 14) \quad (4.36) \\ \frac{160\mu_1}{9a^2} & (n=0) \quad (4.37) \end{cases}$$

$$\sum_n V_{\mu_1}\begin{pmatrix} x & x \\ o & n \end{pmatrix} e^{i\vec{p}.\vec{N}_n}$$

$$= -\frac{128\mu_1}{9a^2} \; C_1C_2C_3 - \frac{16\mu_1}{9a^2} \; (4 \cos 2\pi ak_1 - \cos 2\pi ak_2 - \cos 2\pi ak_3)$$

$$+\frac{160\mu_1}{9a^2} \tag{4.38}$$

where C_i and S_i are defined in (3.19).

(ii) Potential energy corresponding to μ_2, -

$$V_{\mu_2} = \frac{1}{2}\mu_2 \left(\left[\frac{(\vec{s}_1-\vec{s}_3).\vec{n}_{1,3,0}}{a} + \frac{(\vec{s}_1-\vec{s}_o).\vec{n}_{1,0,3}}{\sqrt{3}\frac{a}{2}} \right]^2 \right.$$

$$\left. + \left[\frac{(\vec{s}_3-\vec{s}_1).\vec{n}_{3,1,0}}{a} + \frac{(\vec{s}_3-\vec{s}_o).\vec{n}_{3,0,1}}{\sqrt{3}\frac{a}{2}} \right]^2 \right)$$

(This is the contribution of the type (1) triangle 0, 1, 3)

+ ... (contribution of the twelve type (1) triangles referring to the particle 0).

$$+\left(\left[\frac{(\vec{s}_o-\vec{s}_9).\vec{n}_{0,9,1}}{a} + \frac{(\vec{s}_o-\vec{s}_1).\vec{n}_{0,1,9}}{\sqrt{3}\frac{a}{2}} \right]^2 \right.$$

$$\left. + \left[\frac{(\vec{s}_9-\vec{s}_o).\vec{n}_{9,0,1}}{a} + \frac{(\vec{s}_9-\vec{s}_1).\vec{n}_{9,1,0}}{\sqrt{3}\frac{a}{2}} \right]^2 \right)$$

(This is the contribution of the type (2) triangle 0, 1, 9)

+ ... (contribution of the twenty-four type (2) triangles referring to the particle 0)

+(contribution of all other triangles which do not involve the particle 0). (4.39)

Making use of equations (4.16) to (4.20), (2.16), (2.18) and (2.8), we have

$$V_{\mu_2}\begin{pmatrix} y & x \\ n & o \end{pmatrix} = \begin{cases} -\dfrac{4\mu_2}{3a^2} & (n=1,\ 2,\ 3,\ 4) \qquad (4.40) \\ \dfrac{4\mu_2}{3a^2} & (n=5,\ 6,\ 7,\ 8) \qquad (4.41) \\ 0 & (n=9,\ 10,\ \ldots,\ 14) \qquad (4.42) \\ 0 & (n=0) \qquad (4.43) \end{cases}$$

$$\sum_n V_{\mu_2}\begin{pmatrix} x & y \\ o & n \end{pmatrix} e^{i\vec{p}.\vec{N}_n} = \frac{32\mu_2}{3a^2} \; S_1 S_2 C_3 \qquad (4.44)$$

$$V_{\mu_2}\begin{pmatrix} x & x \\ n & o \end{pmatrix} = \begin{cases} -\dfrac{8\mu_2}{3a^2} & (n=1,\ 2,\ \ldots,\ 8) \qquad (4.45) \\ 0 & (n=9,\ 10) \qquad (4.46) \\ -\dfrac{4\mu_2}{3a^2} & (n=11,\ 12,\ 13,\ 14) \qquad (4.47) \\ \dfrac{80\mu_2}{3a^2} & (n=0) \qquad (4.48) \end{cases}$$

$$\sum_n V_{\mu_2}\begin{pmatrix} x & x \\ o & n \end{pmatrix} e^{i\vec{p}.\vec{N}_n}$$

$$= \frac{80\mu_2}{3a^2} - \frac{64\mu_2}{3a^2} C_1C_2C_3$$

$$- \frac{8\mu_2}{3a^2} (\cos 2\pi ak_2 + \cos 2\pi ak_3) \qquad (4.49)$$

where C_i and S_i are defined in (3.19)

Combination of α_1, α_2, μ_1 and μ_2 -

By combining equations (3.2), (4.9), (4.14), (4.33), (4.38), (4.44) and (4.49), we have a secular equation

$$\begin{vmatrix} P_1 - 4\pi^2\nu^2M & Q_{12} & Q_{13} \\ Q_{21} & P_2 - 4\pi^2\nu^2M & Q_{23} \\ Q_{31} & Q_{32} & P_3 - 4\pi^2\nu^2M \end{vmatrix} = 0 \qquad (4.50)$$

where $P_1 = \Big\{ \left(\frac{8\alpha_1}{3} + \frac{128\mu_1}{9a^2} + \frac{64\mu_2}{3a^2}\right)(1 - C_1C_2C_3) + 4\alpha_2S_1^2 - \frac{16\mu_1}{9a^2} \cdot$

$$\cdot (4\cos 2\pi ak_1 - \cos 2\pi ak_2 - \cos 2\pi ak_3 - 2)$$

$$- \frac{8\mu_2}{3a^2} (\cos 2\pi ak_2 + \cos 2\pi ak_3 - 2) \Big\} \qquad (4.51)$$

$$Q_{12} = 8\left(\frac{\alpha_1}{3} - \frac{8\mu_1}{9a^2} + \frac{4\mu_2}{3a^2}\right) S_1S_2C_3$$

and the others can be obtained by circular permutations of the indices.

This is the same as that obtained by Clark et al. [23] equation (7)) from first principles. The equivalence between the notations α, β, γ_1 and γ_2 used in their paper and those we use, are shown in the following:

$$\left.\begin{aligned} \alpha &= \frac{\alpha_1}{3} \\ \beta &= \alpha_2 \\ \gamma_1 &= \frac{8\mu_1}{9a^2}. \\ \gamma_2 &= \frac{8\mu_2}{9a^2} \end{aligned}\right\} \qquad (4.52)$$

In the long-wave limit as $k \to 0$, with $\rho = 2M/a^3$, the secular equation obtained should be identical with the elasticity secular equation (3.22). Therefore, by comparison, we have

$$2\alpha_2 + \frac{80\mu_1}{9a^2} - \frac{8\mu_2}{3a^2} = a\,c_{11} - a\,c_{44} \qquad (4.53)$$

$$\frac{2\alpha_1}{3} + \frac{16\mu_1}{9a^2} + \frac{24\mu_2}{3a^2} = a\,c_{44} \qquad (4.54)$$

$$\frac{4\alpha_1}{3} - \frac{32\mu_1}{9a^2} + \frac{16\mu_2}{3a^2} = a\,c_{12} + a\,c_{44} \qquad (4.55)$$

(longitudinal)

In the [100] direction, the phonon frequency/at the first Brillouin zone boundary (i.e. $k_1 = 1/a$) is given by

$$\nu_b = \frac{1}{\pi}\left[\frac{1}{3M}\left(4\alpha_1 + \frac{64\mu_1}{3a^2} + \frac{32\mu_2}{a^2}\right]^{1/2}\right. \tag{4.56}$$

Solving equations (4.53) to (4.56), we have

$$\alpha_1 = \frac{3}{4}\, a(\epsilon_{12} - \epsilon_{44}) + \frac{3}{4}\,\pi^2\nu_b{}^2M \tag{4.57}$$

$$\alpha_2 = \frac{1}{4}\, a(2\epsilon_{11} + \epsilon_{12} + 3\epsilon_{44}) - \frac{3}{4}\,\pi^2\nu_b{}^2M \tag{4.58}$$

$$\frac{\mu_1}{a^2} = -\frac{9}{128}\, a(\epsilon_{12} + 3\epsilon_{44}) + \frac{9}{64}\,\pi^2\nu_b{}^2M \tag{4.59}$$

$$\frac{\mu_2}{a^2} = -\frac{3}{64}\, a(\epsilon_{12} - 5\epsilon_{44}) - \frac{3}{32}\,\pi^2\nu_b{}^2M \tag{4.60}$$

By substituting (457), (4.58), (4.59) and (4.60) into (4.50), we have a secular equation

$$\begin{vmatrix} P_1 - 4\pi^2\nu^2M & Q_{12} & Q_{13} \\ Q_{21} & P_2 - 4\pi^2\nu^2M & Q_{23} \\ Q_{31} & Q_{32} & P_3 - 4\pi^2\nu^2M \end{vmatrix} = 0 \tag{4.61}$$

where

$$P_1 = 2\pi^2\nu_b^2 M\,(1-C_1C_2C_3) + (2a\,c_{11}-\pi^2\nu_b^2 M)\,S_1^2 + (2a\,c_{44}-\pi^2\nu_b^2 M)\,(S_2^2+S_3^2)$$

$$Q_{12} = 2a(c_{12} + c_{44})S_1\,S_2\,C_3$$

and the remainder can be obtained by circular permutations of the indices. This is identical with that obtained in the angular force model I, namely equation (3.31). Hence the two angular force models (b.c.c.) are equivalent as far as the frequency spectrum is concerned.

(2) Face-centered Cubic Lattice

(See Fig. 4-3)

Since we only need to use terms of $\left(\frac{\partial^2 V}{\partial u_o\,\partial v_n}\right)_o$, we can treat the potential energy due to the central force interaction and the angular force interaction separately.

(a) Central force (α_1, α_2) interaction -

These are the same as those used in angular force model I (f.c.c. lattice). Therefore, the notations and results in that case are used here, namely, equations (3.38) and (3.44).

(b) Angular force (κ_1, κ_2) interaction -

There are two types of triangles which we are going to consider.

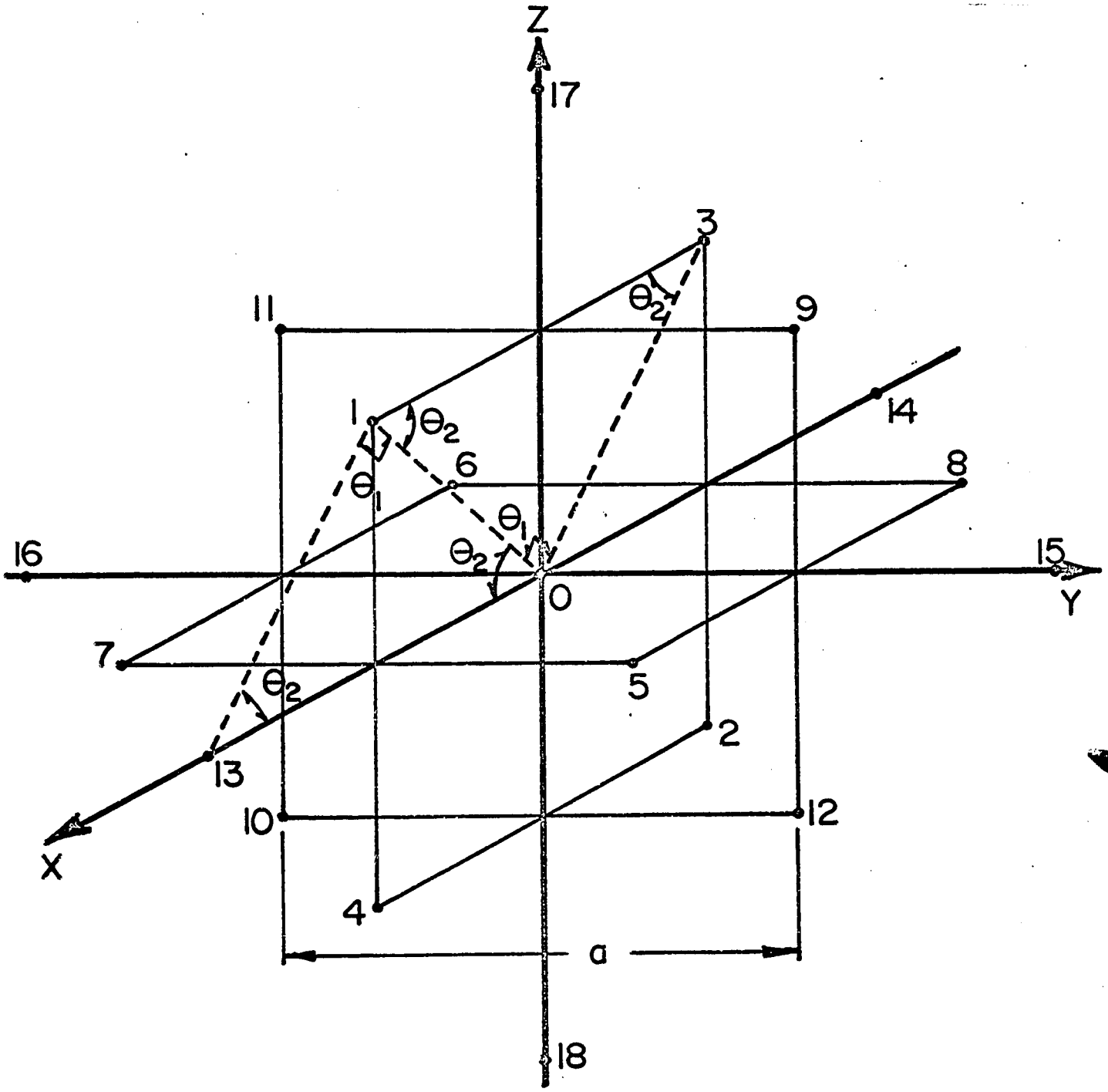

Fig. 4-3. The first and second neighbours of the particle 0 of the f.c.c. lattice.

The first one is that formed by a particle and two of its first neighbours which are both in the same plane of the coordinate axes. They are triangles equivalent to $\Delta 0, 1, 3$ in Fig. 4-3; particles 1 and 3 are both in the X - O - Z plane. This type of triangles is called type (1) triangles. Since we intend to have closer comparison between the two angular force models when applied to both b.c.c. and f.c.c. lattices, we shall limit ourselves to models each consisting of two central force constants and two angular force constants.

The other type is that formed by a particle, one of its first neighbours and one of its second neighbours. They are triangles equivalent to $\Delta 0, 1, 13$; particle 13 is a first neighbour of particle 1. This type of triangles is called type (2) triangles.

There are, in all, twelve type (1) triangles and twenty-four type (2) triangles, with reference to the particle O. As shown in Fig. 4-3, all the thirty-six triangles are identical and each is isosceles with two equal angles θ_2; $\theta_2 = 45°$. We shall associate with each angle θ_1 ($\theta_1 = 90°$) in the triangles an angular force constant κ_1, and each angle θ_2 an angular force constant κ_2.

The unit normals $\vec{n}_{A,B,C}$ in (4.1) are given by

$$\vec{n}_{i,o,j} = \frac{1}{\sqrt{2}} \vec{N}_j = \vec{n}_{o,i,j} \tag{4.62}$$

$$\vec{n}_{i,j,o} = -\frac{1}{2} (\vec{N}_i + \vec{N}_j) = \vec{n}_{j,i,o} \tag{4.63}$$

$$\vec{n}_{i,m,o} = -\frac{1}{\sqrt{2}}\vec{N}_i = \vec{n}_{m,i,o} \tag{4.64}$$

$$\vec{n}_{o,i,m} = \frac{1}{\sqrt{2}}\vec{N}_j = \vec{n}_{i,o,m} \tag{4.65}$$

$$\text{where } \vec{N}_i + \vec{N}_j = \vec{N}_m$$

$$\vec{n}_{m,o,i} = \vec{N}_i - \frac{1}{2}\vec{N}_m = \vec{n}_{o,m,i} \tag{4.66}$$

where i, j denote the first neighbours of particle 0, and m the second neighbours.

We shall deal with the potential energy involving κ_1 first, then that involving κ_2.

(i) Potential energy involving κ_1, -

$$V_{\kappa_1} = \frac{1}{2}\kappa_1 \left\{ \left[\frac{(\vec{s}_o - \vec{s}_1).\vec{n}_{0,1,3}}{a/\sqrt{2}} + \frac{(\vec{s}_o - \vec{s}_3).\vec{n}_{0,3,1}}{a/\sqrt{2}} \right]^2 \right.$$

(This is the contribution of the type (1) triangle 0,1,3)

+ ... (contribution of the twelve type (1) triangles referring to the particle 0)

$$\left. + \left[\frac{(\vec{s}_1 - \vec{s}_o).\vec{n}_{1,0,13}}{a/\sqrt{2}} + \frac{(\vec{s}_1 - \vec{s}_{13}).\vec{n}_{1,13,0}}{a/\sqrt{2}} \right]^2 \right.$$

(This is the contribution of the type (2) triangle 0, 1, 13)
+ ... (contribution of the twenty-four type (2) triangles referring to the particle 0)
+ (contribution of all other triangles which do not involve the particle 0) (4.67)

Making use of equations (4.62) to (4.66), (2.16), (2.18) and (2.8), we have

$$V_{\kappa_1}\begin{pmatrix} y & x \\ n & o \end{pmatrix} = \begin{cases} 0 & (n=1, 2, 3, 4) \quad (4.68) \\ \frac{4\kappa_1}{a^2} & (n=5, 6) \quad (4.69) \\ -\frac{4\kappa_1}{a^2} & (n=7, 8) \quad (4.70) \\ 0 & (n=9, 10, 11, 12) \quad (4.71) \\ 0 & (n=13, 14, \ldots, 18) \quad (4.72) \\ 0 & (n=0) \quad (4.73) \end{cases}$$

$$\sum_n V_{\kappa_1}\begin{pmatrix} x & y \\ o & n \end{pmatrix} e^{i\vec{p}.\vec{N}_n} = -\frac{16\kappa_1}{a^2} S_1 S_2 \quad (4.74)$$

$$V_{\kappa_1}\begin{pmatrix} x & x \\ n & o \end{pmatrix} = \begin{cases} -\dfrac{4\kappa_1}{a^2} & (n=1, 2, \ldots, 8) \quad (4.75) \\ 0 & (n=9, 10, 11, 12) \quad (4.76) \\ -\dfrac{4\kappa_1}{a^2} & (n=13, 14) \quad 4.77) \\ \dfrac{2\kappa_1}{a^2} & (n=15, 16, 17, 18) \quad (4.78) \\ \dfrac{32\kappa_1}{a^2} & (n=0) \quad (4.79) \end{cases}$$

$$\sum_n V_{\kappa_1}\begin{pmatrix} x & x \\ o & n \end{pmatrix} e^{i\vec{p}.\vec{N}_n}$$

$$= \frac{32\kappa_1}{a^2} - \frac{16\kappa_1}{a^2} C_1(C_2+C_3) - \frac{4\kappa_1}{a^2} (2\cos 2\pi ak_1 - \cos 2\pi ak_2 - \cos 2\pi ak_3) \quad (4.80)$$

(ii) Potential energy involving κ_2, -

$$V_{\kappa_2} = \frac{1}{2}\kappa_2 \left\{ \left(\left[\frac{(\vec{s}_1-\vec{s}_3).\vec{n}_{1,3,0}}{a} + \frac{(\vec{s}_1-\vec{s}_o).\vec{n}_{1,0,3}}{a/\sqrt{2}} \right]^2 \right.\right.$$

$$\left.\left. + \left[\frac{(\vec{s}_3-\vec{s}_1).\vec{n}_{3,1,0}}{a} + \frac{(\vec{s}_3-\vec{s}_o).\vec{n}_{3,0,1}}{a/\sqrt{2}} \right]^2 \right)$$

(This is the contribution of the type (1) triangle 0,1,3)

+ ... (contribution of the twelve type (1) triangles referring to the particle 0).

$$+\Big([\frac{(\vec{s}_o-\vec{s}_{13}).\vec{n}_{0,13,1}}{a} + \frac{(\vec{s}_o-\vec{s}_1).\vec{n}_{0,1,13}}{a/\sqrt{2}}]^2$$

$$+ [\frac{(\vec{s}_{13}-\vec{s}_o).\vec{n}_{13,0,1}}{a} + \frac{(\vec{s}_{13}-\vec{s}_1).\vec{n}_{13,1,0}}{a/\sqrt{2}}]^2\Big)$$

(This is the contribution of the type (2) triangle 0,1,13).

+ ... (contribution of the twenty-four type (2) triangles referring to the particle 0).

+ (contribution of all other triangles which do not involve the particle 0) (4.81)

Making use of equations (4.62) to (4.66), (2.16), (2.18) and (2.8), we have

$$V_{\kappa_2}\begin{pmatrix} y & x \\ n & o \end{pmatrix} = \begin{cases} 0 & (n=1, 2, \ldots, 12) \quad (4.82) \\ 0 & (n=13, 14, \ldots, 18) \quad (4.83) \\ 0 & (n=0) \quad (4.84) \end{cases}$$

$$\sum_n V_{\kappa_2}\begin{pmatrix} x & y \\ o & n \end{pmatrix} e^{i\vec{p}.\vec{N}_n} = 0 \quad (4.85)$$

$$V_{\kappa_2}\begin{pmatrix} x & x \\ n & o \end{pmatrix} = \begin{cases} -\frac{4\kappa_2}{a^2} & (n=1, 2, \ldots, 8) \quad (4.86) \\ 0 & (n=9, 10, 11, 12) \quad (4.87) \\ 0 & (n=13, 14, \ldots, 18) \quad (4.88) \\ \frac{32\kappa_2}{a^2} & (n=0) \quad (4.89) \end{cases}$$

$$\sum_n V_{\kappa 2} \begin{pmatrix} x & x \\ o & n \end{pmatrix} e^{i\vec{p}.\vec{N}_n}$$

$$= \frac{32\kappa_2}{a^2} - \frac{16\kappa_2}{a^2} C_1(C_2+C_3) \qquad (4.90)$$

Combination of α_1, α_2, κ_1, κ_2 -

By combining equations (3.2). (3.38), (3.44), (4.74), (4.80), (4.85) and (4.90), we have a secular equation

$$\begin{vmatrix} R_1 - 4\pi^2\nu^2 M & T_{12} & T_{13} \\ T_{21} & R_2 - 4\pi^2\nu^2 M & T_{23} \\ T_{31} & T_{32} & R_3 - 4\pi^2\nu^2 M \end{vmatrix} = 0 \qquad (4.91)$$

Where $R_1 = 2[\alpha_1 + \frac{8}{a^2}(\kappa_1 + \kappa_2)][2 - C_1(C_2 + C_3)] + 4\alpha_2 S_1^2 - \frac{4\kappa_1}{a^2}$ x

$$x(2 \cos 2\pi ak_1 - \cos 2\pi ak_2 - \cos 2\pi ak_3)$$

$$T_{12} = (2\alpha_1 - \frac{16\kappa_1}{a^2}) S_1 S_2$$

and the others can be obtained by circular permutations of the indices. C_i, S_i are defined in (3.19)

In the long-wave limit as $k \to 0$, with $\rho = 4M/a^3$, the secular equation should be identical with the elasticity secular equation (3.22). Therefore, by comparison, we have

$$\alpha_1 + \frac{8}{a^2}(4\kappa_1 + \kappa_2) + 4\alpha_2 = ac_{11} - ac_{44} \tag{4.92}$$

$$\alpha_1 + \frac{8}{a^2}\kappa_2 = ac_{44} \tag{4.93}$$

$$2\alpha_1 - \frac{16}{a^2}\kappa_1 = ac_{12} + ac_{44} \tag{4.94}$$

The phonon frequency (longitudinal) in the [100] direction at the Brillouin zone boundary (i.e. $\kappa_1 = 1/a$), is given by

$$\nu_b = \frac{1}{\pi}\left\{\frac{2}{M}\left[\alpha_1 + \frac{8}{a^2}(\kappa_1 + \kappa_2)\right]\right\}^{1/2} \tag{4.95}$$

Solving equations (4.92) to (4.95), we have

$$\alpha_1 = \frac{1}{2}a(c_{12} - c_{44}) + \frac{1}{2}\pi^2\nu_b{}^2M \tag{4.96}$$

$$\alpha_2 = \frac{1}{4}a(c_{11} + 2c_{44}) - \frac{1}{2}\pi^2\nu_b{}^2M \tag{4.97}$$

$$\frac{\kappa_1}{a^2} = -\frac{1}{8} ac_{44} + \frac{1}{16} \pi^2 \nu_b{}^2 M \tag{4.98}$$

$$\frac{\kappa_2}{a^2} = -\frac{1}{16} a(c_{12} - 3c_{44}) - \frac{1}{16} \pi^2 \nu_b{}^2 M \tag{4.99}$$

By substituting (4.96), (4.97), (4.98) and (4.99) into (4.91), we have a secular equation

$$\begin{vmatrix} R_1 - 4\pi^2 \nu^2 M & T_{12} & T_{13} \\ T_{21} & R_2 - 4\pi^2 \nu^2 M & T_{23} \\ T_{31} & T_{32} & R_3 - 4\pi^2 \nu^2 M \end{vmatrix} = 0 \tag{4.100}$$

where $R_1 = \pi^2 \nu_b{}^2 M [2 - C_1(C_2 + C_3)] + (ac_{11} - \pi^2 \nu_b{}^2 M) S_1{}^2$

$$+ (ac_{44} - \tfrac{1}{2} \pi^2 \nu_b{}^2 M) (S_2{}^2 + S_3{}^2)$$

$$T_{12} = a(c_{12} + c_{44}) S_1 S_2$$

and the others can be obtained by circular permutations of the indices. Comparing (3.61) and (4.100), we find that

$$K_i \neq R_i \tag{4.101}$$

but

$$L_{ij} \equiv T_{ij} \tag{4.102}$$

CHAPTER V

DATA AND CALCULATIONS

The frequency histograms are obtained following the method used by Varshni and Shukla [26] by means of a 1620 IBM computer. The first Brillouin zone is divided into identical cubes each of edge equal to 1/40 of the distance between Γ and X points of the Brillouin zone. The total number of such cubes in the first zone is 64000, and that of frequencies is 192000. Because of symmetric properties, we need only consider 1/48 of the first zone. This has 1686 points; each point is weighed according to the number of points equivalent to it. Special attention has to be paid to those points lying on the surfaces, edges and corners of the first zone. The frequencies are obtained by solving the appropriate secular equations. The frequency histograms are then obtained by Blackman's sampling method.

For all the metals which we deal with, except nickel and sodium, the histograms are obtained from data at 0°K and the dispersions curves from data at temperatures at which the experimental dispersion curves are obtained. For the cases of nickel and sodium, the histograms are obtained at temperatures other than 0°K because no elastic constant data at 0°K are available.

Because experimental values of phonon frequency (longitudinal) at the first zone boundary in the [100] direction at 0°K, ($\nu_b(0)$) are not

available, we obtain these values by means of the following method.

It is well known that for longitudinal elasticity waves in the [100] direction (see, e.g., de Launay's article [12], equation (10.10)),

$$\nu_{k_{(\text{elast.})}}(t) \propto \left[\frac{c_{11}(t)}{\rho(t)}\right]^{1/2} \tag{5.1}$$

where $\nu_{k_{(\text{elast.})}}(t)$ is the frequency of the elasticity wave (longitudinal) in the [100] direction and at t°K. With $\rho(t) = \frac{2M}{a^3(t)}$ for b.c.c. lattice or $\rho(t) = \frac{4M}{a^3(t)}$ for f.c.c. lattice, we have

$$\frac{\nu_{k_{(\text{elast.})}}(0)}{\nu_{k_{(\text{elast.})}}(t)} = \left[\frac{c_{11}(0)\, a^3(0)}{c_{11}(t)\, a^3(t)}\right]^{1/2} \tag{5.2}$$

We assume that this relation is true for all values of k,

$$\text{i.e.,} \quad \frac{\nu_k(0)}{\nu_k(t)} = \left[\frac{c_{11}(0)\, a^3(0)}{c_{11}(t)\, a^3(t)}\right]^{1/2} \tag{5.3}$$

for all k.

In particular, we have

$$\frac{\nu_b\,(0)}{\nu_b\,(t)} = \left[\frac{c_{11}\,(0)\,a^3\,(0)}{c_{11}\,(t)\,a^3\,(t)}\right]^{1/2} \tag{5.4}$$

where $\nu_b\,(t)$ is the boundary phonon frequency (longitudinal) in the [100] direction and at t°K.

The lattice specific heats at constant volume are then calculated from the expression,

$$C_v = 3R\int_o^{\nu_m} \frac{x^2\,e^x}{(e^x - 1)^2}\; g\,(\nu)\; d\nu \tag{5.5}$$

where $x = \frac{h\nu}{kT}$

and

$$\int_o^{\nu_m} g\,(\nu)\; d\nu = 1$$

The equivalent Debye temperatures are then calculated from the relation

$$\frac{C_v}{3R} = \frac{4\pi^4}{5}\left(\frac{T}{\theta}\right)^3 - \frac{3\theta/T}{e^{\theta/T}-1} + 12\log\left(1-e^{-\theta/T}\right) - 36\,\frac{T}{\theta}\sum_{n=1}^{\infty}\left\{\left[1+\frac{2T}{n\theta}+\frac{2}{n^2}\left(\frac{T}{\theta}\right)^2\right]x\right.$$

$$\left. x\,\frac{e^{-n\theta/T}}{n^2}\right\} \tag{5.6}$$

(1) Face-centered Cubic Lattice -

The metals which we deal with are copper, aluminum and nickel. The lattice constant (a), elastic constants (c_{11}, c_{12}, c_{44}) and the phonon frequency (longitudinal) at the zone boundary in the [100] direction (ν_b) of these metals are shown in Table 2.

Table 2. The lattice constant (a), the elastic constants (c_{11}, c_{12}, c_{44}) and the phonon frequency (longitudinal) at the zone boundary in the [100] direction, (ν_b) of copper, aluminum and nickel.

Group	Element	Temp. (°K)	a (10^{-8} cm.)	C_{11} (10^{11} dynes/cm.^{2})	C_{12} (10^{11} dynes/cm.^{2})	C_{44} (10^{11} dynes/cm.^{2})	Ref.	Temp. (°K)	[100] ν_b (10^{12} cps)
1b	Cu	0	3.6029[a]	17.62	12.494	8.177	c	0	7.43[f]
		300	3.6147[b]	16.839	12.142	7.539	c	300	7.3 [g]
3b	Al	0	4.0328[a]	11.430	6.192	3.162	d	0	9.73[f]
		80	4.0338[b]	11.373	6.191	3.128	d	80	9.71[h]
8	Ni	296	3.5236[b]	24.6	15.0	12.2	e	296	8.55[i]

[a] Calculated from the room temperature value by the method of Corruccini and Gniewek [29].

[b] A.I.P. Handbook [30].

[c] Overton and Gaffney [31].

[d] Kamm and Alers [32].

[e] de Klerk [33].

[f] Derived from the experimental value at higher temperature as explained in the text (equation (5.4)).

[g] Sinha [34] and Svensson, Brockhouse and Rowe [35].

[h] Stedman and Nilsson [36].

[i] Birgeneau et al. [37].

(I) Angular force model I -

The values of the interparticle force constants α_1, α_2, σ_1 and σ_2 are obtained from equations (3.57), (3.58), (3.59) and (3.60). These are shown in Table 3.

Table 3. The interparticle force constants α_1, α_2, σ_1 and σ_2 of copper, aluminum and nickel in the angular force model I.

Group	Metal	Temp. (°K)	α_1	α_2	σ_1	σ_2
			(10^3 dynes/cm.)			
1b	Cu	0	32.99	1.500	-4.248	2.304
		300	31.66	1.344	-3.913	1.833
3b	Al	0	19.90	1.058	1.035	-2.562
		80	19.82	1.047	1.025	-2.569
8	Ni	296	41.54	4.087	-6.377	5.144

The theoretical dispersion curves are obtained from equation (3.52) and are shown in Fig. 6-1 (copper), Fig. 6-6 (aluminum) and Fig. 6-11 (nickel) along with the experimental points.

The frequency histograms are shown in Fig. 6-3 (copper), Fig. 6-8 (aluminum) and Fig. 6-13 (nickel).

The equivalent Debye temperatures obtained from equation (5.6)

are shown in Fig. 6-5 (copper), Fig. 6-10 (aluminum) and Fig. 6-15 (nickel) together with the experimental values.

(II) Angular force model II -

The values of the interparticle force parameters α_1, α_2, $\kappa_1/(a^2)$ and $\kappa_2/(a^2)$ are obtained from equations (4.96), (4.97), (4.98) and (4.99).

These are shown in Table 4.

Table 4. The interpaticle force parameters α_1, α_2, $\kappa_1/(a^2)$ and $\kappa_2/(a^2)$ of copper, aluminum and nickel in angular force model II.

Group	Metal	Temp. (°K)	α_1	α_2	$\kappa_1/(a^2)$	$\kappa_2/(a^2)$
			(10^3 dynes/cm.)			
1b	Cu	0	36.52	1.859	-0.090	-0.882
		300	36.06	1.098	0.0617	-1.102
3b	Al	0	27.04	-3.031	1.022	-1.786
		80	27.02	-3.067	1.028	-1.801
8	Ni	296	40.10	7.997	-0.9776	0.3610

The dispersion curves obtained from equation (4.91) are shown in Fig. 6-2 (copper), Fig. 6-7 (aluminum) and Fig. 6-12 (nickel).

The frequency histograms are shown in Fig. 6-4 (copper),

Fig. 6-9 (aluminum) and Fig. 6-14 (nickel), and the equivalent Debye temperatures obtained from equation (5.6) are shown in Fig. 6-5 (copper), Fig. 6-10 (aluminum) and Fig. 6-15 (nickel).

(2) Body-centered Cubic Lattice -

The following metals have been considered: sodium, tantalum, molybdenum, tungsten, and iron. The lattice constant (a), the elastic constants (c_{11}, c_{12}, c_{44}) and the phonon frequency (longitudinal) at the zone boundary in the [100] direction (ν_b) of these metals are shown in Table 5.

Table 5. The lattice constant (a), the elastic constants (c_{11}, c_{12}, c_{44}) and the phonon frequency (longitudinal) at the zone boundary in the [100] direction (ν_b) of sodium, tantalum, Molybdenum, tungsten and iron.

Group	Element	Temp. (°K)	a (10^{-8} cm.)	C_{11} (10^{11}dyn/cm^2)	C_{12} (10^{11}dyn/cm^2)	C_{44} (10^{11}dyn/cm^2)	Ref.	Temp. (°K)	[100] ν_L (10^{12} cps)
1a	Na	78	4.2353[a]	.815	.679	.578	c	90	3.58[g]
5a	Ta	0	3.2979[a]	26.632	15.816	8.736	d	0	5.07[h]
		300	3.3026[b]	26.091	15.743	8.182	d	296	5.03[i]
6a	Mo	0	3.1470[a]	45.002	17.292	12.503	d	0	6.357[j]
		300	3.1500[b]	44.077	17.243	12.165	d	296	6.3[k]
	W	0	3.1620[a]	53.255	20.495	16.313	d	0	5.54[h]
		300	3.1648[b]	52.327	20.453	16.072	d	room	5.50[l]
8	Fe	0	2.8608[a]	24.31	13.81	12.19	e	0	8.433[h]
		289	2.8665[b]	23.35	13.55	11.8	e,f	289	8.29[m]

a Calculated from the room temperature value [30] by the method of Corruccini and Gniewek [29].

b A.I.P. Handbook [30].

c Diederich and Trivisonno [38].

d Featherston and Neighbours [39].

e Rayne and Chandrasekhar [40].

f Low [41].

g Woods et al. [42].

h Derived from the experimental value at higher temperature as explained in the text (equation 5.4)).

i Woods [43].

j Derived from the room temperature value (6.3×10^{12} cps.) as explained in the text (equation (5.4))

k Woods and Chen [44]. This is not the experimental value but rather the value given by the force constant model used by these authors. It was found that this value gives a better overall agreement with the dispersion curves.

l Chen and Brockhouse [45].

m Low [41].

(I) Angular force model I -

The values of the interparticle force constants α_1, α_2, n_1 and n_2 are obtained from equations (3.27), (3.28), (3.29) and (3.30). These are shown in Table 6.

Table 6. The interparticle force constants α_1, α_2, n_1 and n_2 of sodium, tantalum, molybdenum, tungsten and iron in angular force model I.

Group	Metal	Temp. (°K)	α_1	α_2	n_1	n_2
			(10^3 dynes/cm)			
1a	Na	78	3.8690	0.5187	-0.1237	0.0168
5a	Ta	0	59.54	24.86	-1.187	-4.651
		300	58.26	24.33	-0.997	-5.246
6a	Mo	0	62.77	54.93	-7.557	3.789
		300	61.92	53.82	-7.558	3.559
	W	0	81.31	61.08	-5.979	2.673
		300	80.58	60.02	-6.114	2.647
8	Fe	0	53.46	18.50	-2.324	1.165
		289	52.06	17.74	-2.442	1.188

(II) Angular force model II -

The values of the interparticle force parameters α_1, α_2, $\mu_1/(a^2)$ and $\mu_2/(a^2)$ are obtained from equations (4.57), (4.58), (4.59) and (4.60). These are shown in Table 7.

Table 7. The interparticle force parameters α_1, α_2, $\mu_1/(a^2)$ and $\mu_2/(a^2)$ of sodium, tantalum, molybdenlum, tungsten and iron in angular force model II.

Group	Metal	Temp. (°K)	α_1	α_2	$\mu_1/(a^2)$	$\mu_2/(a^2)$
			(10^3 dynes/cm.)			
1a	Na	78	3.942	0.6593	-0.0395	0.0137
5a	Ta	0	74.68	21.39	0.974	-2.839
		300	75.00	20.08	1.195	-3.138
6a	Mo	0	58.96	66.27	-3.191	0.715
		300	58.80	64.94	-3.127	0.585
	W	0	79.27	69.73	-2.433	0.383
		300	78.75	68.78	-2.464	0.3430
8	Fe	0	52.29	21.99	-0.981	0.220
		289	50.94	21.37	-1.021	0.210

Because equations (3.31) and (4.61) are identical, the two

angular force models for the b.c.c. lattice are equivalent as far as the frequency spectrum is concerned. We can use any one of equations (3.20), (3.31) (i.e. (4.61)) and (4.50) for obtaining the dispersion curves, frequency histograms and hence the equivalent Debye temperatures.

We use equation (4.50) to obtain the dispersion curves. These are shown together with the experimental points in Fig. 6-16 (sodium), Fig. 6-19 (tantalum), Fig. 6-22 (molybdenum), Fig. 6-25 (tungsten) and Fig. 6-28 (iron).

The frequency histograms are obtained from equation (4.50) and are shown in Fig. 6-17 (sodium), Fig. 6-20 (tantalum), Fig. 6-23 (molybdenum), Fig. 6-26 (tungsten) and Fig. 6-29 (iron).

With the specific heats obtained from equation (5.5), the equivalent Debye temperatures are obtained from equation (5.6) and are shown in Fig. 6-18 (sodium), Fig. 6-21 (tantalum), Fig. 6-24 (molybdenum), Fig. 6-27 (tungsten) and Fig. 6-30 (iron) along with the experimental values.

CHAPTER VI

RESULTS, DISCUSSIONS AND CONCLUSION

As mentioned in Chapter I, the most general force constant model is the tensor-force model. In the following, we shall discuss the interpretation of the two angular force models (AFM-I and AFM-II) in terms of the tensor force model, and the results we obtained.

(1) Face-centered Cubic Lattice -

Upon equating secular equation (3.52) and the secular equation of a tensor-force model with first neighbour and second neighbour interactions for the f.c.c. lattice*, we find that, as far as the frequency spectrum is concerned, the angular force model I for f.c.c. lattice is equivalent to a particular case of the tensor-force model with

$$\overset{110}{\alpha_1} = \frac{1}{2}(\alpha_1 + \sigma_1) \tag{6.1}$$

$$\overset{110}{\alpha_3} = 2\sigma_1 \tag{6.2}$$

---

* See, e.g., Squires' article [21], Table II. The second term in MA_{11} for the f.c.c. lattice should read $\left\{ \overset{110}{2\alpha_3} \ (1-\cos\theta_2 \cos\theta_3) \right\}$.

$$\beta_3^{110} = \frac{1}{2}(\alpha_1 - \sigma_1) \tag{6.3}$$

$$\alpha_1^{200} = \alpha_2 \tag{6.4}$$

and

$$\alpha_2^{200} = \sigma_2 \tag{6.5}$$

where α_1^{110}, α_3^{110}, β_3^{110}, α_1^{200} and α_2^{200} are notation used by Squires [21] to denote the force parameters for the first and the second neighbours, used in the tensor-force model. From (6.1), (6.2) and (6.3), we have a relation between the first neighbour tensor-force parameters,

$$2\alpha_1^{110} - \alpha_3^{110} - 2\beta_3^{110} = 0 \tag{6.6}$$

Upon equating secular equation (4.91) and the secular equation of a tensor-force model with first neighbour and second neighbour interactions for the f.c.c. lattice (see footnote in p. 74), we find that, as far as the frequency spectrum is concerned, the angular force model II for f.c.c. lattice is equivalent to a particular case of the tensor-force model with

$$\alpha_1^{110} = \frac{1}{2}\alpha_1 + \frac{4}{a^2}(\kappa_1 + \kappa_2) \tag{6.7}$$

$$\alpha_3^{110} = 0 \tag{6.8}$$

$$\beta_3^{110} = \frac{1}{2}\alpha_1 - \frac{4}{a^2}\kappa_1 \tag{6.9}$$

$$\alpha_1^{200} = \alpha_2 + \frac{4}{a^2}\kappa_1 \tag{6.10}$$

$$\alpha_2^{200} = -\frac{2}{a^2}\kappa_1 \tag{6.11}$$

Dispersion curves by the angular force model I for the face-centered cubic lattice —

From equation (3.61), we have obtained equations for the dispersion curves along some axes of symmetry.

(i) [100] direction.

Longitudinal lattice wave frequency,

$$\nu(L) = \frac{1}{2\pi}\left\{\frac{1}{M}\left[2\pi^2\nu_b^2 M(1-C_1) + (a\,c_{11} - \pi^2\nu_b^2 M)S_1^2\right]\right\}^{1/2} \tag{6.12}$$

Transverse lattice wave frequency,

$$\nu(T) = \frac{1}{2\pi}\left\{\frac{1}{M}\left[(ac_{12} + ac_{44} - 2\pi^2\nu_b{}^2M)\ (C_1-1)\right.\right.$$

$$\left.\left. + (\tfrac{1}{2}ac_{12} + \tfrac{3}{2}ac_{44} - \pi^2\nu_b{}^2M)\ S_1{}^2\right]\right\}^{1/2} \qquad (6.13)$$

(ii) [110] direction.

Longitudinal lattice wave frequency,

$$\nu(L) = \frac{1}{2\pi}\left\{\frac{1}{M}\left[(ac_{12} + ac_{44} - 2\pi^2\nu_b{}^2M)\ (C_1-1)\right.\right.$$

$$\left.\left. + (ac_{11} + \tfrac{3}{2}ac_{12} + \tfrac{5}{2}ac_{44} - \pi^2\nu_b{}^2M)\ S_1{}^2\right]\right\}^{1/2} \qquad (6.14)$$

Transverse lattice waves' frequencies,

$$\nu(T_1) = \frac{1}{2\pi}\left\{\frac{1}{M}\left[(ac_{12} + ac_{44} - 2\pi^2\nu_b{}^2M)\ (C_1-1)\right.\right.$$

$$\left.\left. + (ac_{11} - \tfrac{1}{2}ac_{12} + \tfrac{1}{2}ac_{44} - \pi^2\nu_b{}^2M)\ S_1{}^2\right]\right\}^{1/2} \qquad (6.15)$$

and

$$\nu(T_2) = \frac{1}{2\pi}\left\{\frac{1}{M}\left[2\pi^2\nu_b{}^2M\ (1-C_1) + (2ac_{44} - \pi^2\nu_b{}^2M)\ S_1{}^2\right]\right\}^{1/2} \qquad (6.16)$$

(iii) [111] direction

Longitudinal lattice wave frequency,

$$\nu(L) = \frac{1}{2\pi} \left\{ \frac{a}{M} [c_{11} + 2c_{12} + 4c_{44}] \right\}^{1/2} S_1 \qquad (6.17)$$

Transverse lattice wave frequency,

$$\nu(T) = \frac{1}{2\pi} \left\{ \frac{a}{M} [c_{11} - c_{12} + c_{44}] \right\}^{1/2} S_1 \qquad (6.18)$$

Dispersion curves by the angular force model II for the face-centered cubic lattice -

From equation (4.100), we have obtained equations for the dispersion curves along some axes of symmetry.

(i) [100] direction.

Longitudinal lattice wave frequency,

$$\nu(L) = \frac{1}{2\pi} \left\{ \frac{1}{M} [2\pi^2 \nu_b^2 M (1-C_1) + (ac_{11} - \pi^2 \nu_b^2 M) S_1^2] \right\}^{1/2} \qquad (6.19)$$

Transverse lattice wave frequency

$$\nu(T) = \frac{1}{2\pi} \left\{ \frac{1}{M} [\pi^2 \nu_b^2 M (1-C_1) + (ac_{44} - \tfrac{1}{2} \pi^2 \nu_b^2 M) S_1^2] \right\}^{1/2} \qquad (6.20)$$

(ii) [110] direction

Longitudinal lattice wave frequency,

$$\nu(L) = \frac{1}{2\pi}\left\{\frac{1}{M}\left[\pi^2\nu_b{}^2M\,(1-C_1) + (ac_{11} + ac_{12} + 2ac_{44} - \frac{1}{2}\pi^2\nu_b{}^2M)\,S_1{}^2\right]\right\}^{1/2}$$

Transverse lattice waves' frequencies,

(6.21)

$$\nu(T_1) = \frac{1}{2\pi}\left\{\frac{1}{M}\left[\pi^2\nu_b{}^2M\,(1-C_1) + (ac_{11} - ac_{12} - \frac{1}{2}\pi^2\nu_b{}^2M)S_1{}^2\right]\right\}^{\frac{1}{2}} \qquad (6.22)$$

$$\nu(T_2) = \frac{1}{2\pi}\left\{\frac{1}{M}\left[2\pi^2\nu_b{}^2M\,(1-C_1) + (2ac_{44} - \pi^2\nu_b{}^2M)\,S_1{}^2\right]\right\}^{1/2} \qquad (6.23)$$

(iii) [111] direction

Longitudinal lattice wave frequency,

$$\nu(L) = \frac{1}{2\pi}\left\{\frac{a}{M}\left[c_{11} + 2c_{12} + 4c_{44}\right]\right\}^{1/2} S_1 \qquad (6.24)$$

Transverse lattice wave frequency,

$$\nu(T) = \frac{1}{2\pi}\left\{\frac{a}{M}\left[c_{11} - c_{12} + c_{44}\right]\right\}^{1/2} S_1 \qquad (6.25)$$

On comparing equations (6.12) and (6.19), (6.16) and (6.23), (6.17) and (6.24), (6.18) and (6.25), we find that the longitudinal dispersion curves in the [100] direction, the transverse dispersion curves

T_2 (vibrating along the [001] direction) in the [110] direction, the longitudinal and the transverse dispersion curves in the [111] direction, are identical for the two angular force models. This is also seen in the corresponding figures.

Upon examining Tables 3 and 4 in Chapter V, we find that for both models, in general, the first neighbour central force parameter, α_1, is of magnitude ten to twenty times those of the corresponding second neighbour force parameter, α_2. For the metals investigated, all α_1 and α_2 are positive except α_2 of aluminum in Model II. In general, the angular force parameters in Model I, σ_1 and σ_2 are of the same order of magnitude as α_2 while those in Model II are smaller. The angular force parameters in Model II are smaller in magnitude than those in Model I. Their signs vary from metal to metal and from model to model. In the case of copper, $\kappa_1/(a^2)$ is very small in comparison with the others.

Copper

On examining the dispersion curves of copper (Figs. 6-1 and 6-2), we find that in the [ζ00] and the [ζζ0] direction, Model II gives reasonably good result while the transverse dispersion curve along the [ζ00] direction and the dispersion curve T_2 in the [ζζ0] direction in Model I gives values below that of the experimental points by about 15%. The dispersion curves in the [ζζζ] direction are satisfactory. (They are identical for these two models). The experimental values shown in the

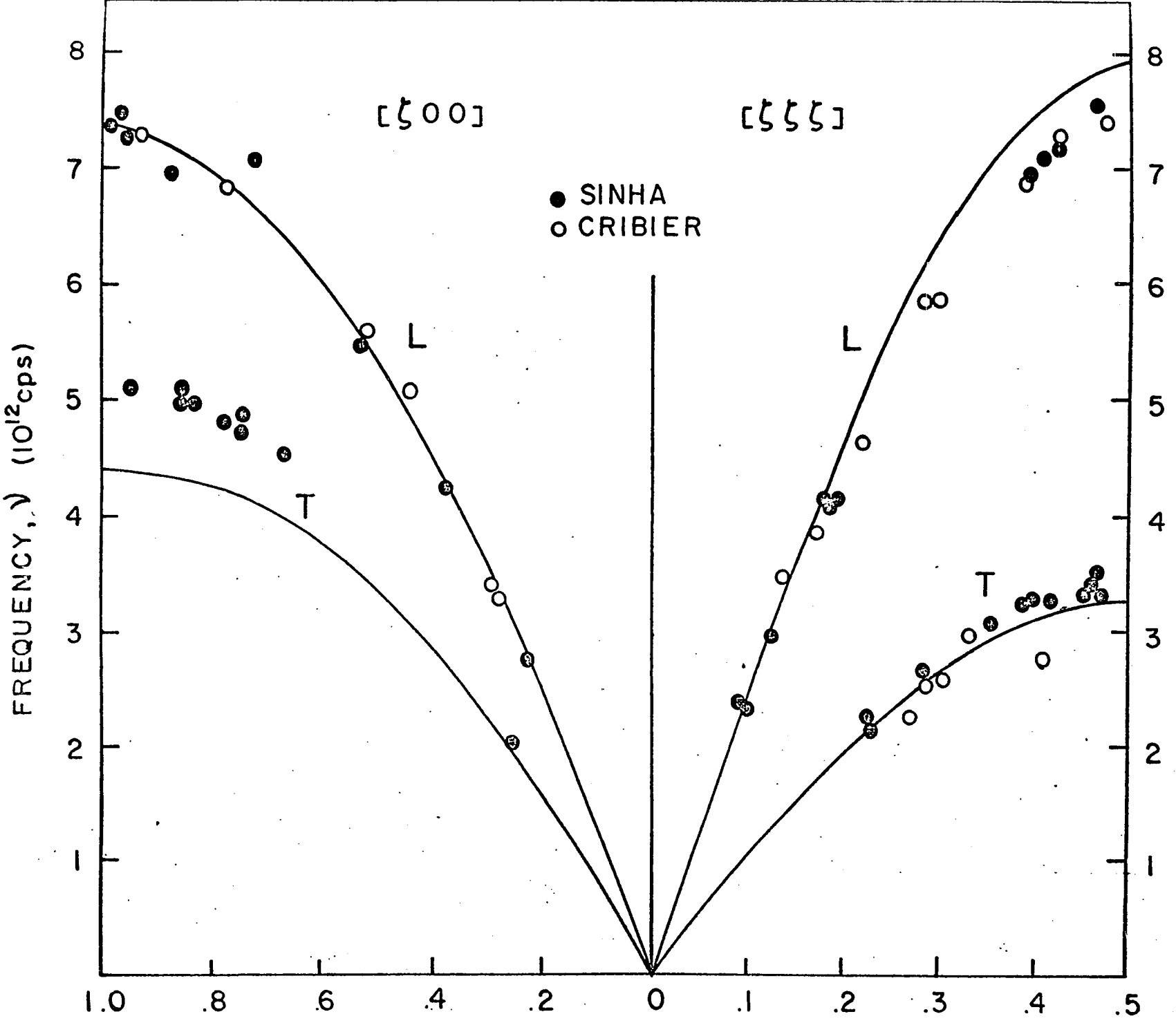

Fig. 6-1 (a) Copper (AFM-1, 300°K)

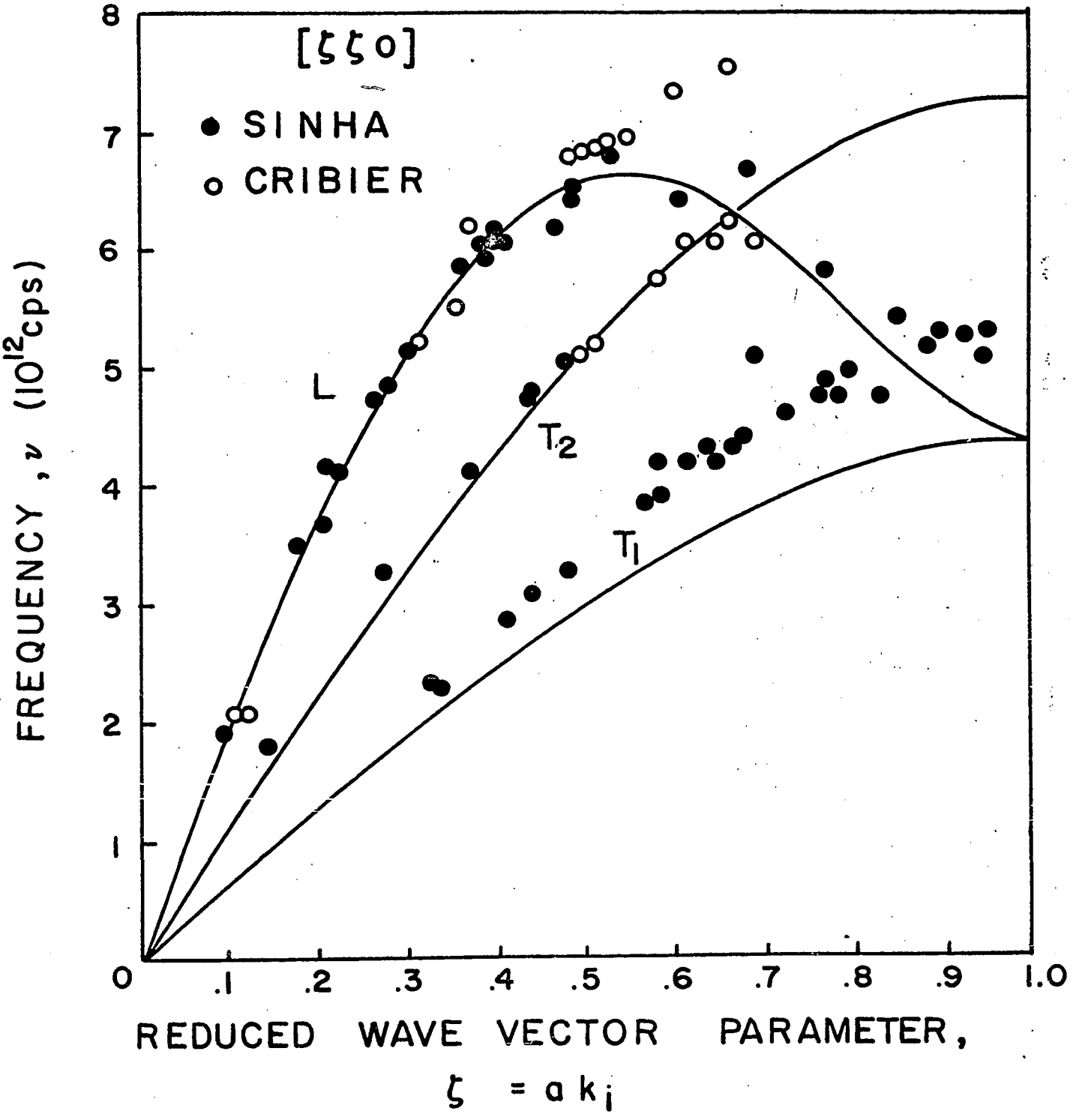

Fig. 6-1(b) Copper (AFM-II, 300°K)

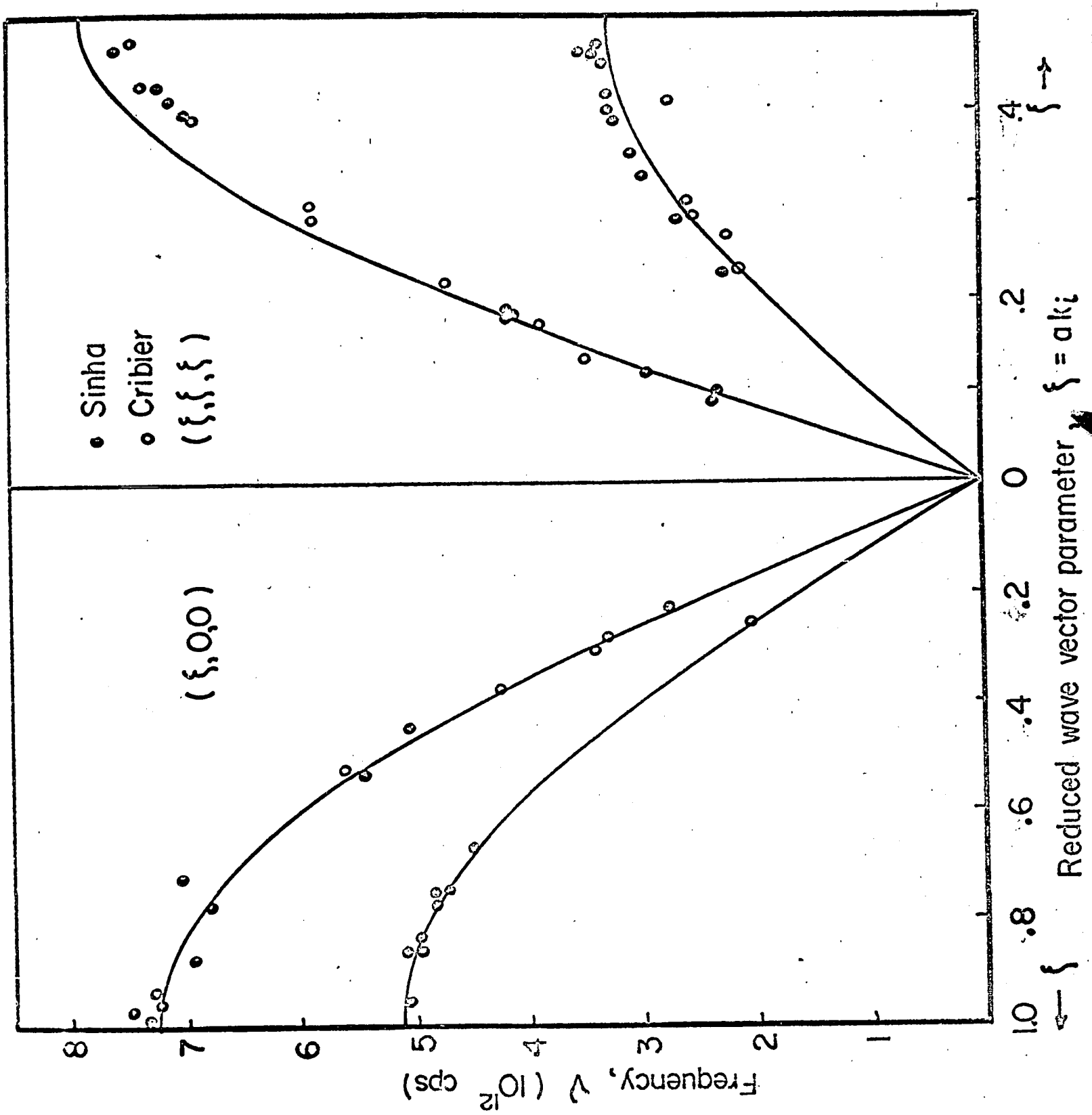

Fig. 6-2(a). Dispersion curves of copper by AFM-II at 300°K.

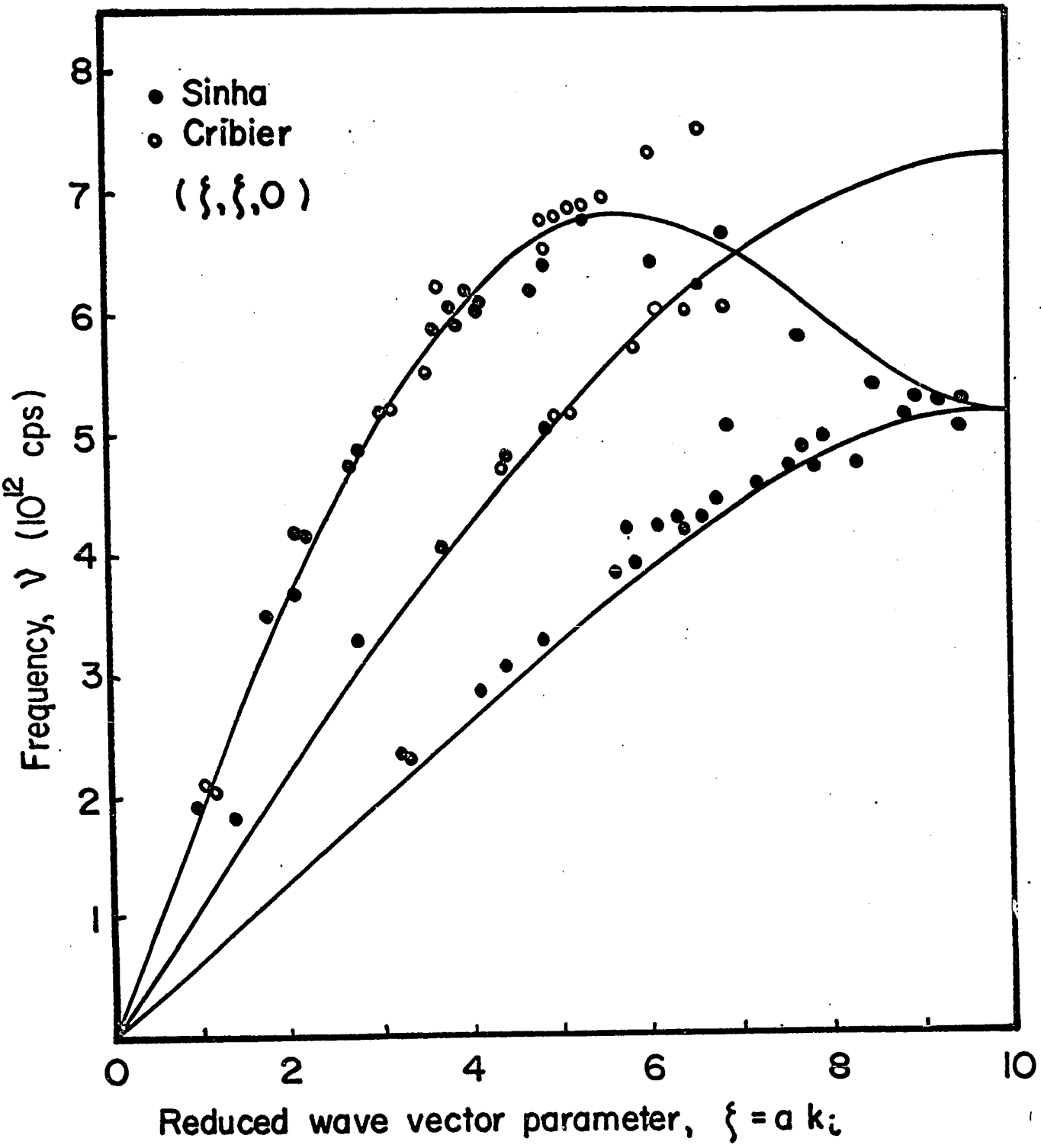

Fig. 6-2(b) Dispersion curves of copper by AFM-II at 300°K.

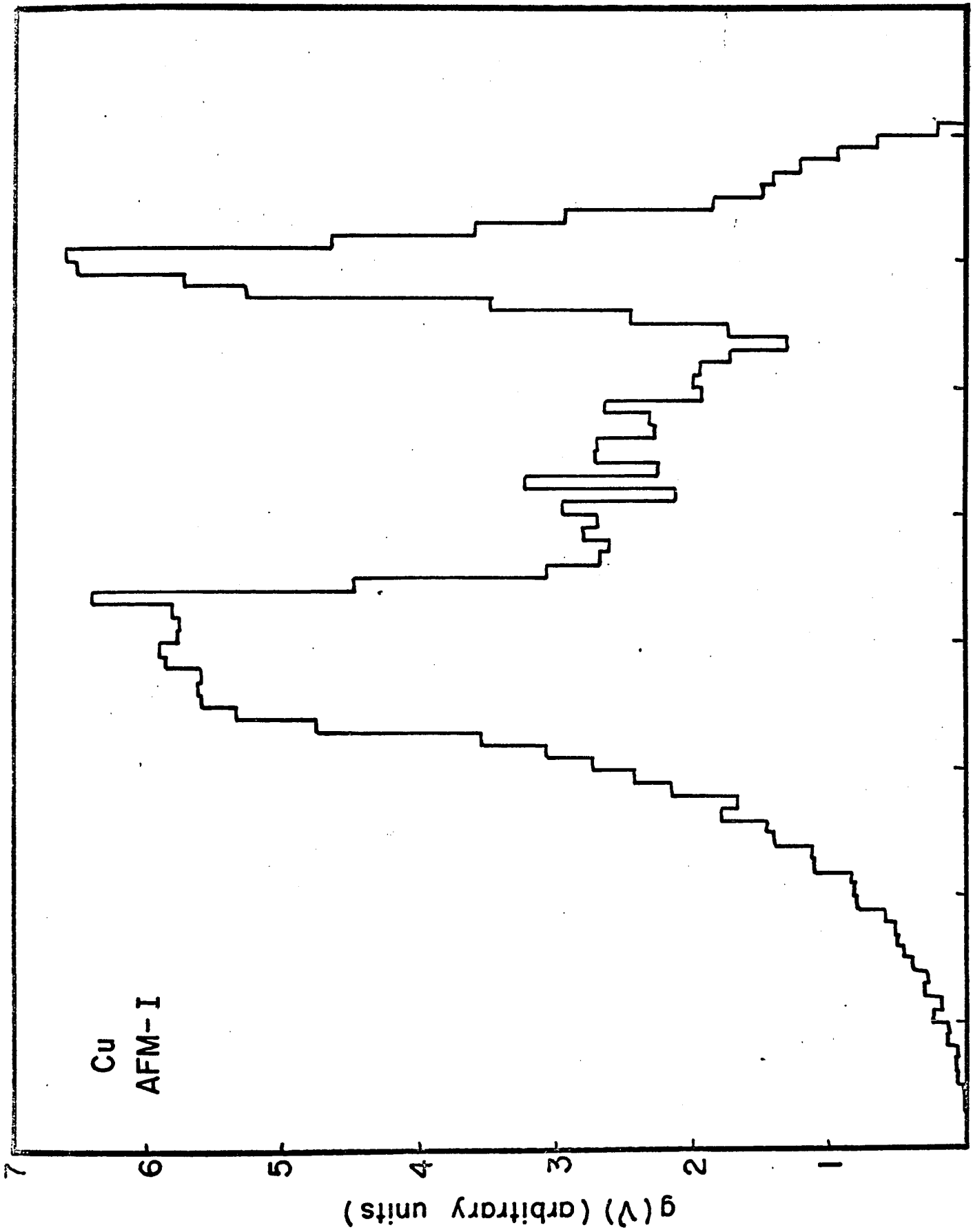

Fig. 6-3.

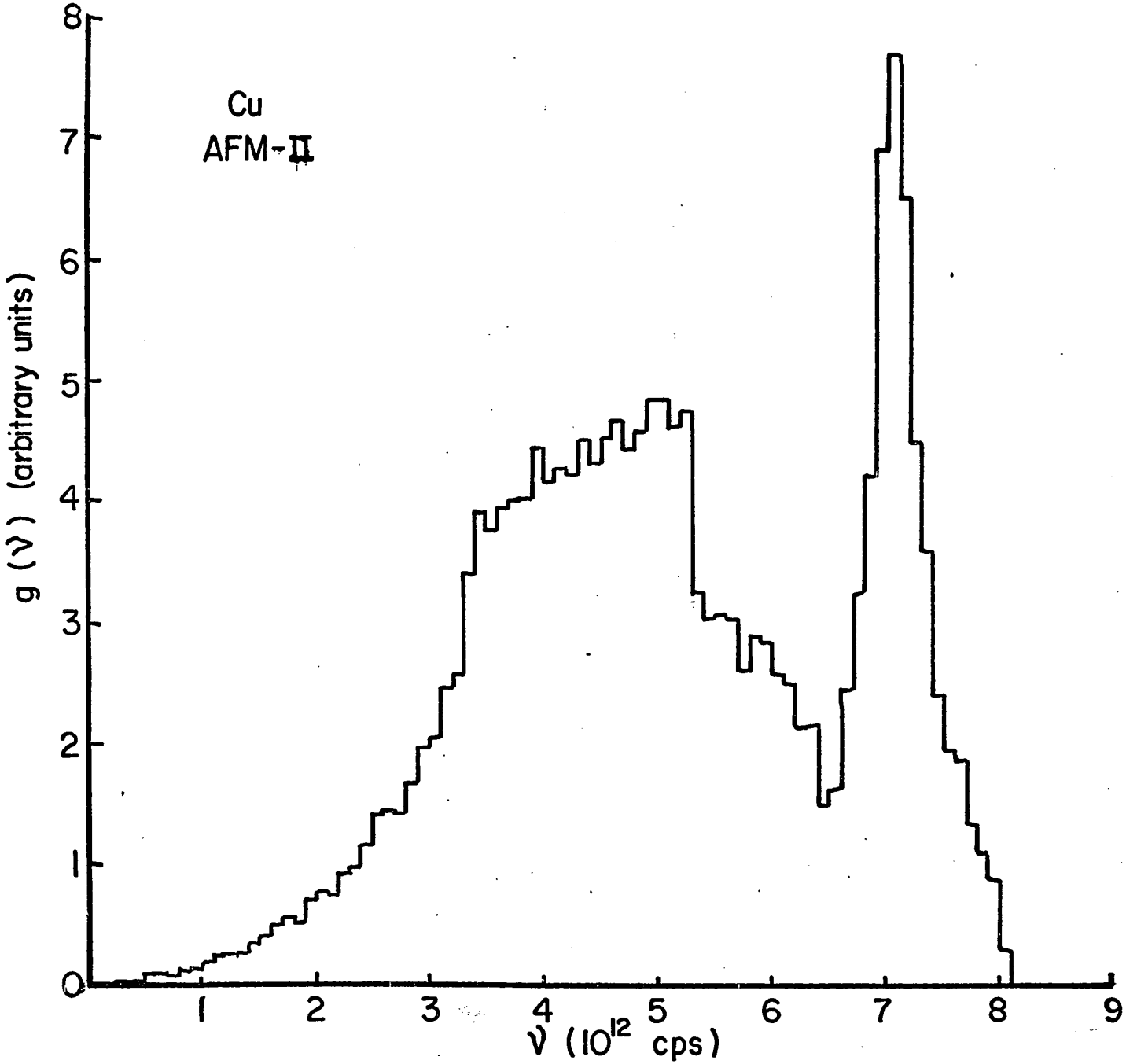

Fig. 6-4. Frequency Spectra of Copper.

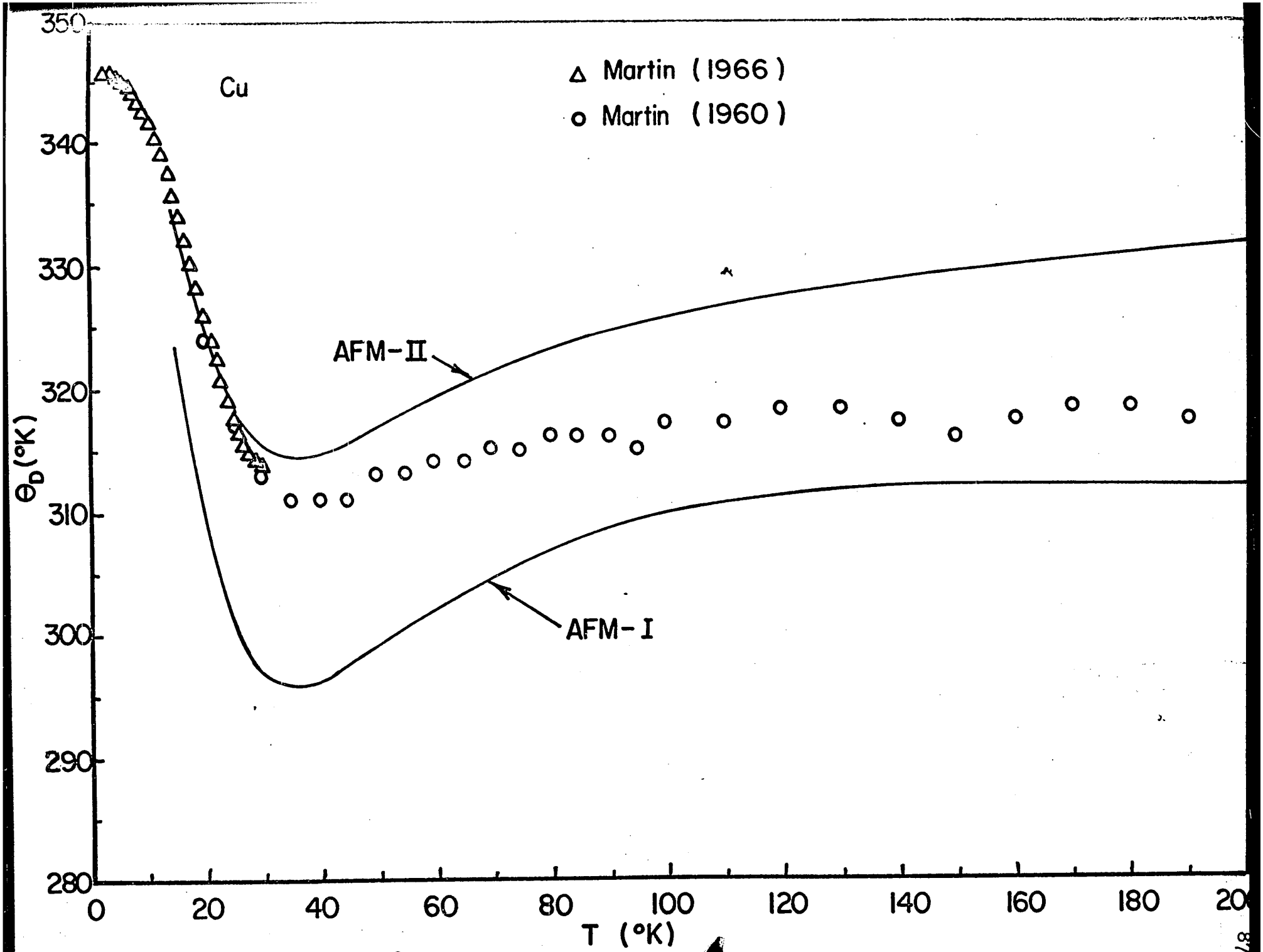

Fig. 6-5. Debye temperature of copper.

diagrams are due to Sinha [34] and Cribier [46]. Very similar results have been obtained by Svensson, Brockhouse and Rowe [35] by a different method.

The frequency spectrum of copper in model I (Fig. 6-3) has a broad peak at frequency about 4×10^{12} cps and a sharp peak of approximately the same height at a frequency of 7×10^{12} cps. The frequency spectrum of copper in model II (Fig. 6-4) has a broad peak at about 45×10^{12} cps and a sharp peak of about double its height at 7×10^{12} cps. This spectrum is in good agreement with that obtained by Varshni and Shukla [26], using a third-neighbour tensor-force model.

The Debye temperature curves of copper for the two models are of the same shape (Fig. 6-5). Model II gives better agreement with the experimental results at low temperature while model I gives better results at higher temperature. Moreover, it approaches to a constant value of about 312°K for temperatures higher than 140°K. The experimental values of Debye temperatures are from Martin [47, 48].

Aluminum

In the case of aluminum, Model II gives better result of dispersion curves than that of Model I (Figs. 6-6 and 6-7). The longitudinal dispersion curve in the $[\zeta 00]$ direction, the transverse dispersion curve T_2 in the $[\zeta\zeta 0]$ direction and the transverse dispersion curve in the $[\zeta\zeta\zeta]$ direction are reasonable. The experimental values have been obtained by Stedman and Nilsson [36] at 80°K.

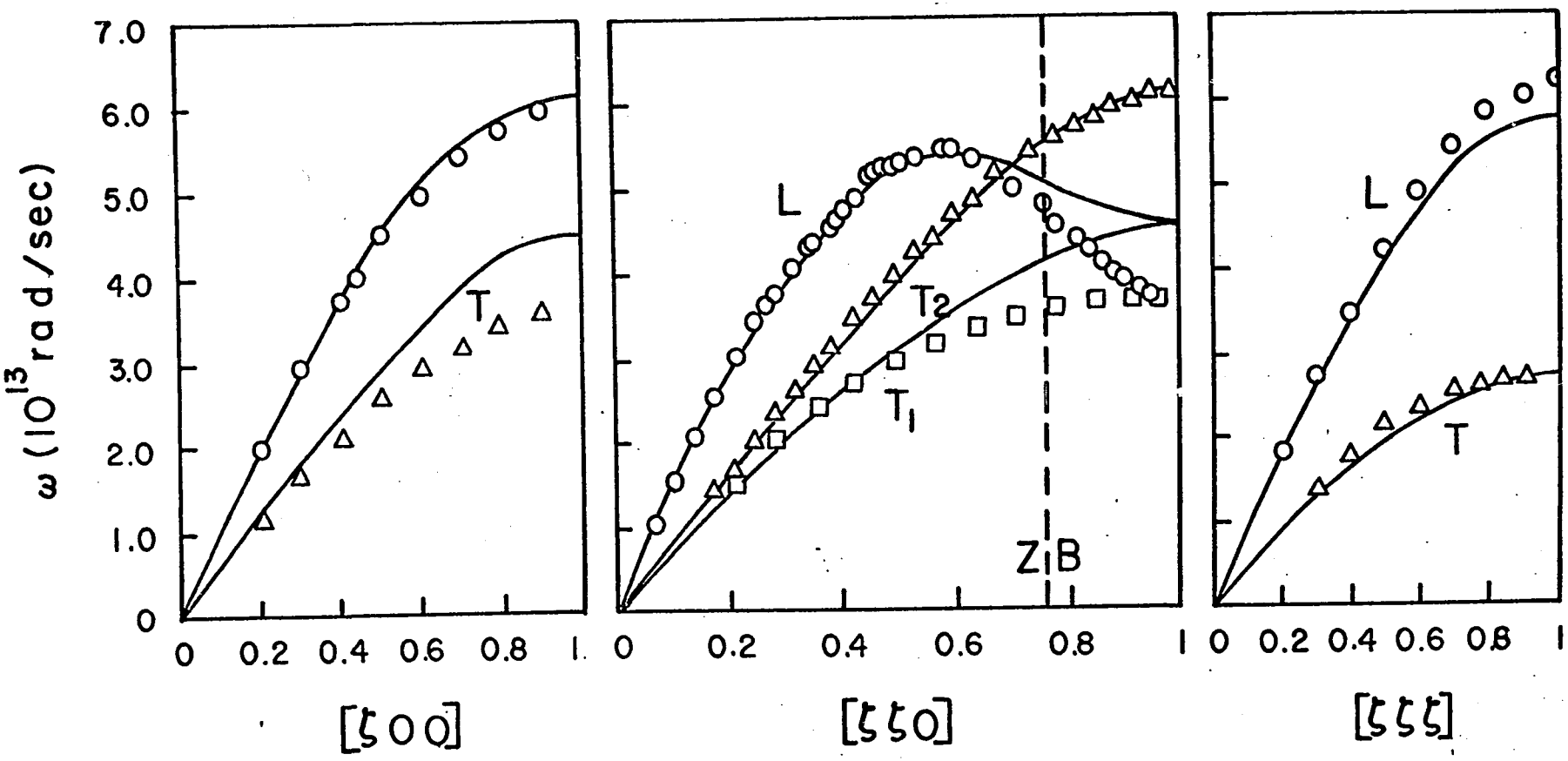

REDUCED WAVE VECTOR PARAMETER, $\zeta = ak_i$

Fig. 6-6 Aluminum (AFM-1, 80°K)

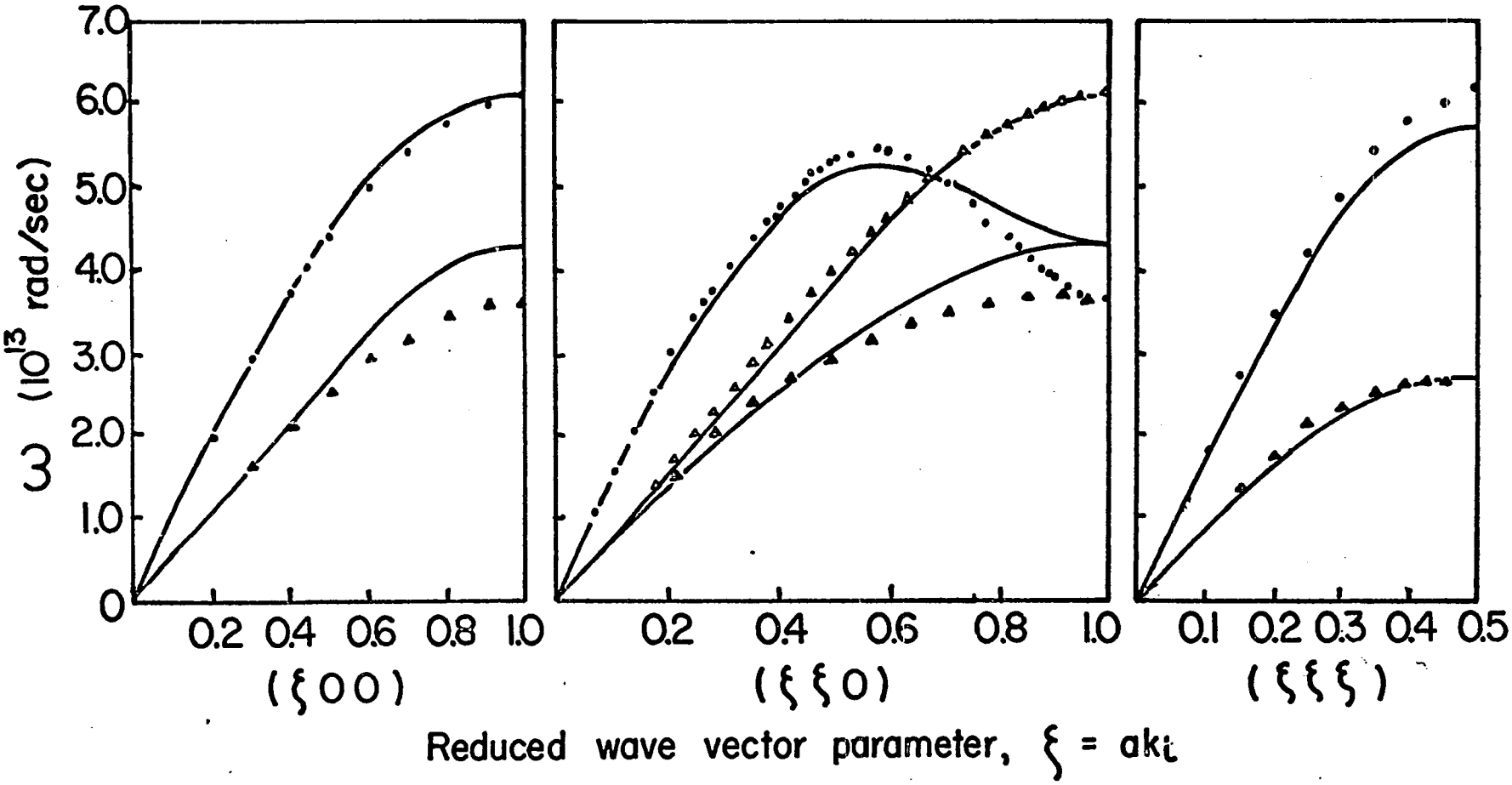

Fig. 6-7. Dispersion curves of Aluminum by AFM-II (80°K).

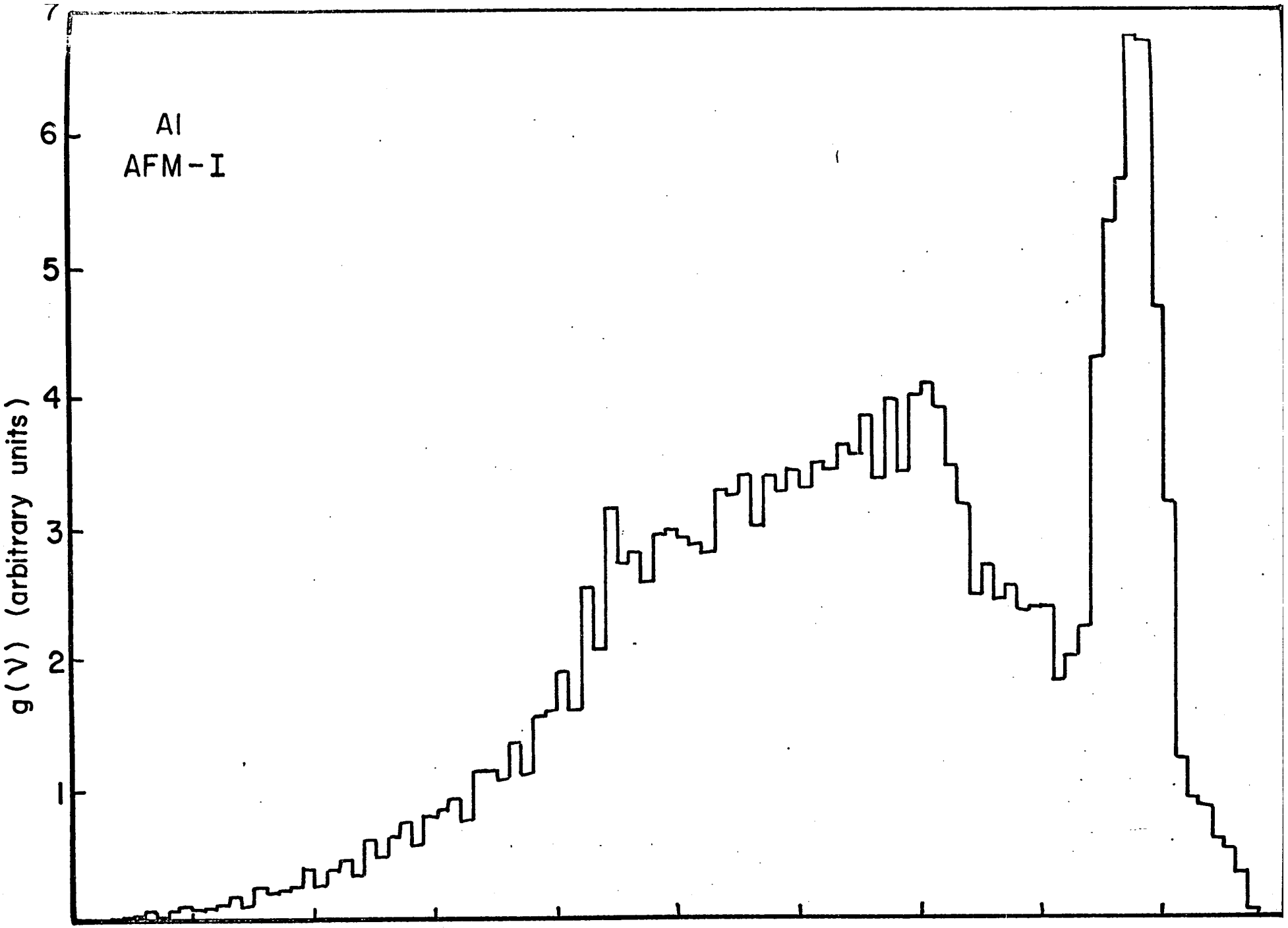

Fig. 6-8.

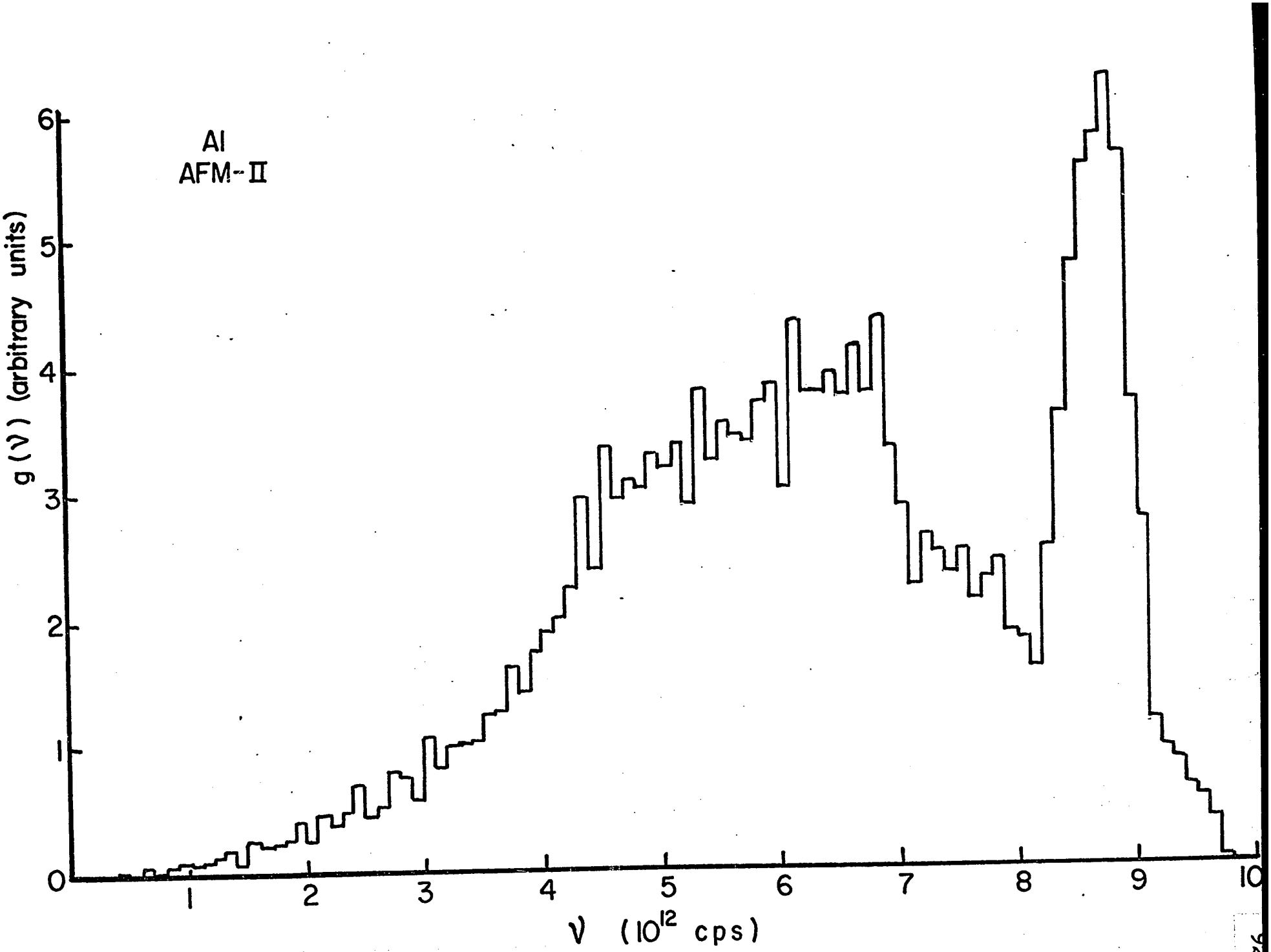

Fig. 6-9. Frequency Spectra of Aluminum.

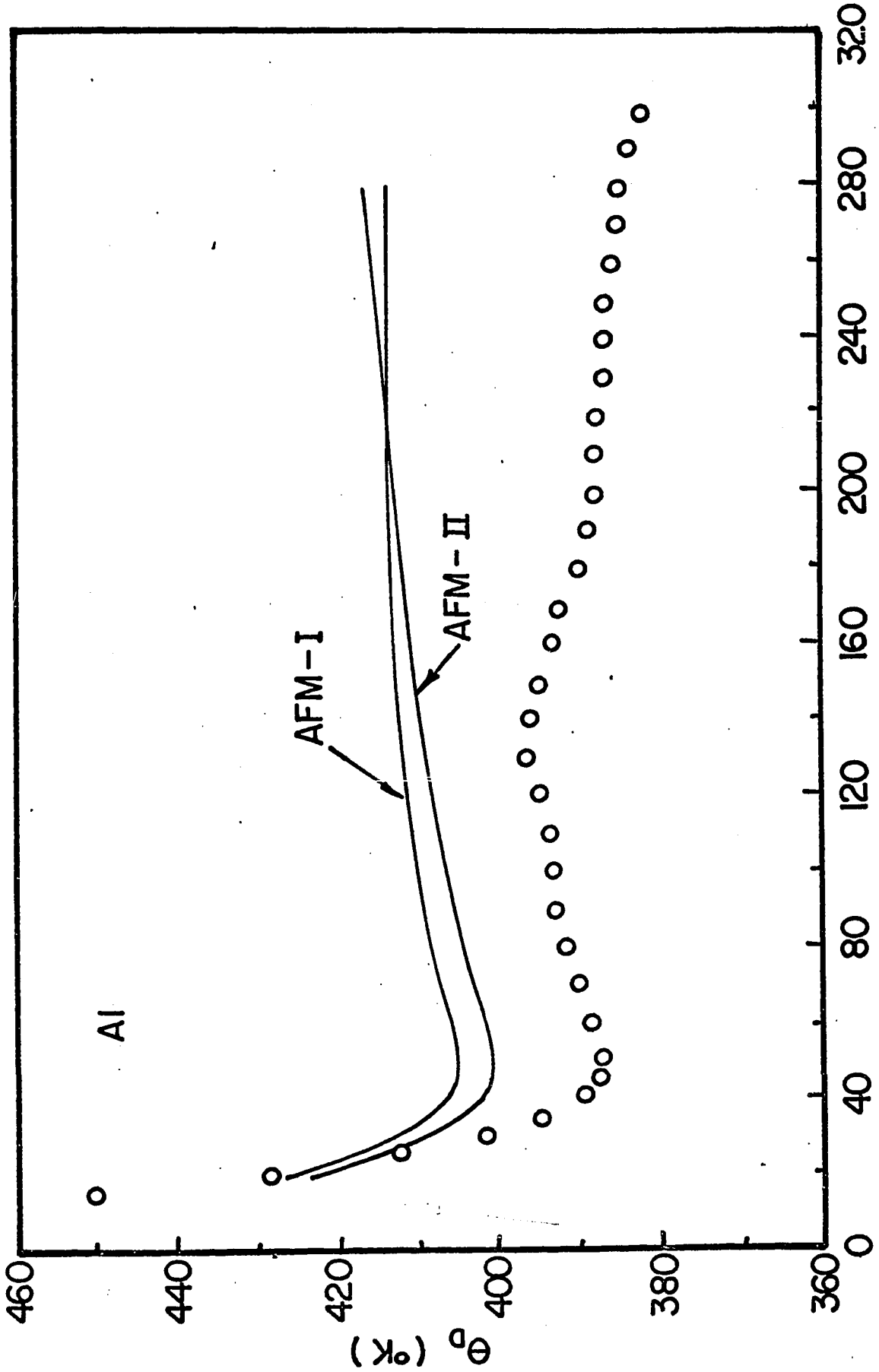

Fig. 6-10. Debye temperature of Aluminum.

The frequency spectra of aluminum for the two models are similar (Figs. 6-8 and 6-9). Both give a broad peak in the range of ν from 5×10^{12} cps to 7×10^{12} cps, and a sharper and higher peak at about 8.8×10^{12} cps. These are compatible with that obtained by Varshni and Shukla [26], using an axially symmetric model.

The Debye temperature curves for the two models show the same characteristic as those of copper, namely, Model II gives better result in low temperatures while Model I gives better result (which approaches to a constant value), at higher temperatures (Fig. 6-10). Except for the 0°K point the experimental θ's are from the work of Giauque and Meads [49] corrected for the electronic contribution [50]. The 0°K value is due to Phillips [50].

Nickel

Model II gives reasonably good result of dispersion curves of nickel (Fig. 6-12) except the longitudinal dispersion curves in the [ζζζ]. direction. This result is better than that provided by Model I. (Fig. 6-11).

The frequency spectrum of nickel in Model II has a broad peak in the range of frequency between 4.5×10^{12} cps and 6×10^{12} cps, and a sharper and higher peak at about 8.3 cps (Fig. 6-14). This is in good agreement with that calculated by Birgeneau et al. [37] using a fourth-neighbour tensor-force model, and the experimental results obtained by Tchernoplekov et al. [51], Brugger [52], and Mozer et al. [53]. The spectrum provided by Model I is not so encouraging. (Fig. 6-13).

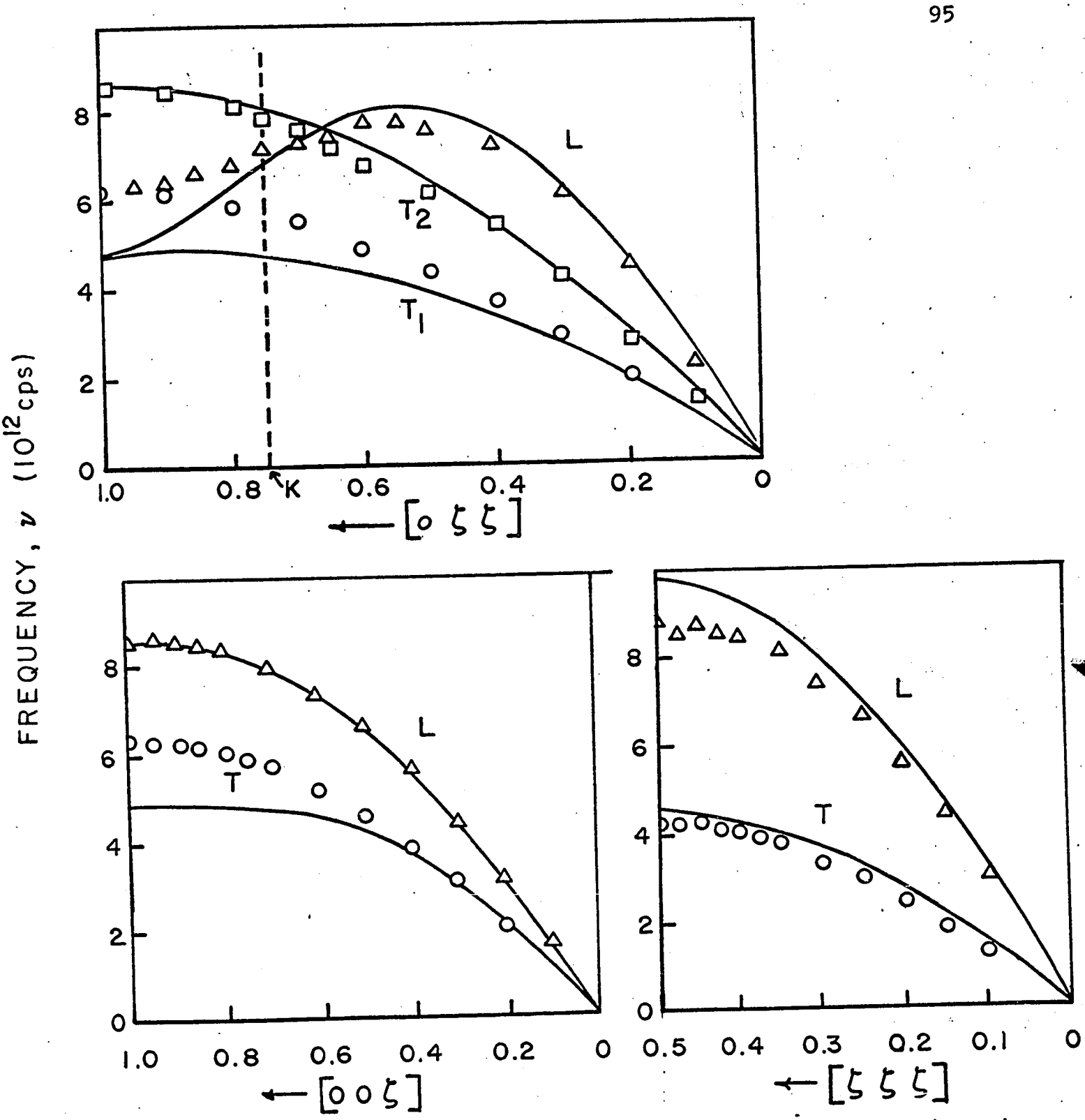

Fig. 6-11 Nickel (AFM - 1, 296°K)

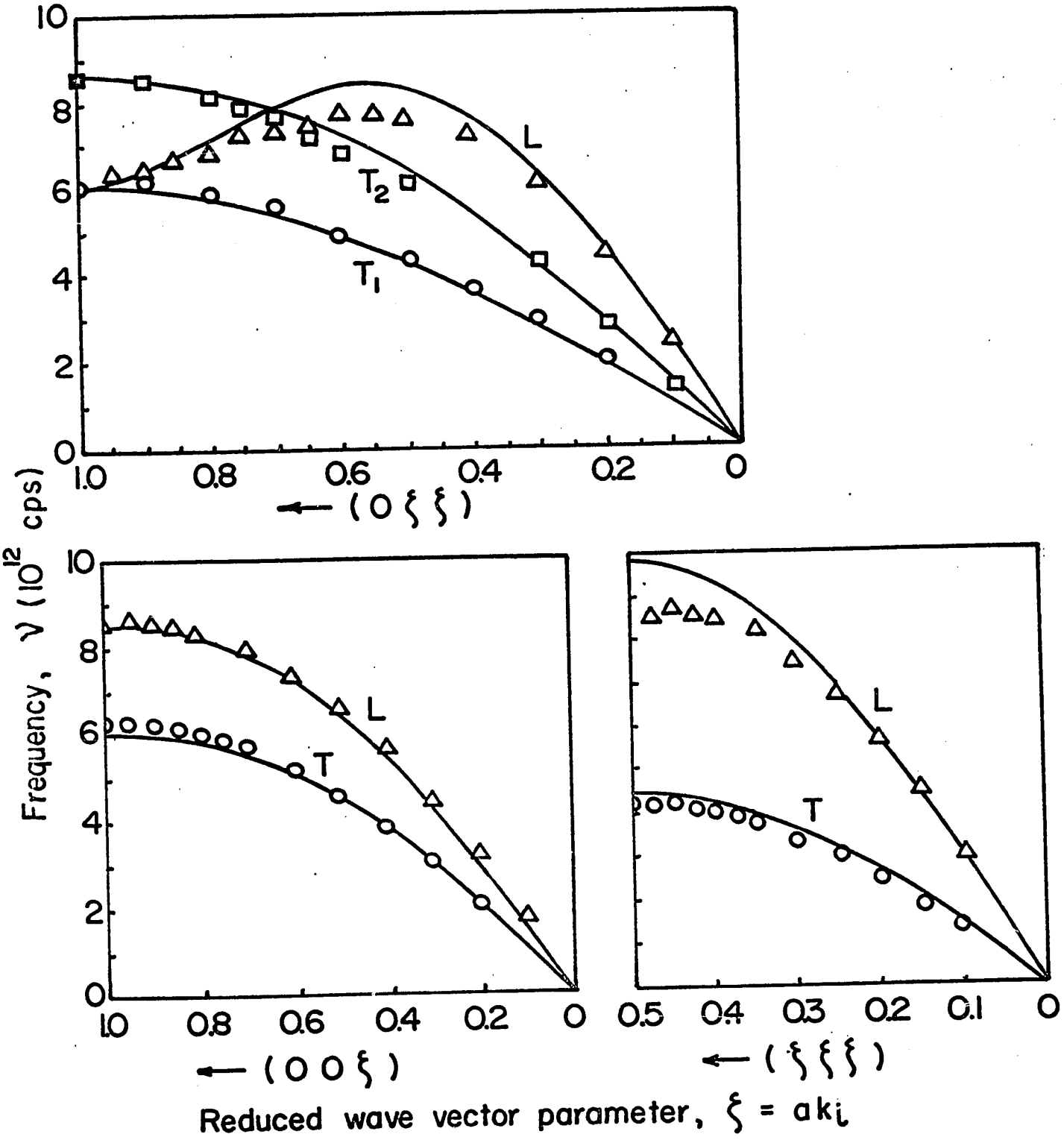

Fig. 6-12. Dispersion curves of Nickel by AFM-II at 296°K.

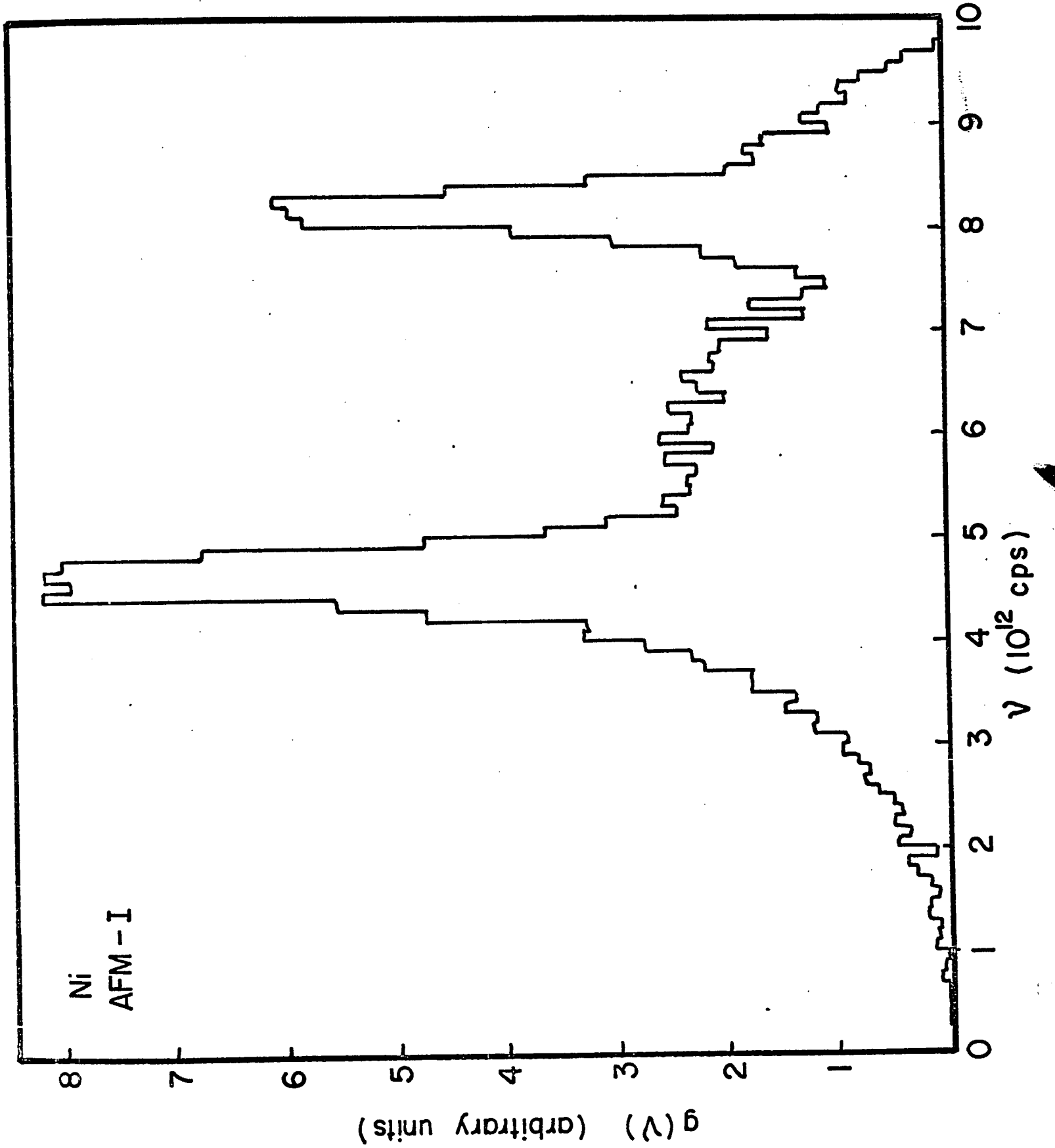
Ni
AFM-I
g(V) (arbitrary units)
ν (10^12 cps)
0
1
2
3
4
5
6
7
8
9
10

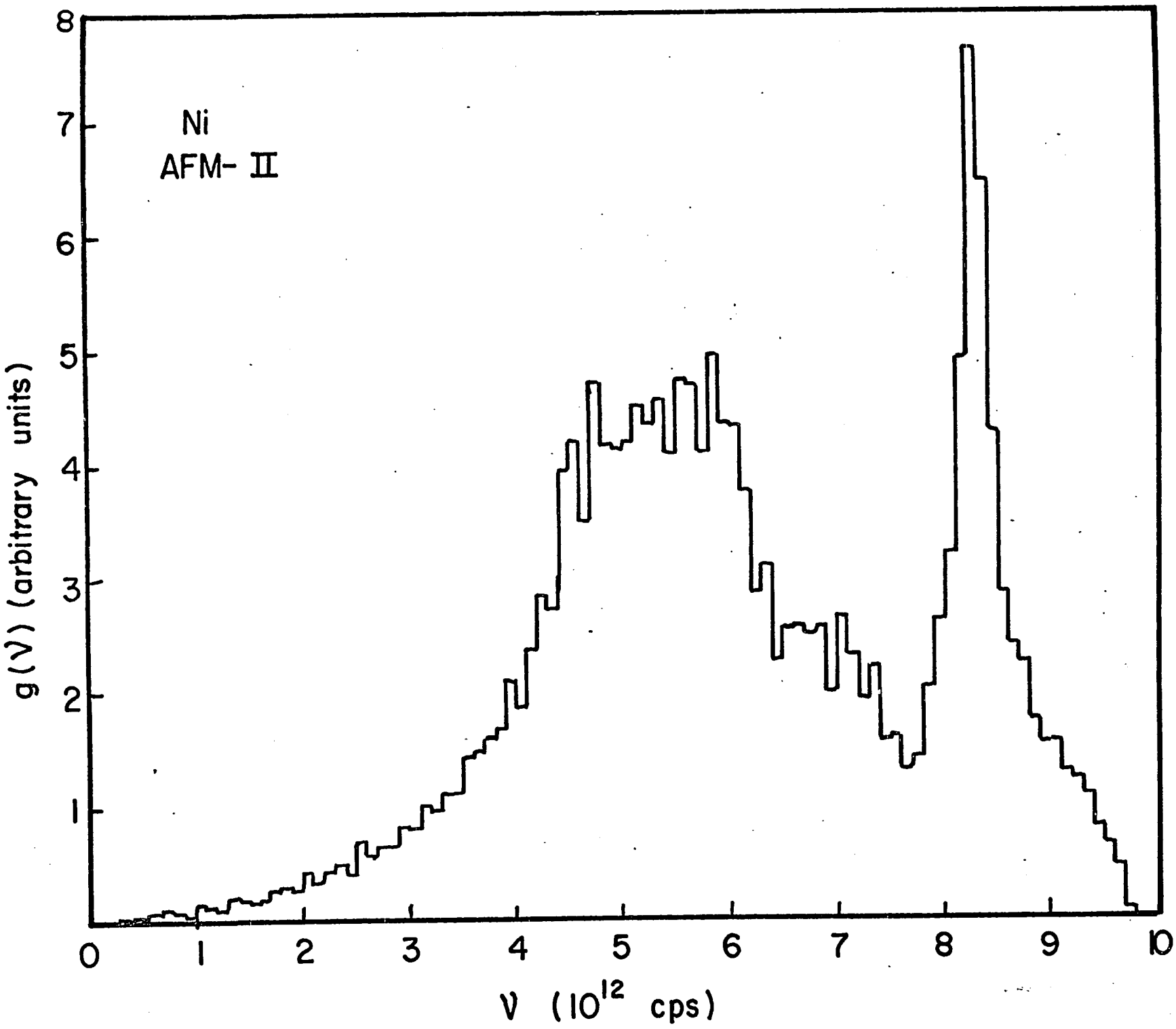

Fig. 6-14

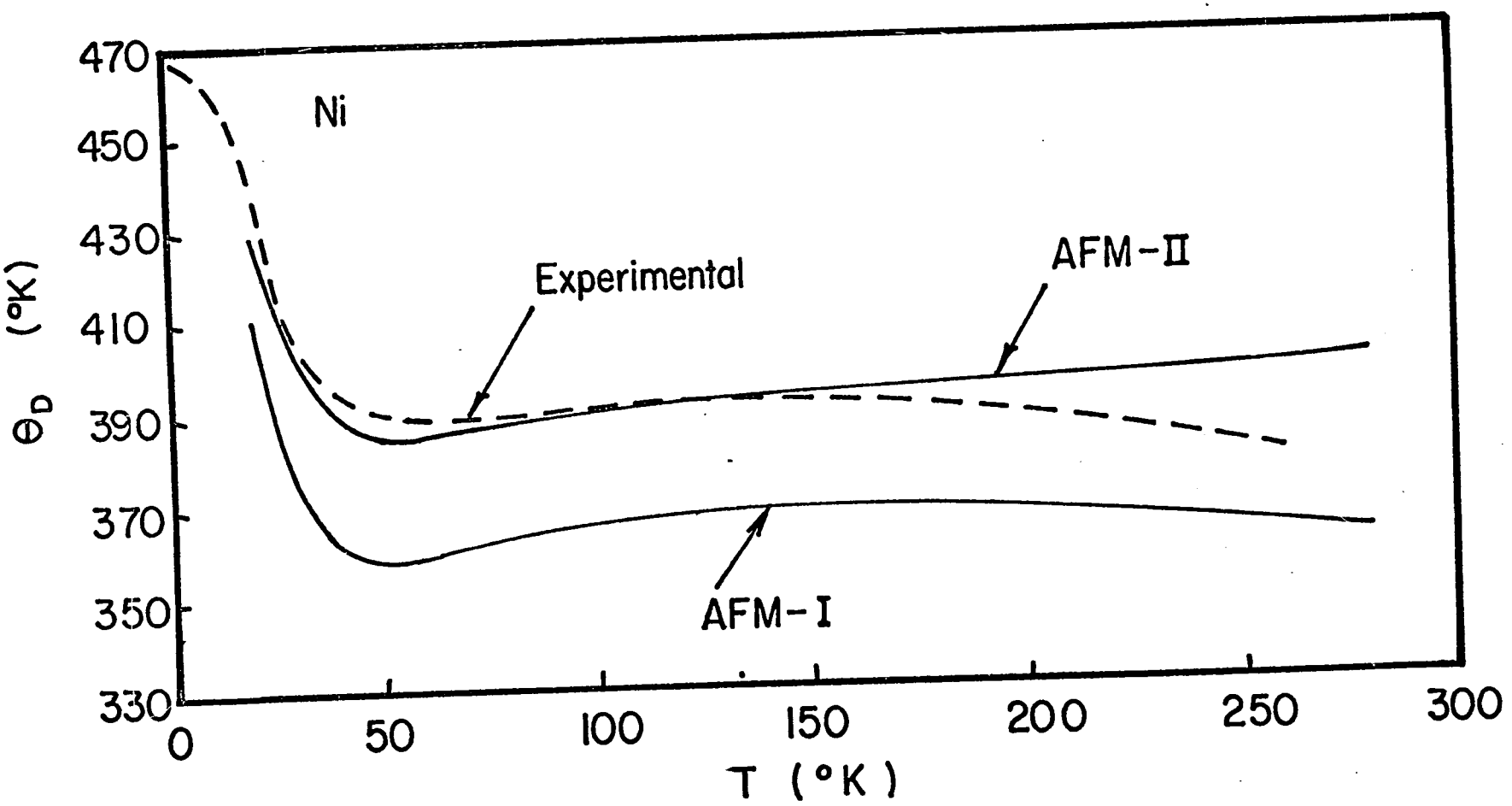

Fig. 6-15. Debye temperature of Nickel.

The "experimental" curve for Debye temperatures shown in Fig. 6-15 represents the experimental heat capacity data of Busey and Giauque [54] and of Rayne and Kemp [55] as interpreted by the latter authors. The analysis of heat capacity (C_v) data for nickel is complicated by the existence of a magnetic contribution C^m, in addition to the usual conduction electron (C^e) and lattice (C^l) terms. Thus an analysis of $C_v(T)$ for $T < 10°K$ by means of the formula,

$$C_v = C^e + C^l = \gamma T + \beta T^3$$

is quite inadequate in the case of nickel. In the absence of a magnetic field, the dominant term [56] in C^m is of the form $AT^{3/2}$ for low T. The existing C_v data for nickel are not sufficiently precise to determine the value of A. This can be found, however, from saturation magnetization measurements, and the appropriate allowance for C^m made in the analysis of C_v. In this way, Rayne and Kemp [55] have deduced the "experimental" curve shown in Fig. 6-15. Model II provides reasonable result in comparison with the experimental curve. The theoretical curve tends to a constant at higher temperature. On the other hand at temperatures higher than 260°K, it seems that the results by Model I are in better agreement.

As a conclusion, we find that the angular force Model II provides reasonably good results for dispersion curves, frequency spectra, and Debye temperatures. Though only four force parameters are used, the results

are comparable to those obtained from models with more parameters.

The histograms and Debye temperatures for copper and aluminum were calculated from the force constants at 0°K. It is possible that the disagreement with Debye temperatures at high temperatures could be lessened if force constants appropriate to those temperatures are used.

(2) Body-centered cubic lattice -

Upon equating the secular equation (3.20) and the secular equation of a second neighbour tensor-force model for the b.c.c. lattice (see footnote in p. 74), we find that, as far as the frequency spectrum is concerned, the angular force Model I for b.c.c. lattice is equivalent to the second-neighbour tensor-force model with the following identities,

$$\frac{4}{3}(\alpha_1 + 2\eta_1) = \overset{111}{\alpha_1} \tag{6.26}$$

$$\alpha_2 = \overset{200}{\alpha_1} \tag{6.27}$$

$$\eta_2 = \overset{200}{\alpha_2} \tag{6.28}$$

and

$$\frac{1}{3}(\alpha_1 - \eta_1) = \overset{111}{\beta_1} \tag{6.29}$$

The angular force Model II for b.c.c. lattice, which also involves 4 constants is equivalent to the second neighbour tensor-force model with

the following identities,

$$\frac{\alpha_1}{3} + \frac{16\mu_1}{9a^2} + \frac{8\mu_2}{3a^2} = \overset{111}{\alpha_1} \tag{6.30}$$

$$\alpha_2 + \frac{32\mu_1}{9a^2} = \overset{200}{\alpha_1} \tag{6.31}$$

$$-\frac{8\mu_1}{9a^2} + \frac{4\mu_2}{3a^2} = \overset{200}{\alpha_2} \tag{6.32}$$

$$\frac{\alpha_1}{3} - \frac{8\mu_1}{9a^2} + \frac{4\mu_2}{3a^2} = \overset{111}{\beta_1} \tag{6.33}$$

If in equation (3.20), we use $\overset{111}{\alpha_1}$, $\overset{200}{\alpha_1}$, $\overset{200}{\alpha_2}$ and $\overset{111}{\beta_1}$ as the parameter instead of α_1, α_2, η_1, η_2, that is, by substituting (6.26), (6.27), (6.28) and (6.24) into (3.20), we get a secular equation which would be identical to that obtained by substituting $\overset{111}{\alpha_1}$, $\overset{200}{\alpha_1}$, $\overset{200}{\alpha_2}$ and $\overset{111}{\beta_1}$ into equation (4.50). From this, it is obvious that the two angular force models are equivalent as far as the frequency spectrum is concerned.

An examination of Tables 6 and 7 in Chapter V, shows that in both models, in general, the first neighbour force parameter α_1, is of magnitudes two or three timesthose of the second neighbour force parameter

α_2. In the case of molybdenum in Model II the values of α_2 are larger than those of α_1. The signs of the values of α_1 and α_2 in both models are positive.

In general, the values of the angular force parameters, η_1 or μ_1/a^2 are smaller than α_1 by a factor of thirty or forty. η_1 values are greater than η_2 values and $\mu_1/(a^2)$ values are greater than $\mu_2/(a^2)$ values with the exception for Ta. In general, the values of η_1 are greater than those of $\mu_1/(a^2)$ and the values of η_2 are greater than those of $\mu_2/(a^2)$. In the cases of molybdenum, tungsten and iron, the values of $\mu_2/(a^2)$ are around one-tenth of those of $\mu_1/(a^2)$ and are negligible in comparison with those of α_1. This is why Clark et al. [23] have obtained reasonable result for dispersion curves of iron, by means of a three constant angular force model.

The signs of η_1 are all negative. The signs of η_2 and $\mu_2/(a^2)$ are all positive except those for tantalum. The signs of $\mu_1/(a^2)$ are all negative except those for tantalum.

The magnitude and signs of the angular force parameters of tantalum show that its behaviour is different from the other metals considered here.

Sodium

The dispersion curves of sodium in Fig. 6-16 are in good accord with the experimental results of Woods et al [42].

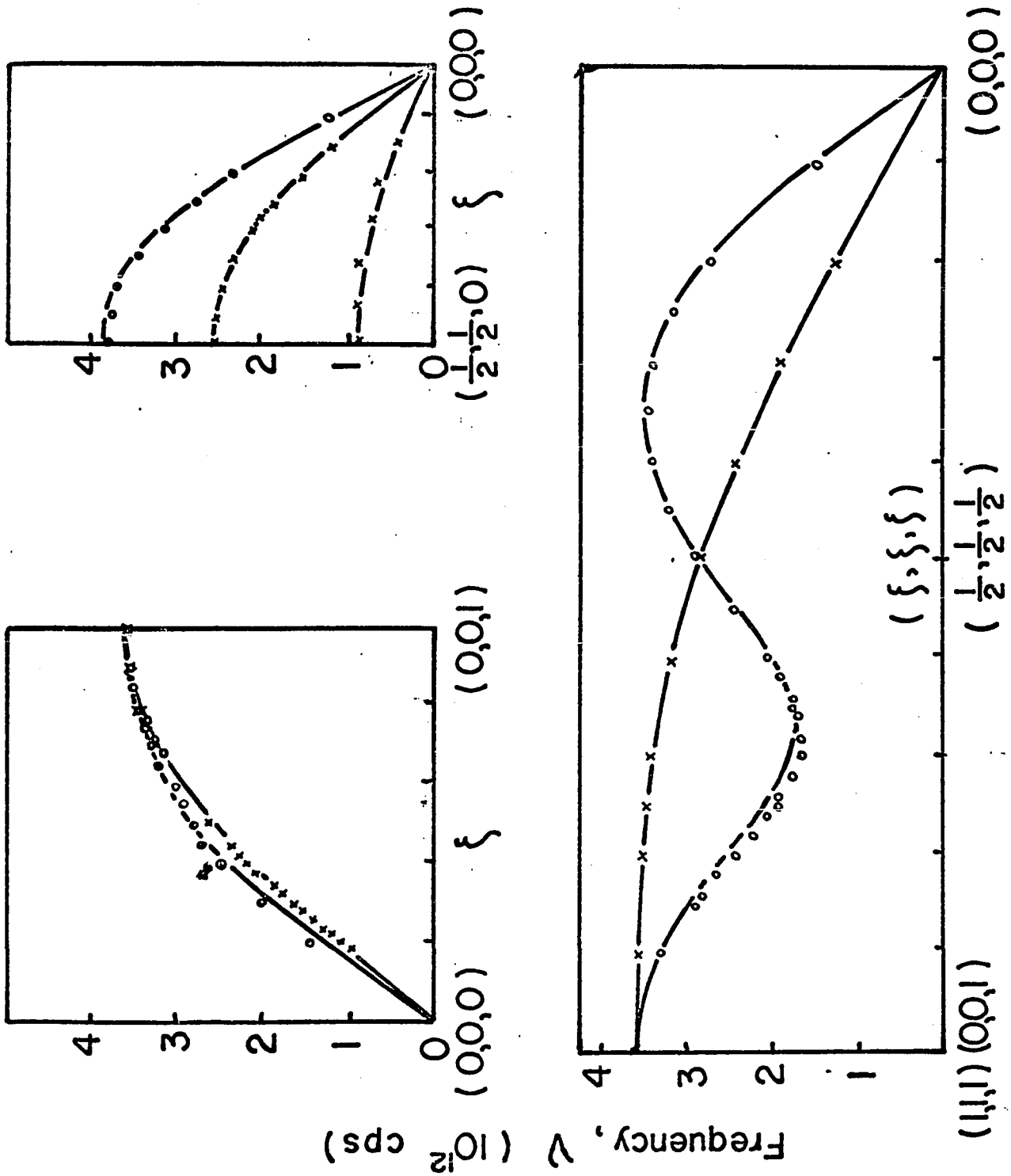

Fig. 6-16. Dispersion curves of sodium at 90°K.

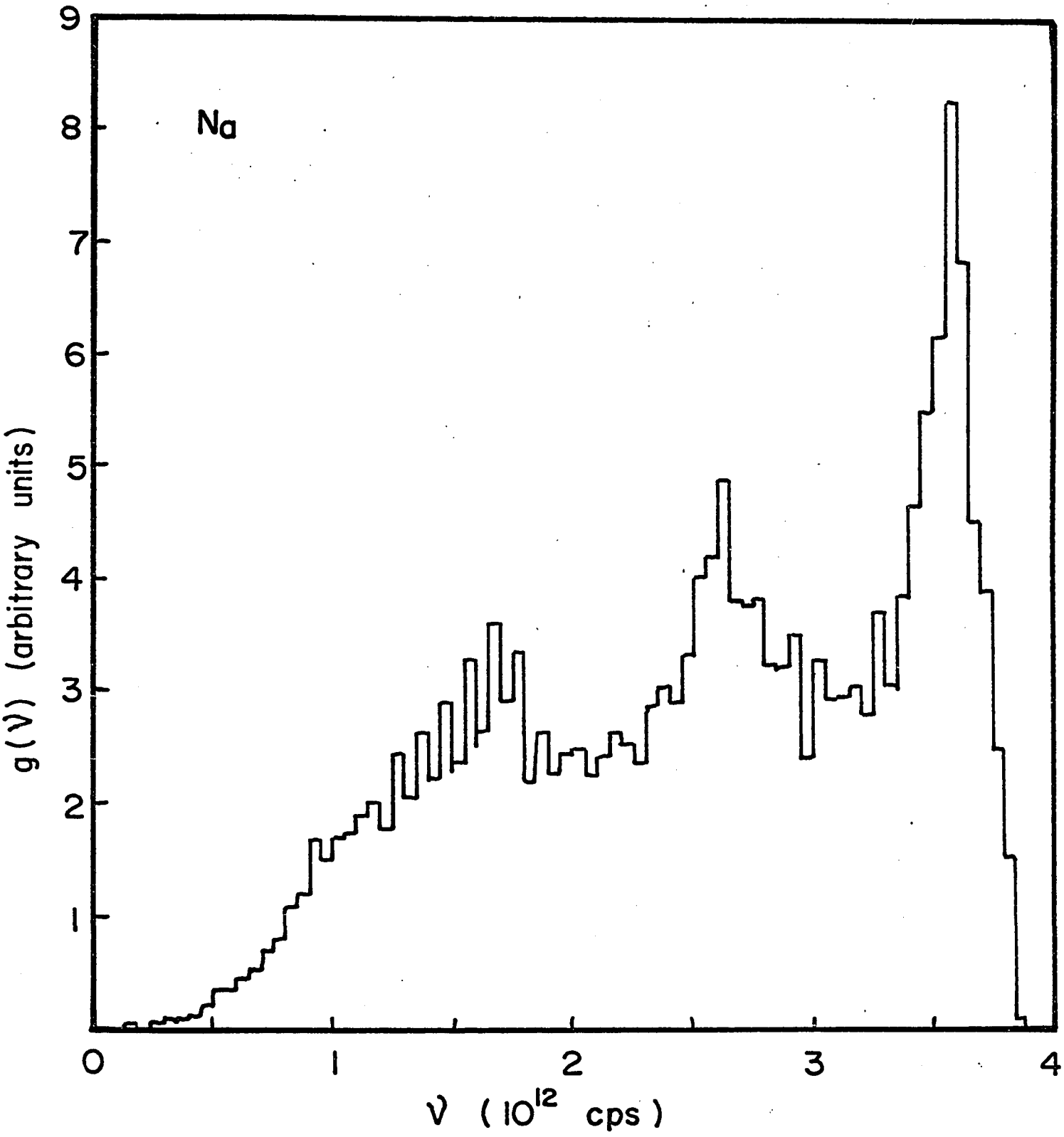

Fig. 6-17. Frequency Spectra of sodium.

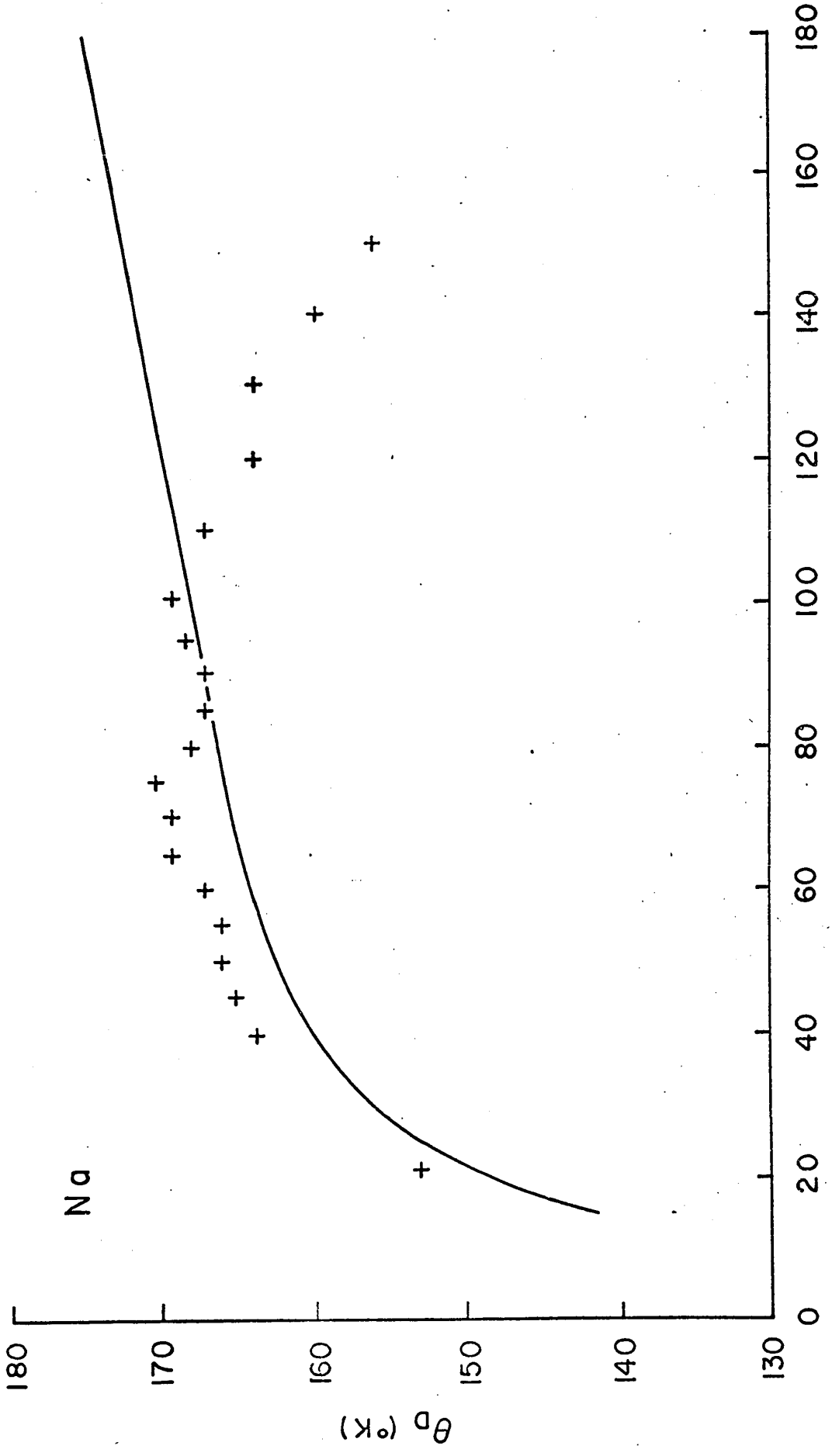
Na
θ_D (°K)
T (°K)
180
170
160
150
140
130
0
20
40
60
80
100
120
140
160
180

Fig. 6 - 18

The frequency spectrum of sodium in Fig. 6-17 has a peak at about 1.7×10^{12} cps, a higher one at 2.6×10^{12} cps and a highest one at 3.6×10^{12} cps. This is in good agreement with that obtained by Dixon Woods and Brockhouse [57] using a fifth-neighbour tensor-force model.

The experimental points of Debye temperatures shown in Fig. 6-18 were derived by Dixon et al. [57] from experimental heat capacity data of Martin [58]. The theoretical Debye temperature curve shows better agreement with experimental values at temperatures below 100°K. For higher temperatures, the theoretical value increases with increasing temperature while the experimental value decreases .

Tantalum

The dispersion curves of tantalum have been measured by Woods [43].

The transition metals show a number of perplexing properties and it is also reflected in their measured dispersion curves, which are known to be quite complicated. It is therefore not surprising that in the case of tantalum, the theoretical curves do not show a good agreement with the experimental results. In the [100] direction, for $\zeta > .5$ the longitudinal branch takes a dip and goes below the transverse branch. It is not possible to reproduce such a behaviour with only four force constants.

We have mentioned earlier the discordance of the magnitude and

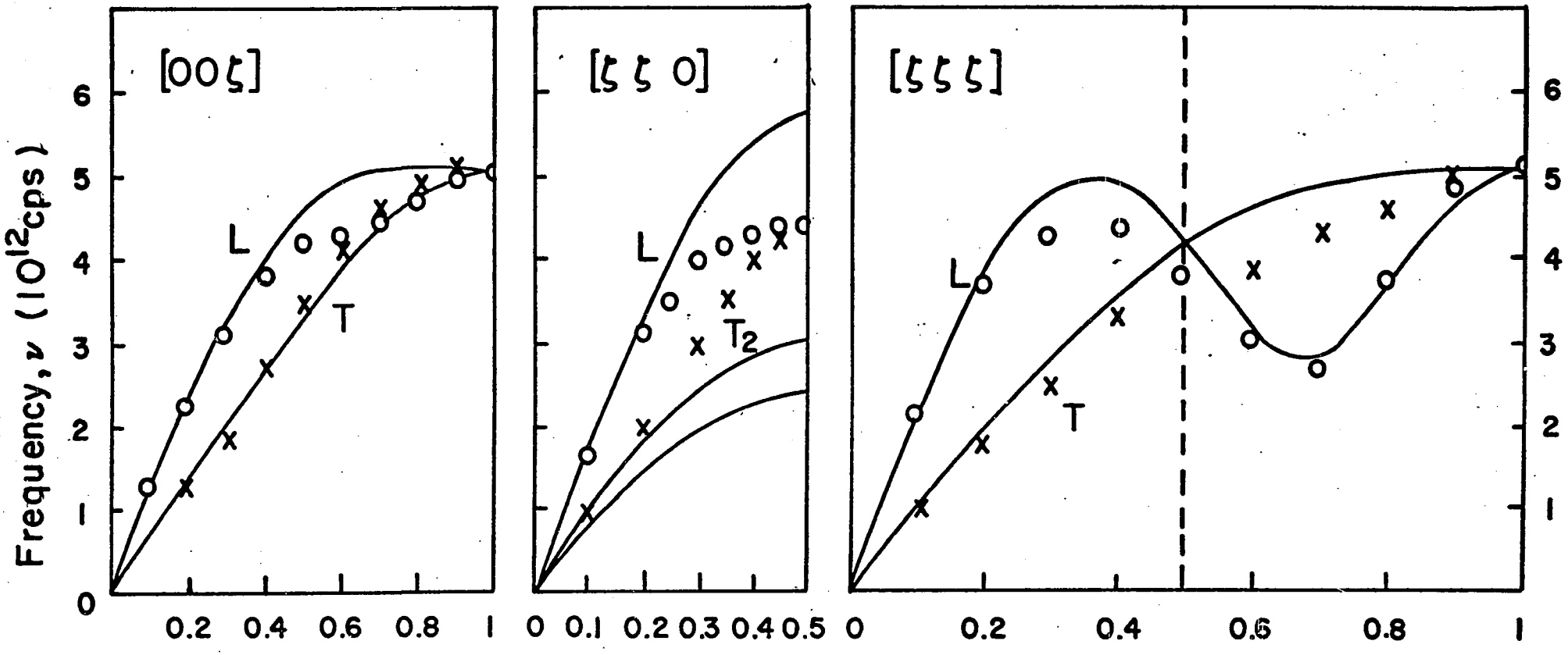

FIG. 6-19 Tantalum (296°K)

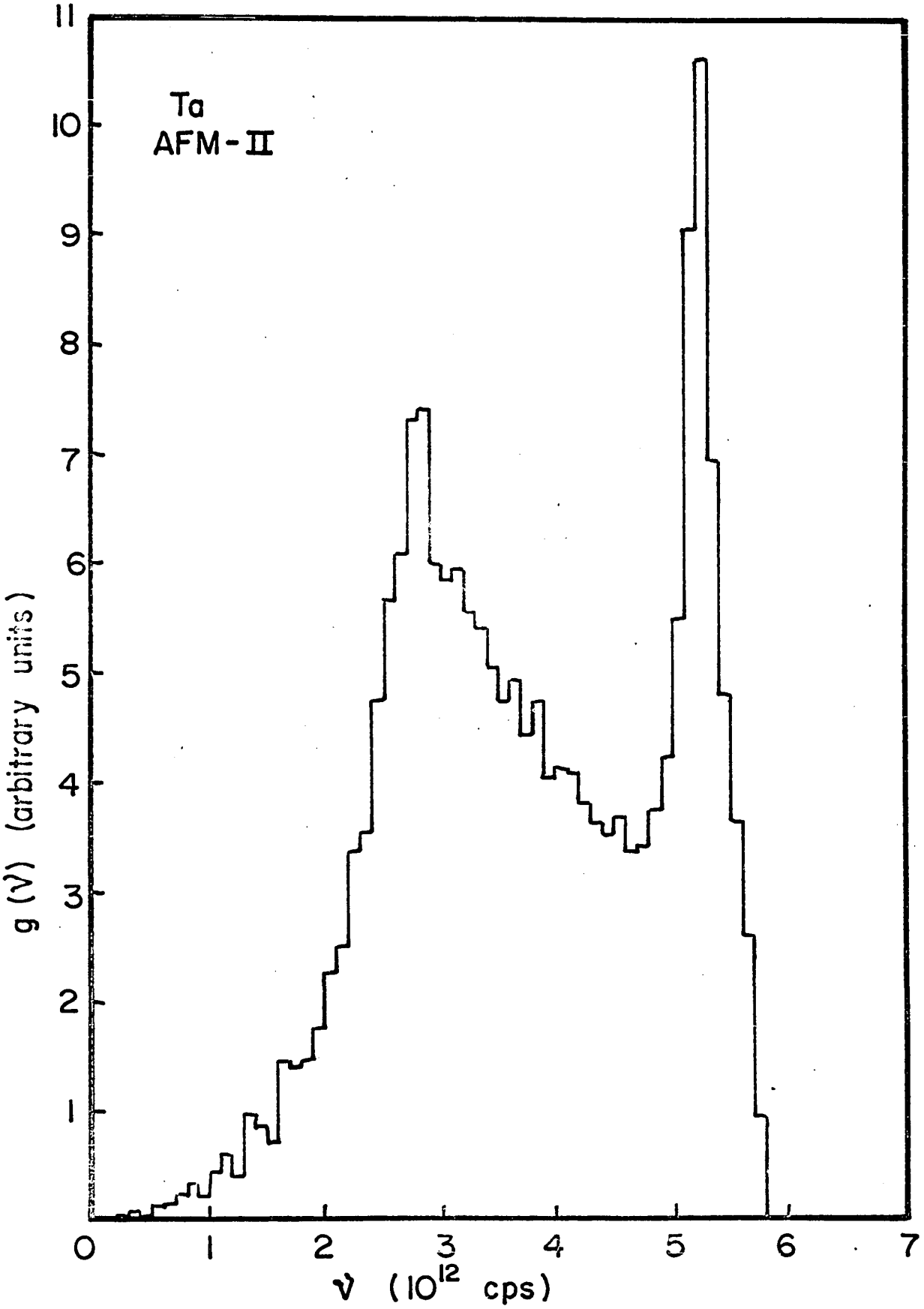
Ta
AFM-II
g (ν) (arbitrary units)
ν (10^12 cps)
0
1
2
3
4
5
6
7
1
2
3
4
5
6
7
8
9
10
11

Fig. 6-20.

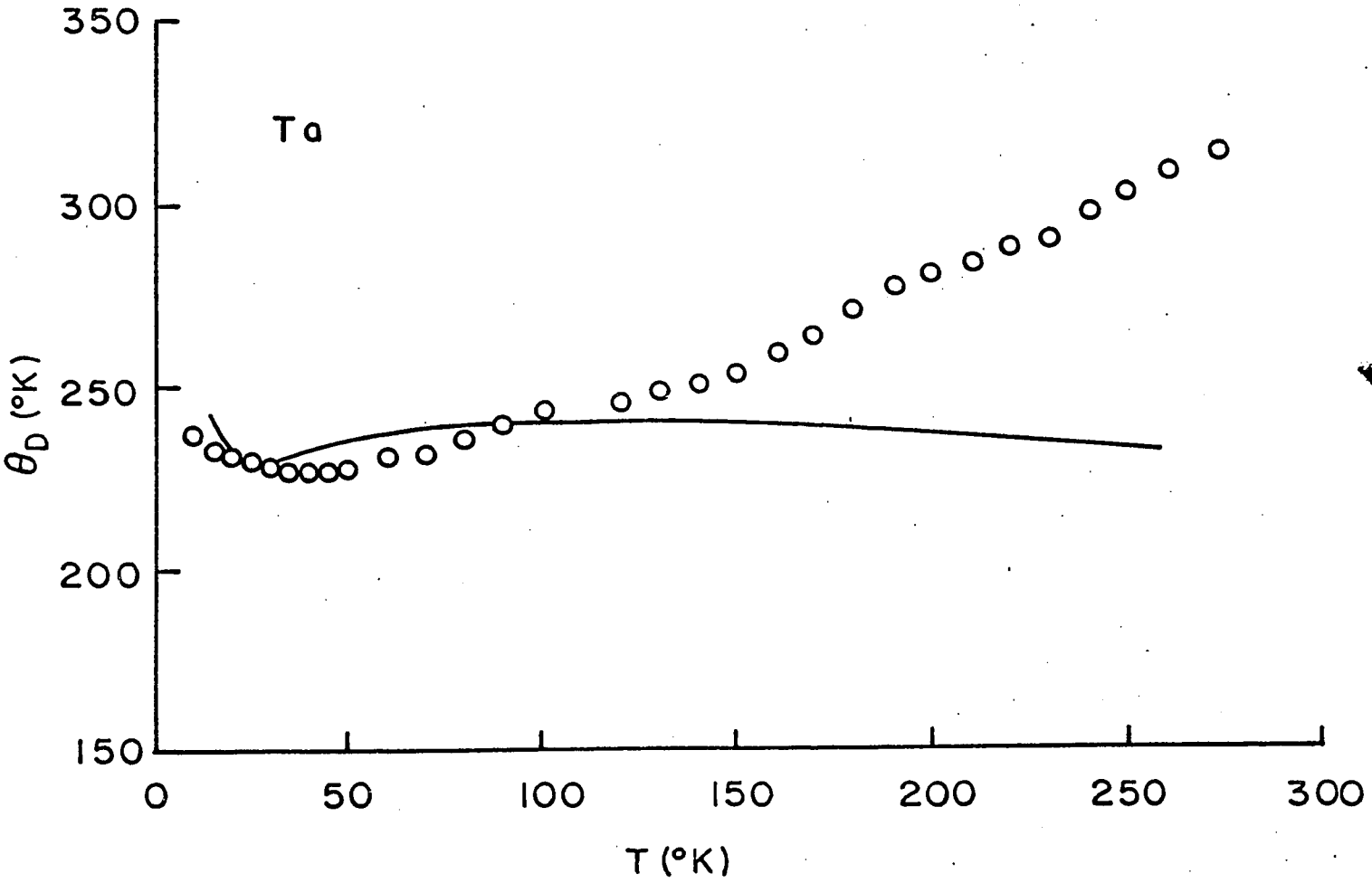

Fig. 6 - 21

signs of the force constants of tantalum in comparison with other metals.

The frequency spectrum of tantalum has one peak at 2.8×10^{12} cps and a higher and sharper peak at 5.2×10^{12} cps (Fig. 6-20). Its shape is similar to that obtained by Woods [43], calculated from the seventh-neighbour general force model.

Heat capacity measurements on tantalum have been carried out by Clusius and Losa [59]. The experimental points for θ's were obtained by subtracting the electronic heat capacity from their results. A number of values of γ have been proposed. A majority of them are close to $14. \times 10^{-4}$ cal/(g. at. deg.^{2}) (Gschneider [60]) and this value was also adopted here.

The theoretical Debye temperature curve (Fig. 6-21) has reasonable agreement with the experimental values for temperatures below 100°K. For higher temperatures, the experimental value increases rapidly with increasing temperature, while the theoretical value remains almost constant. It appears that the value of γ used here is not completely satisfactory.

Molybdenum

The dispersion curves of molybdenum (Fig. 6-22) in the direction [00ζ] have better agreement with the experimental values [44] than that of the dispersion curves in the other directions.

The frequency spectrum of molybdenum has a sharp peak at

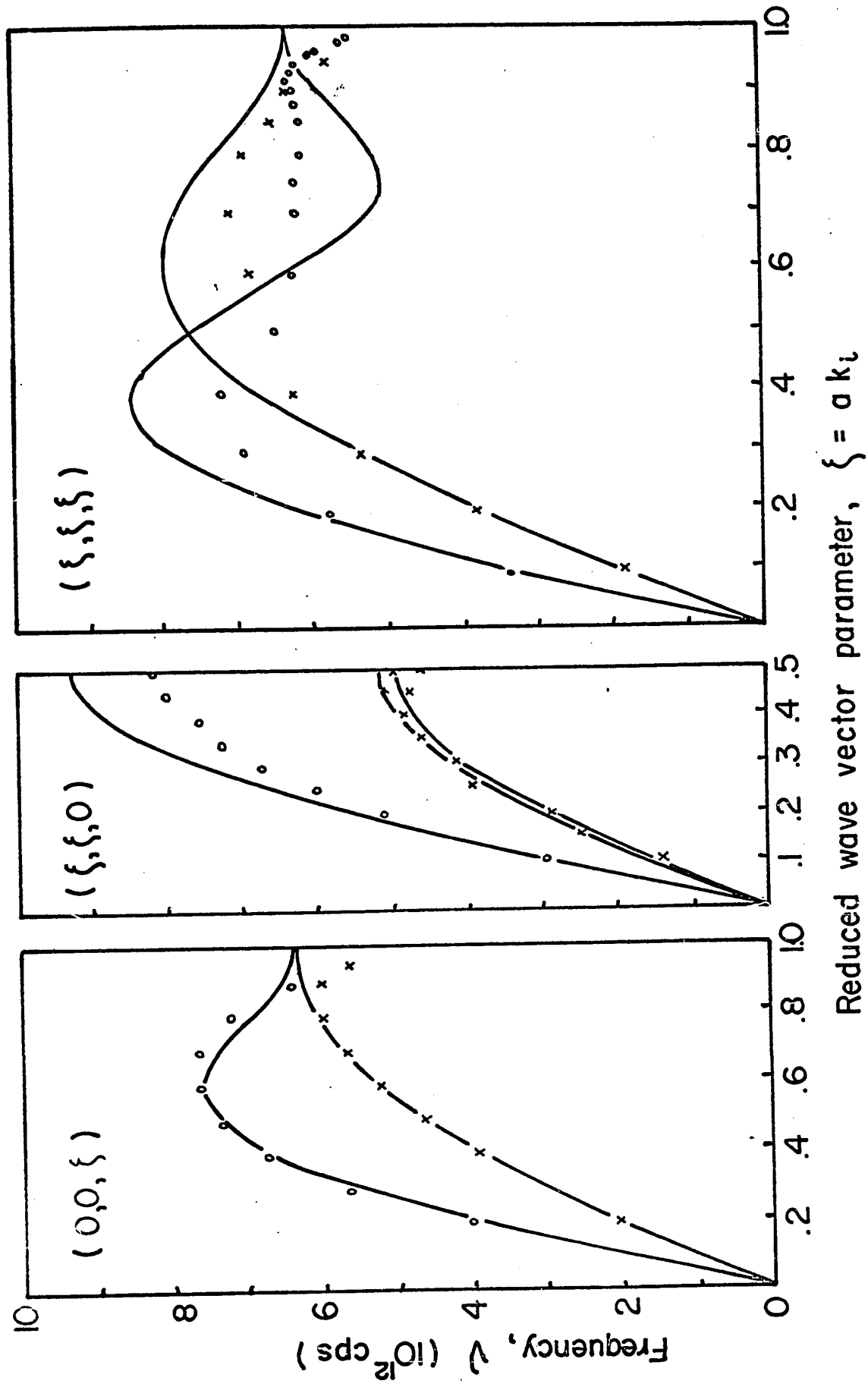

Fig. 6-22. Dispersion curves of Molybdenum (296°K)

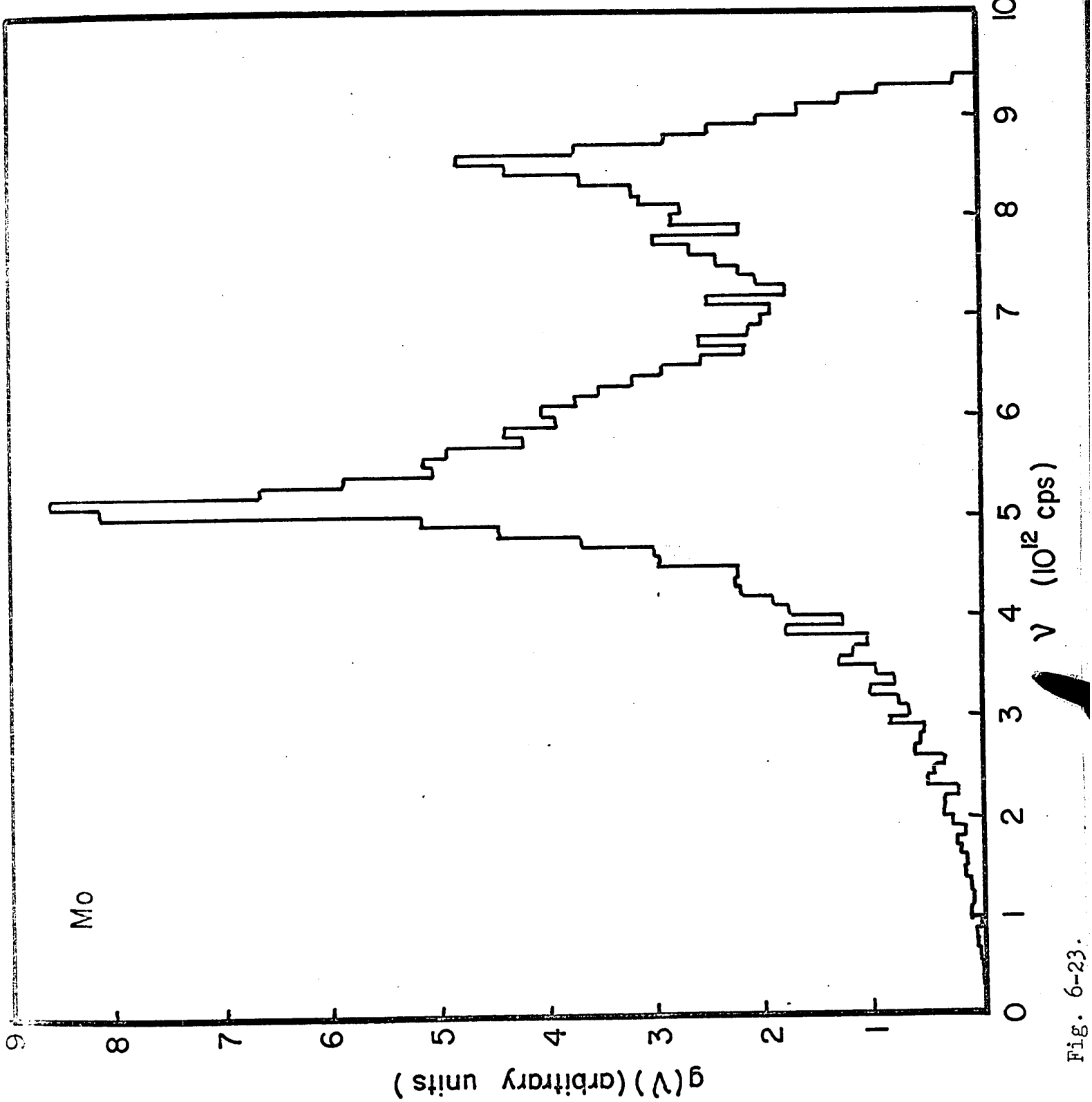

Fig. 6-23.

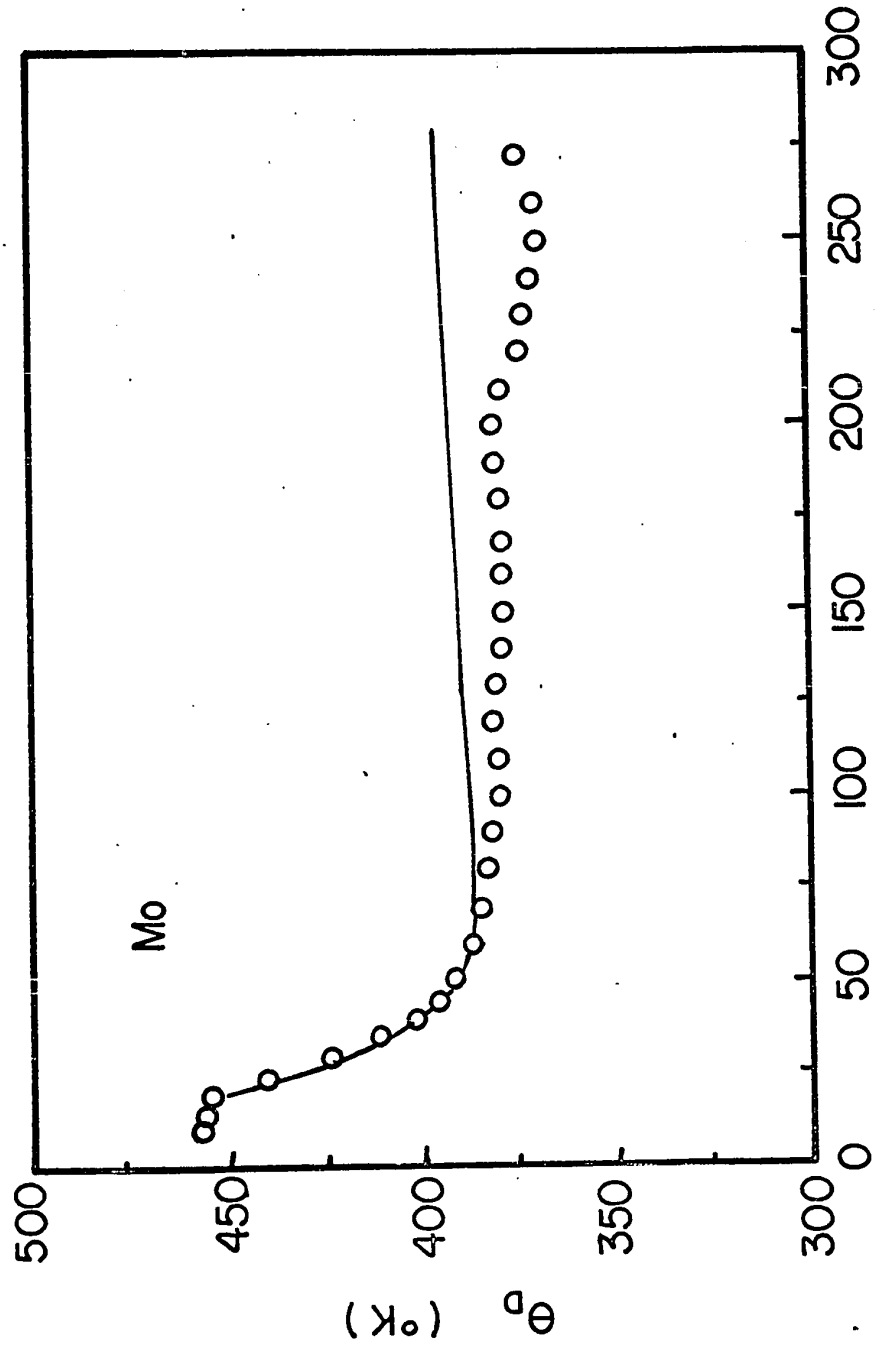

Fig. 6-24. Debye temperature of Molybdenum.

5.1×10^{12} cps and a lower one at 8.5×10^{12} cps. (Fig. 6-23).

The Debye temperature curve of molybdenum agrees with experimental values for temperatures lower than 100°K (Fig. 6-24). At higher temperatures, the theoretical value increases gradually with increasing temperature, while the experimental value fluctuates.

The experimental values were derived from the heat capacity measurements of Clusius and Franzosini [61] using $\gamma = 5.02 \times 10^{-4}$ cal/(g-at. deg.^{2}) (Gschneider [60]).

Tungsten

The dispersion curve of tungsten show better agreement with experimental points in the [00ζ] direction than in the others. (Fig. 6-25). The experimental values have been obtained by Chen and Brockhouse [45].

The histograms of tungsten has a sharp peak at 4.1×10^{12} cps and a lower one at 6.7×10^{12} cps (Fig. 6-26).

The Debye temperature curves of tungsten shows reasonable agreement with the experimental values. For temperature higher than 200°K, the theoretical value remains constant while the experimental value decreases with increasing temperature.

The experimental values were obtained from the heat capacity measurements of Clusius and Frazosini [61] using $\gamma = 2.92 \times 10^{-4}$ cal/g-at. deg.^{2}) (Gschneider [60]).

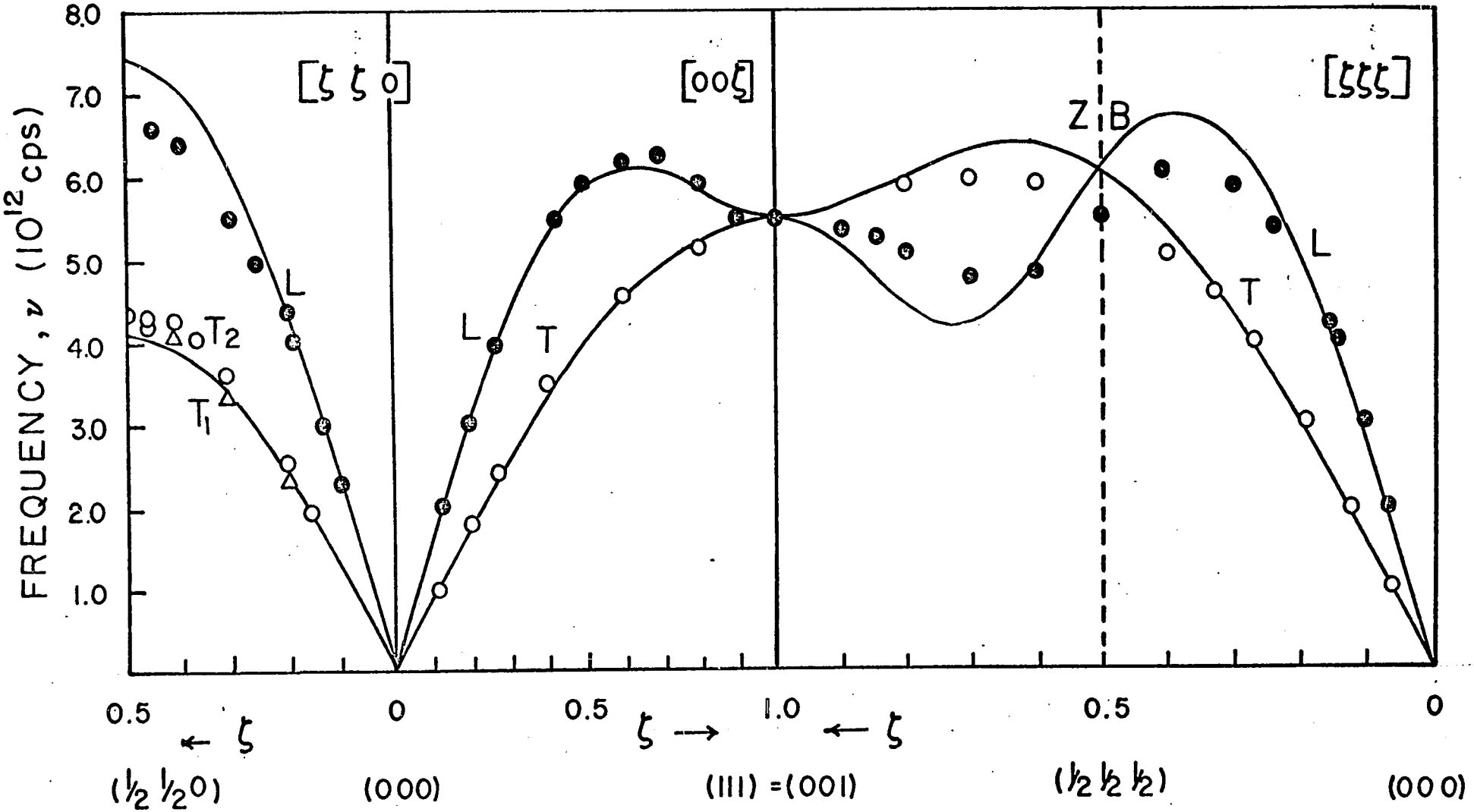

REDUCED WAVE VECTOR PARAMETER, $\zeta = a k_i$

Fig. 6-25 Tungsten (room temperature)

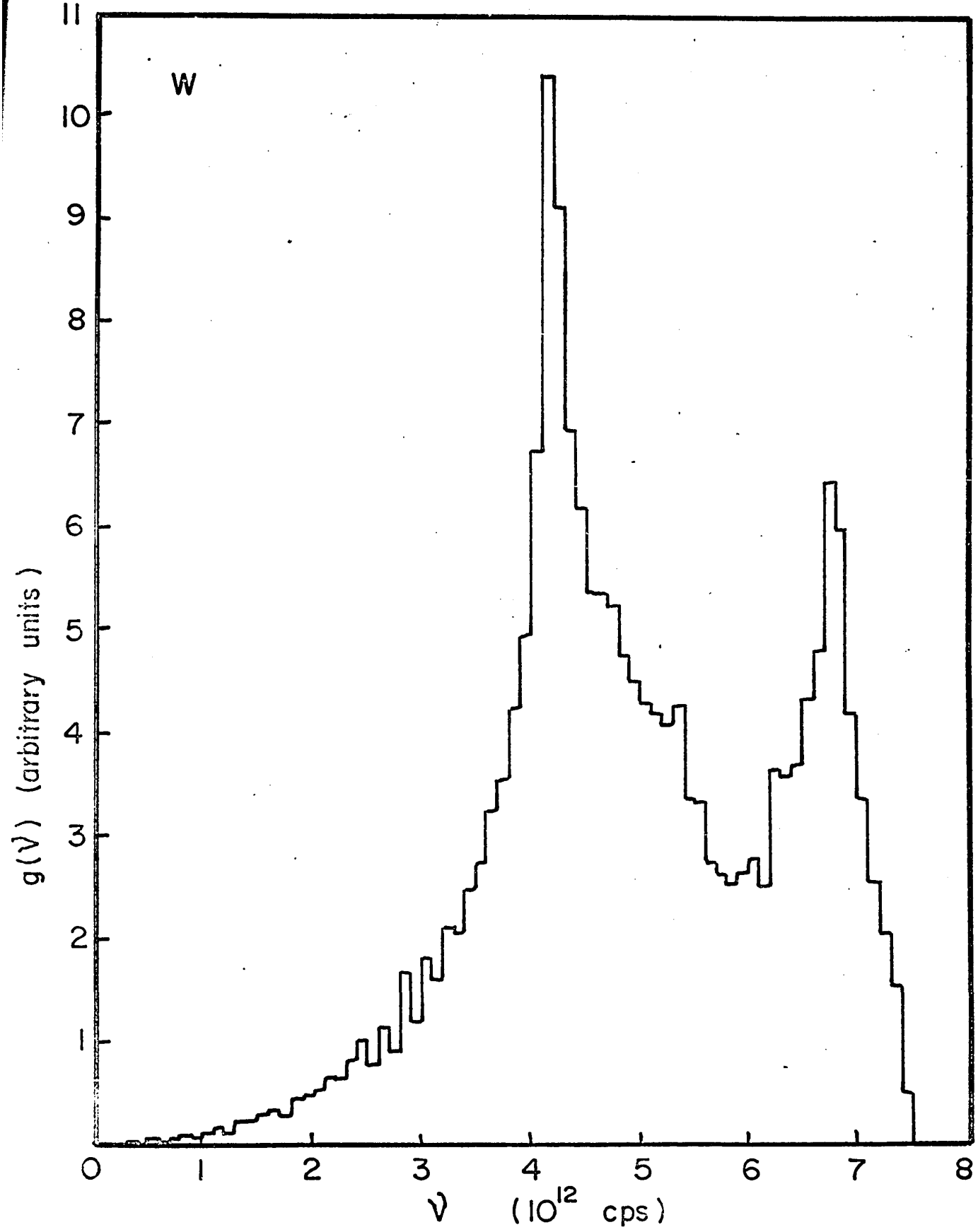

Fig. 6-26. Frequency spectra for Tungsten.

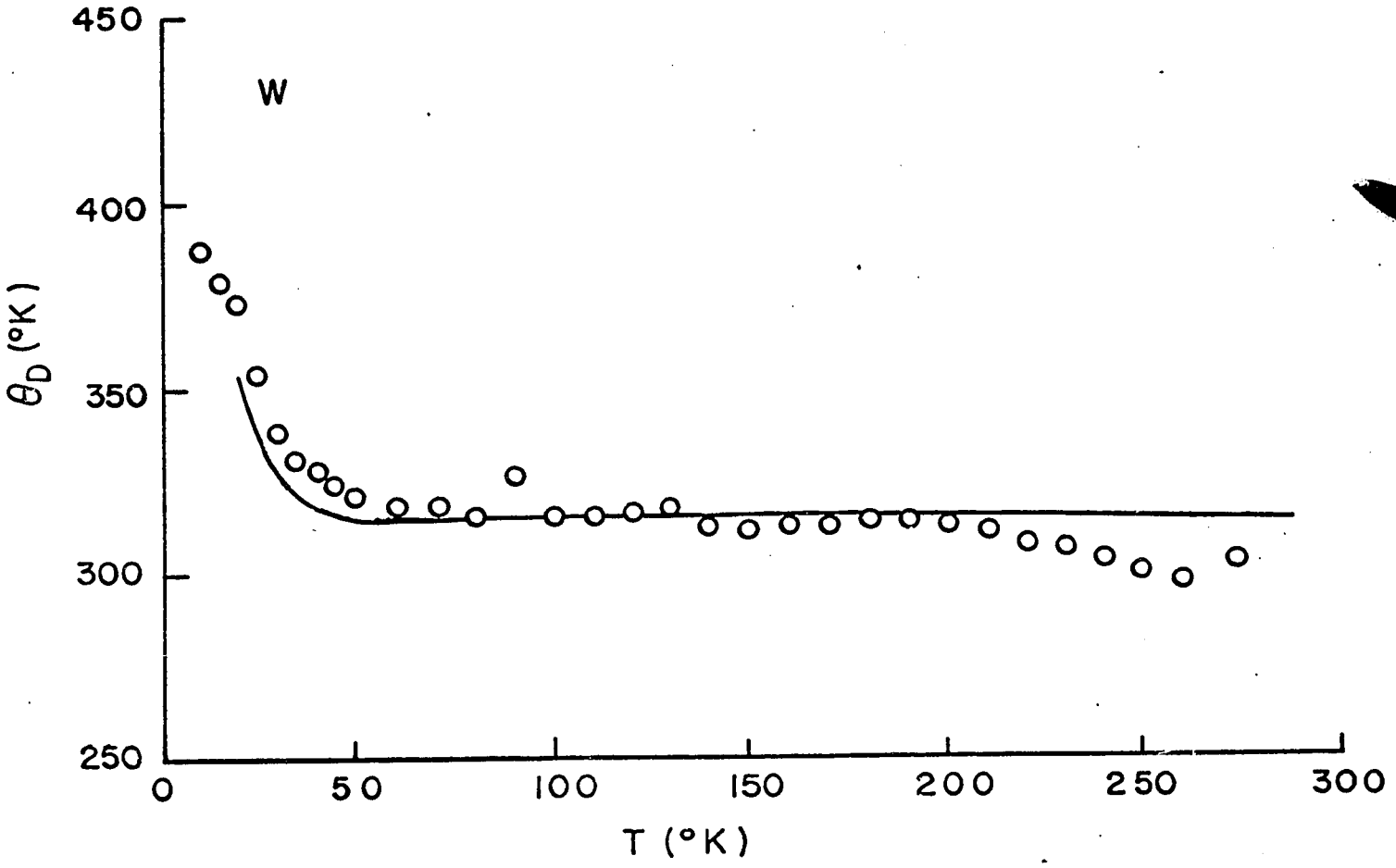

Fig 6 - 27

Iron

The dispersion curves of iron (Fig. 6-28) are in good agreement with the experimental points obtained by Low [41].

The frequency spectrum of iron has a plateau in the frequency range 4.5×10^{12} cps to 7.5×10^{12} cps and a sharp peak at 9×10^{12} cps (Fig. 6-29).

As in the case for nickel, the specific heat of iron has a spin-wave contribution ($\alpha T^{3/2}$) in addition to the usual conduction electron (γT) and lattice terms. Different experimenters have found somewhat different values of α and γ. Recent experiments of Dixon et al. [62] give $\gamma = (11.34 \pm 0.03) \times 10^{-4}$ cal/(mole deg^2) and $\alpha = (1.15 \pm 0.09) \times 10^{-5}$ cal/(mole deg$^{5/2}$). Mahesh and Dayal [63] have used these values of α and γ to derive Debye temperatures from the experimental values of C_v measured by Dmyckaerts [64] and Kelley [65]; these experimental values are reproduced in Fig. 6-30. The theoretical curve is very similar to that calculated by Mahesh and Dayal [63] by using an extended Krebs model [66]. The agreement between the experimental values and the theoretical curve is not unsatisfactory.

In conclusion we find that for those metals whose dispersion curves are not complicated (e.g. Na, Fe) the second-neighbour tensor-force model can be used with fair success. For others though it may not be very satisfactory for the dispersion curves, it still can give a reasonable description of the average frequency spectrum and specific heat.

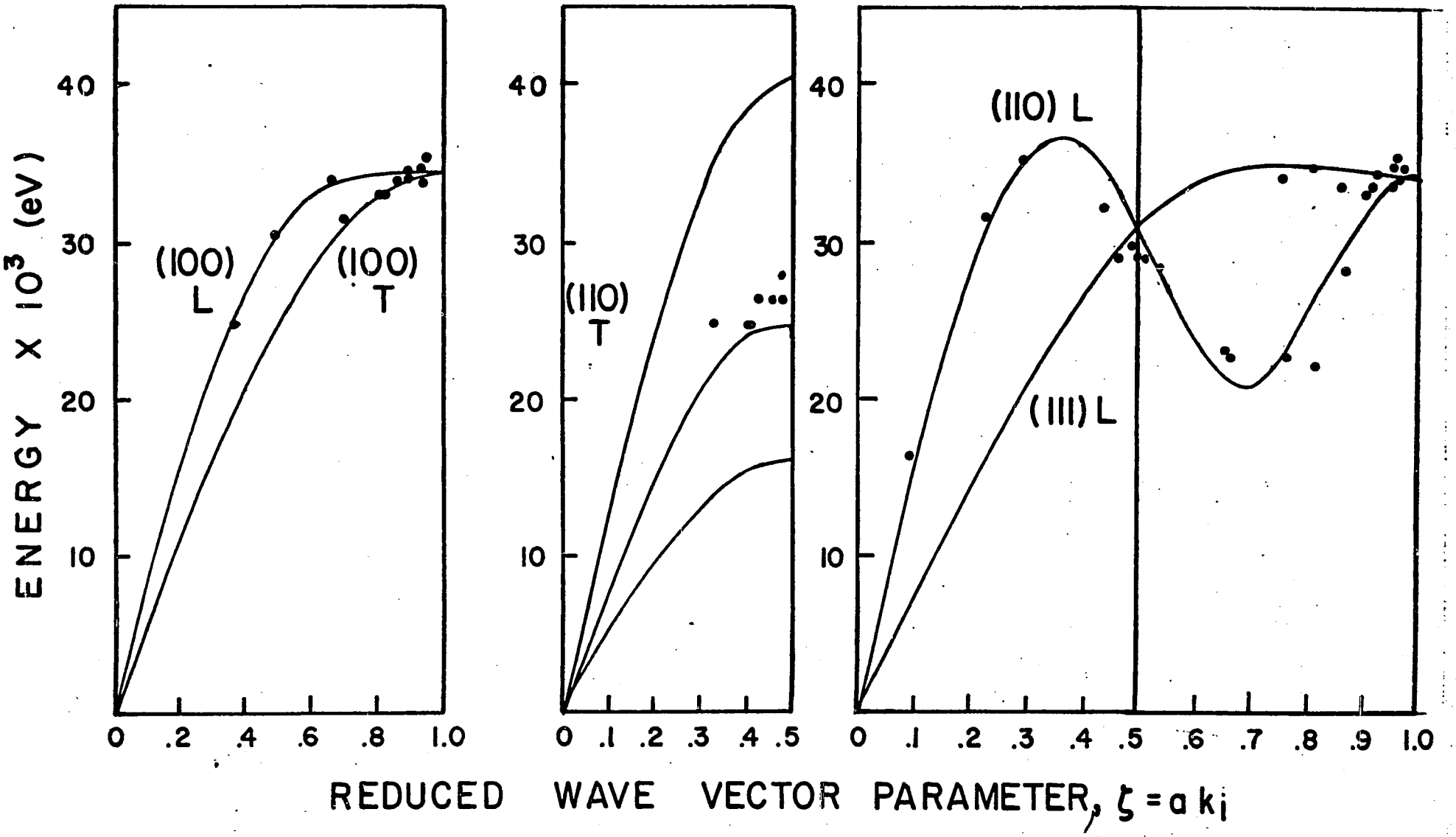

Fig. 6 - 28, Iron (289°K)

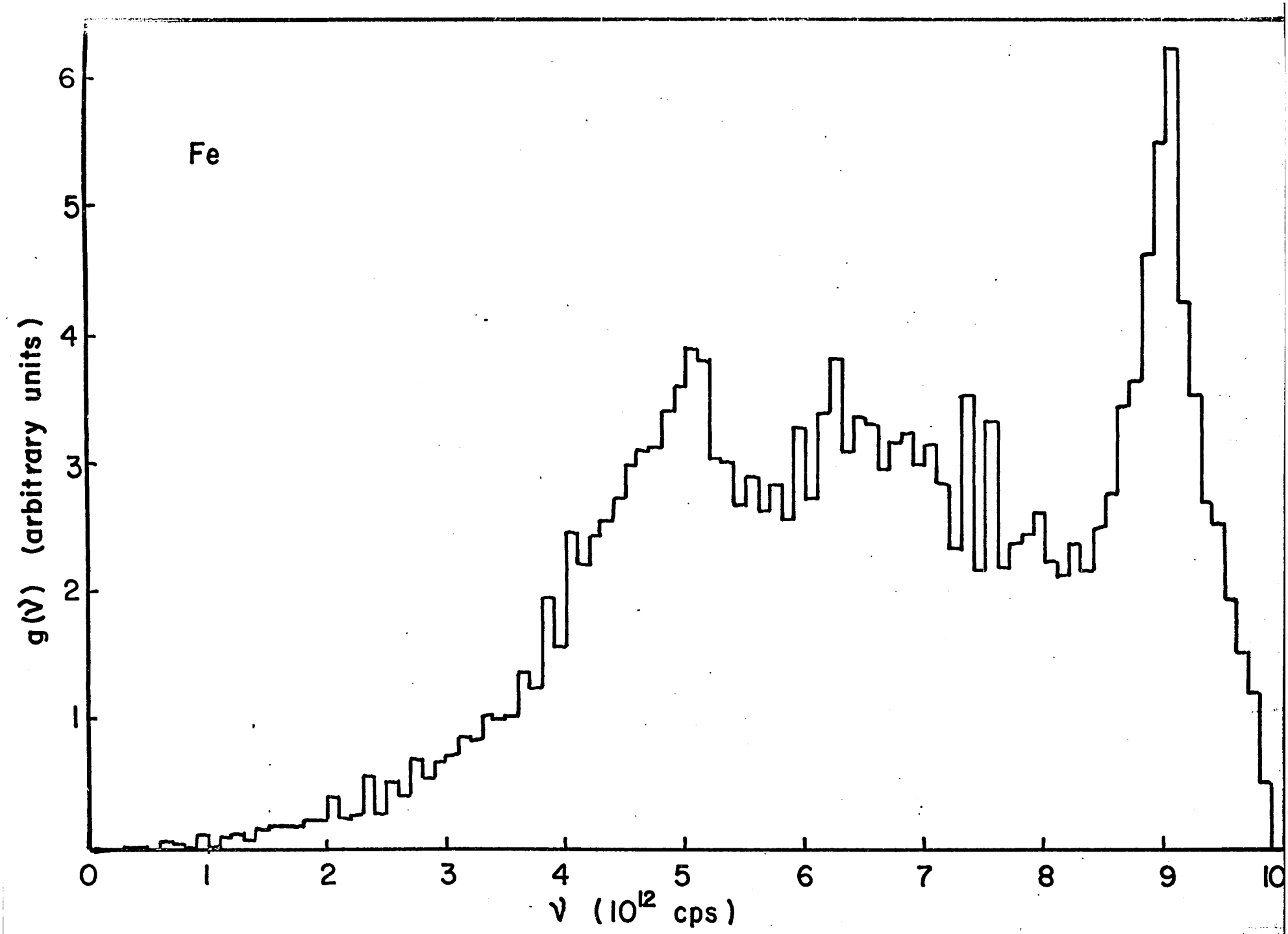

Fig. 6-29 Frequency spectra for Iron.

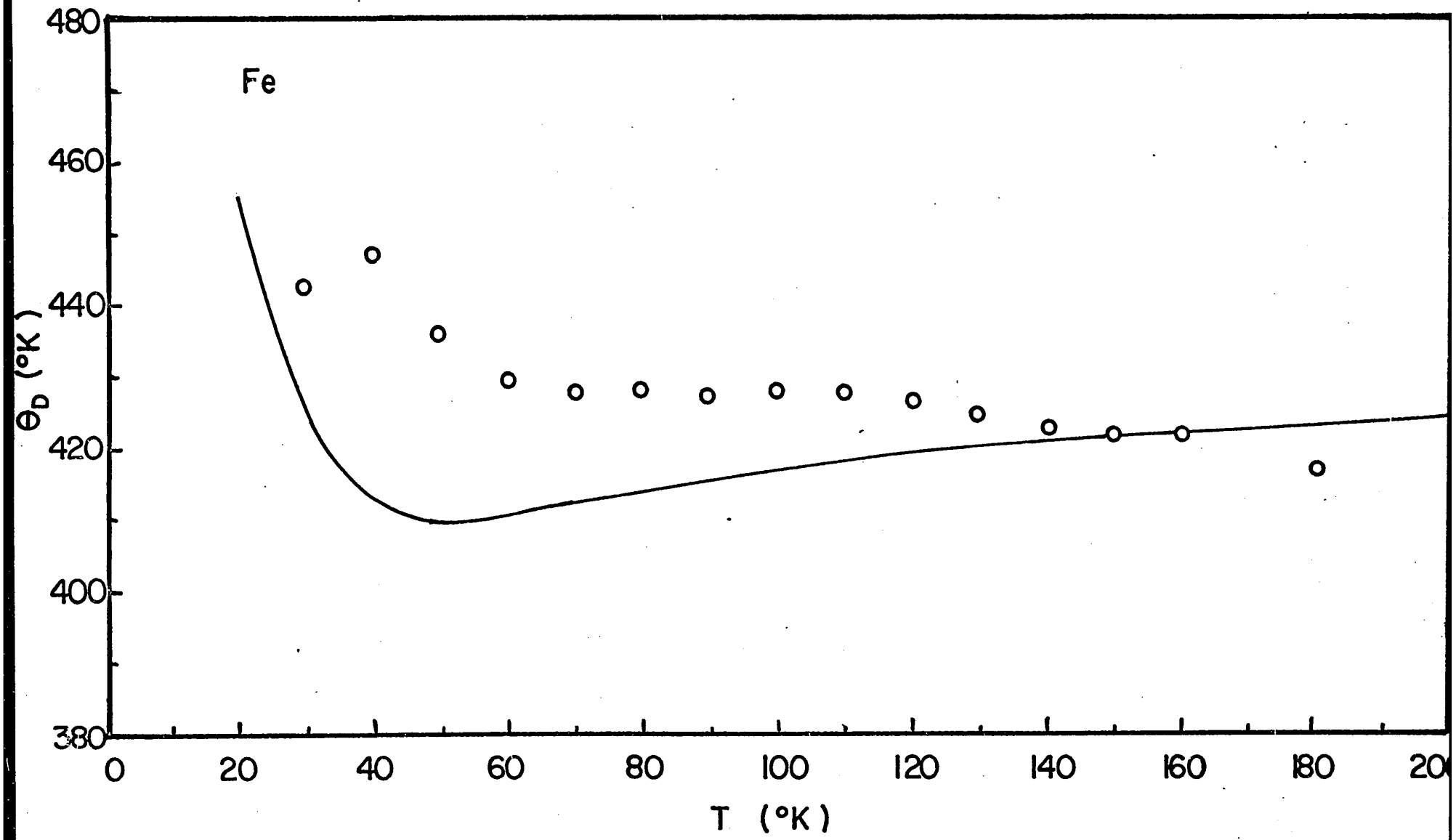

Fig. 6-30. Debye temperature of Iron.

REFERENCES

1. A. Einstein, Ann. Physik 22, 180 (1907).
2. P. Debye, Ann. Physik 39, 789 (1912). An English translation of this paper can be found in "The Collected Papers of Peter J.W. Debye", (Interscience, New York, 1954).
3. M. Born and Th. von Karman, Phys. Zeit. 13, 297 (1912).
4. M. Born, Atomtheorie des festen Zustandes, (2nd ed., Teubner, 1923).
5. M. Blackman, Proc. Roy. Soc. A148, 365, 385 (1935); ibid A149, 117, 126 (1935).
6. E.W. Montroll, J. Chem. Phys. 15, 575 (1947).
7. W.A. Bowers and H.B. Rosenstock, J. Chem. Phys. 18, 1056 (1950).
8. P.C. Fine, Phys. Rev. 56, 355 (1939).
9. R.B. Leighton, Revs. Mod. Phys. 20, 165 (1948).
10. M. Blackman, in Handbuch der Physik, VII/I, p. 325 (1955) (Springer-Verlag, Berlin).
11. M. Born and K. Huang, "Dynamical Theory of Crystal Lattices", (Oxford University Press, 1962).
12. J. de Launay, in "Solid State Physics", edited by F. Seitz and D. Turnbull (Academic Press, Inc., New York, 1956) Vol. 2.
13. W. Cochran, Repts. Prog. Phys. 26, 1 (1963).
14. A.A. Maradudin, E.W. Montroll and G.H. Weiss, Theory of Lattice Dynamics in the Harmonic Approximation (Academic Press, 1963).

15. G.H. Begbie and M. Born, Proc. Roy. Soc. (London) A188, 179 (1947).

16. G.H. Begbie, Proc. Roy. Soc. (London) A188, 189 (1947).

17. H. Curien, Bull. Soc. Franc., Mineral et Crystallographie 75, 197 (1952).

18. D.N. Singh and W.A. Bowers, Phys. Rev. 116, 279 (1959).

19. J.B. Hendricks, H.N. Riser and C.B. Clark, Phys. Rev. 130, 1377 (1963).

20. G.L. Squires, in "Inelastic Scattering of Neutrons in Solids and Liquids, Vol. II", p. 55 (Proceedings, International Atomic Energy Agency, Vienna, 1963).

21. G.L. Squires, in "Inelastic Scattering of Neutrons in Solids and Liquids, Vol. II", p. 71 (Proceedings, International Atomic Energy Agency, Vienna, 1963).

22. M. Born, Ann. Physik 44, 605 (1914).

23. B.C. Clark, D.C. Gazis and R.F. Wallis, Phys. Rev. 134, A1486 (1964).

24. D.C. Gazis, R. Herman and R.F. Wallis, Phys. Rev. 119, 533 (1960).

25. G.W. Lehman, T. Wolfram and R.E. De Warnes, Phys. Rev. 128, 1593 (1962); 130, 2599 (1963).

26. Y.P. Varshni and R.C. Shukla, J. Chem. Phys. 43, 3966 (1965).

27. H. Goldstein, "Classical Mechanics", (Addison-Wesley Publishing Company, Inc., 1959).

28. R.A. Smith, "Wave Mechanics of Crystalline Solids", (Chapman & Hall Ltd., 1961).

29. R.J. Corruccini and J.J. Gniewek, N.B.S. Monograph 29, (1961) (National Bureau of Standards, Washington).

30. American Institute of Physics Handbook (edited by D.E. Gray), Second Edition, Table 9a-2, (McGraw Hill Book Co., New York, 1963).

31. W.C. Overton Jr. and J. Gaffney, Phys. Rev. 98, 969 (1955).

32. G.N. Kamm and G.A. Alers, J. Appl. Phys. 35, 327 (1964).

33. J. de Klerk, Proc. Phys. Soc. 73, 337 (1959).

34. S.K. Sinha, Phys. Rev. 143, 422 (1966).

35. E.C. Svensson, B.N. Brockhouse and J.M. Rowe, preprint.

36. R. Stedman and G. Nilsson, "Inelastic Scattering of Neutrons in Solids and Liquids", International Atomic Energy Agency 58/35, Bombay (1964).

37. R.J. Birgeneau, J. Cordes, G. Dolling and A.D.B. Woods, Phys. Rev., 136, A1359 (1964).

38. M.E. Diederich and J. Trivisonno, J. Phys. Chem. Solids, 27, 637 (1966).

39. F.H. Featherston and J.R. Neighbours, Phys. Rev., 130, 1324 (1963).

40. J.A. Rayne and B.S. Chandrasekhar, Phys. Rev. 122, 1714 (1961).

41. G.G.E. Low, Proc. Phys. Soc. 79, 479 (1962).

42. A.D.B. Woods, B.N. Brockhouse, R.H. March, A.T. Stewart and R. Bowers, Phys. Rev. 128, 1112 (1962).

43. A.D.B. Woods, Phys. Rev. 136, A781, (1964).

44. A.D.B. Woods and S.H. Chen, Solid State Commun. 2, 233 (1964).

45. S.H. Chen and B.N. Brockhouse, Solid State Commun. 2, 73 (1964).

46. D. Cribier, B. Jacrot and D. Saint-James, Inelastic Scattering of Neutrons Solids Liquids Proc. Symp., (I.A.E.A.), p. 549 (1961).

47. D.L. Martin, Can. J. Phys. 38, 17 (1960).

48. D.L. Martin, Phys. Rev. 141, 576 (1966).

49. W.F. Giauque and P.F. Meads, J. Am. Chem. Soc. 63, 1897 (1941).

50. N.E. Phillips, Phys. Rev. 114, 676 (1959).

51. N.A. Tchernoplekov, M.G. Zemlyanov, A.G. Tchetserin and B.G. Lyasht-Lyashtchenko, Inelastic Scattering of Neutrons in Solids and Liquids (International Atomic Energy Agency, Vienna 1962), Vol. 2, p. 159.

52. R.M. Brugger, A.E.R.E. (Harwell) Report R4562 (1964), quoted in Birgeneau et al [37].

53. B. Mozer, K. Otnes and H. Palevsky, Lattice Dynamics (Proc. Internat. Conf., Copenhagen) p. 63, (Pergamon Press 1964).

54. R.H. Busey and W.F. Giauque, J. Am. Chem. Soc. 74, 3157 (1952).

55. J.A. Rayne and W.R.G. Kemp, Phil. Mag. 1, 918 (1956).

56. F.J. Dyson, Phys. Rev. 102, 1217 (1956).

57. A.E. Dixon, A.D.B. Woods and B.N. Brockhouse, Proc. Phys. Soc. 81, 973 (1963).

58. D.L. Martin, Proc. Roy. Soc. A254, 433 (1960).

59. K. Clusius and C.G. Losa, Z. Naturforsch. 10a, 939 (1955).

60. K.A. Gschneider Jr., Solid State Physics 16, 276 (1964).

61. K. Clusius and P. Franzosini, A. Naturforsch. 14a, 99 (1959).

62. M. Dixon, F.E. Hoare, T.M. Holden and D.E. Moody, Proc. Roy. Soc. (London) A285, 561 (1965).

63. P.S. Mahesh and B. Dayal, Phys. Rev. 143, 443 (1966).

64. G. Duyckaerts, Physica, 6, 401 (1939).

65. K.K. Kelley, J. Chem. Phys. 11, 16 (1943).

66. K. Krebs , Phys. Rev. 138, A143, (1965).

VITA

Name: Pui Sum Yuen

Born: Hong Kong, 1942

Education:

Primary: Watson Primary School, Hong Kong, 1950-1953
The Primary School Section of the Pui Ying Secondary School, Hong Kong, 1953-1954

Secondary: Pui Ying Secondary School, Hong Kong, September, 1954 - January, 1956
Kau Yan College, Hong Kong, January, 1956 - July, 1956
Wellington College, Hong Kong, 1956-1957
New Method College, Hong Kong, 1957-1960

University: Hong Kong Technical College, Hong Kong, 1960-1963
University of Ottawa, 1963-1966

Courses: Electrical Engineering, 1960-1963
Physics, 1963-1966

Degrees: Higher Diploma (E.E.), 1963
Hon. B.Sc. (Physics), 1965